Winter 1-1-2012

Natural Killer Cell Recruitment and Activation Following Orthopoxviral Infection

Melissa Anne Pak-Wittel
Washington University in St. Louis

WASHINGTON UNIVERSITY IN ST. LOUIS

Division of Biology and Biomedical Sciences

Immunology

Dissertation Examination Committee:
Wayne M. Yokoyama, Chair
John P. Atkinson
Marco Colonna
Anthony R. French
Deborah J. Lenschow
Emil R. Unanue

Natural Killer Cell Recruitment and Activation Following Orthopoxviral Infection

by

Melissa A. Pak-Wittel

A dissertation presented to the
Graduate School of Arts and Sciences
of Washington University in
partial fulfillment of the
requirements for the degree of
Doctor of Philosophy

December 2012

Saint Louis, Missouri

TABLE OF CONTENTS

LIST OF FIGURES AND TABLES

CHAPTER 5

CHAPTER 6

LIST OF ABBREVIATIONS

CFSE	carboxyfluorescein diacetate
CPXV	Cowpox virus
DCs	Dendritic cells
DNA	deoxyribonucleic acid
dpi	days post infection
ECTV	Ectromelia virus
FLT-3	FMS-related tyrosine kinase-3 ligand
GCPR	g-coupled protein receptor
GDP/GTP	guanosine diphosphate / guanosine triphosphate
GMCSF	granulocyte macophage colony-stimulating factor
g-protein	guanine nucleotide binding protein
IFN	inteferon
IL	interleukin
IN	intranasal
IP	intraperitoneal
IV	intravenous
kb	kilobase
LN	lymph node
MDA 5	melanoma differentiation associate gene 5
MHC I	major histocompatibility class I
mL	milliliter
ms	mouse
MVA	modified vaccinia Ankara

NK	natural killer
ORF	open reading frame
PBS	phosphate buffered solution
PMA	phorbol myristle acetate
polyI:C	polyinosinic:polycytidylic acid
PRR	pattern recognition receptor
RIG I	retinoic acid inducible receptors
RNA	ribonucleic acid
TNFα	tumor necrosis factor α
µg	microgram
µl	microliter
VARV	Variola virus
VV	Vaccinia virus

Acknowledgements

Herein I would like to acknowledge the many people who have mentored and encouraged me during my thesis work. First I would like to thank Wayne Yokoyama for supporting me, both financially and scientifically, during my graduate career. Inasmuch as Wayne has allowed me freedom while still providing guidance, I have learned to think more critically, proceed cautiously and interpret my data systemically.

I would also like to extend my sincere thanks to my thesis committee: Drs. John Atkinson, Marco Colonna, Tony French, Debbie Lenschow and Emil Unanue. Their critiques and suggestions challenged me to grow, be more skeptical and have made me a better scientist. I appreciate the enthusiasm and support that they have provided during my graduate education and training.

Fellow members of the Yokoyama lab also deserve many thanks. In addition to mentoring me, they have provided scientific and personal support throughout my endeavors. In particular, I would like to acknowledge Dorothy Sojka for providing guidance and contributing to my work, and Beatrice Plougastel and Bijal Parikh who always provided insight, discussion and helped me overcome scientific hurdles. I must also thank Liping Yang and Josh Rivenbark; my experiments could not have been done without their kind assistance. I would also like to acknowledge Jennifer Laurent, Lorraine Schwartz, Tammy Derleth and Darryl Higuchi for all their help ensuring my project ran smoothly. Past and present members of the lab including Jimmy Ma, Melissa Berrien, Tammy Cheng, Paul Klekotka, Peter Keyel, Joe Wahle, John Sunwoo, Stephen Ferris, Megan Cooper, Jian Gao, Syste Piersma, Diana Beckman, Samantha Taffner, Maria Gainey, and Takashi Ebihara have provided a stimulating and fun environment to learn and work.

I would also like to acknowledge my fellow graduate students in the lab who have been not just co-workers, but true friends. I thank Claudia Vargas and Julie (Elliott) Chase who were always willing to listen. Thanks also to Minji Byun, who taught me so much about the cowpox virus system, to Helena Jonsson, whose interest always challenged me, and thanks to Chris Affolter, who has been a pillar of support through many challenges.

The Washington University community has been a wonderful family during my graduate career and I have made many great friends here. I am grateful for their support, shared advice, protocols and reagents. In particular, I would like to thank Beverly (Illian) Strong, Danielle Atibalentja, Anja Fuchs, Monica (Walker) Drylewicz, Clara Moon, Holly (Smith) Akilesh and Elizabeth Miller.

My family and friends from California have also been a source of encouragement and support throughout the years. I want to thank my parents, grandparents, brothers and sister-in-law for believing in and supporting me throughout my entire education. In particular, my younger brother, Arthur, and his wife, Julie, were graduate students at the same time and have commiserated with me and provided helpful advice. I would also like to acknowledge my best friends: Freecia Wang, Charlene Betts-Ng and Robin Carle, who always reminded me that I could do this.

Finally, I would like to acknowledge my husband, Gregory Wittel. He has celebrated the high points and carried me through the low points. His belief in my ability as a scientist has been constant and a source of motivation throughout all these years.

ABSTRACT OF THE DISSERTATION

Natural Killer Cell Recruitment and Activation Following Orthopoxviral Infection

by

Melissa A. Pak-Wittel

Doctor of Philosophy in Biology and Biomedical Sciences
Immunology

Washington University in St Louis, 2012

Professor Wayne M. Yokoyama, Chairperson

The orthopoxviridae are large, complex DNA viruses with important historical and clinical significance. Members of this genus encode numerous proteins known to subvert the immune response to infection, providing a useful system to probe required host responses for resistance and survival. Natural killer (NK) cells provide an essential innate response to infection through direct lysis of infected cells and cytokine production. The innate anti-viral response following infection is associated with NK cell population expansion in draining LNs, where they are normally a rare population. We have identified mechanisms underlying NK cell expansion following orthopoxviral infection and have examined viral inhibition of the NK cell-mediated host response.

Since close contact with cowpox virus (CPXV), a natural pathogen of rodents, causes zoonotic infections in humans, we employed a footpad model of infection in mice to determine the requirement of NK cells for resistance to orthopoxviral infection. Systemic depletion of NK cells prior to CPXV infection resulted in increased viral replication and systemic dissemination. Recruitment of NK cells to the draining LN was pertussis toxin sensitive indicating chemokine receptor dependence. Candidate chemokine receptors were identified by comprehensive analysis of chemokine mRNA

expression in the draining LN in conjunction with chemokine receptor expression on NK cells. We determined that CXCR3 was intrinsically required for NK cell recruitment to the draining LN in an interferon-γ– (IFN-γ) dependent manner. Additionally, a non-overlapping requirement for subcapsular sinus macrophages was required for NK cell recruitment.

CPXV inhibited full maturation of NK cells leading to incomplete activation following infection. We found that NK cells recruited to the draining LN did not produce IFN-γ or up-regulate surface activation markers. The inhibition of NK cell production of IFN-γ was CPXV specific, multifactorial and complex. Despite this phenotype, cytotoxic function of NK cells was preserved through uninhibited production of granzyme B. We have demonstrated that the innate response to CPXV infection induces chemokine-mediated recruitment of NK cells to the draining LN where they limit replication and dissemination despite specific inhibition by CPXV.

CHAPTER 1:

Introduction

Orthopoxviruses, Cross Protective Vaccination and Zoonotic Infections

Orthopoxviruses are large, complex DNA viruses whose genus includes historically and clinically important viruses. Among these is variola virus (VARV), the causative agent of smallpox infection, which had devastating consequences on the human population due to its significant morbidity and morality (1). Cross-protection conferred by another orthopoxvirus, vaccinia virus (VV), allowed eradication of naturally occurring smallpox disease during a campaign led by the World Health Organization. The basis of cross-protection was demonstrated by Edward Jenner who deliberately inoculated an eight year old boy first with freshly isolated cowpox virus (CPXV) from a lesion on a dairy maid and subsequently with VARV (2). Jenner's hypothesis that immunization with CPXV would confer protection to smallpox challenge was confirmed when the child displayed no signs of smallpox disease.

Despite eradication of natural smallpox infection, the possibility of deliberate release of VARV during a potential bioterrorist event remains. Additionally, other orthopoxviruses increasingly cause emerging zoonotic infection including monkeypox virus, which is primarily localized to Africa but caused a recent outbreak in the Midwestern United States (3-5). There have also been increasing reports of zoonotic CPXV infection in Europe, where CPXV is endemic in the rodent population (6-10). Despite reports of increasing zoonotic infections, vaccination is no longer routinely recommended or practiced. While most immunocompetent individuals tolerate vaccination with little to no problem, significant side effects have been reported in patients who are immunocompromised and those with eczema and atopic dermatitis (9, 11). In addition, the protective immune response diminishes over time in vaccinated

individuals (12-14). This has resulted in a population that is increasingly susceptible to zoonotic orthopoxvirus infections.

The origin of VV is unknown, although there is some speculation that VV arose following multiple passages of CPXV during the course of smallpox eradication (15). Due to the widespread propagation of VV strains that were ultimately used to eradicate smallpox, VV became the prototypical orthopoxvirus for study of immunomodulation and host-pathogen interactions (16). Some studies have examined immune evasion by VV with the goal of generating safer vaccines. These studies have resulted in the development of attenuated vaccine strains including ACAM200 and modified vaccinia Ankara (MVA), which were derived from serial *in vitro* passaging and targeted deletions of immunomodulatory genes, respectively (17, 18). Since VV also elicits a strong cellular and humoral immune response, other studies have examined its use as a vector to bolster immunizations against other pathogens (18). These studies have demonstrated that VV-vectored immunization increases the immune response to cancer antigens and several pathogens including human immunodeficiency virus and rabies virus. Thus, many studies have both examined immunomodulation of the host immune system and exploited the immunostimulatory response by VV.

Increasing numbers of reports indicate that zoonotic CPXV infections are predominantly caused by skin scratch inoculation following interaction with an infected animal (6-9) whereas zoonotic infection with VV very rarely occurs, especially as the host reservoir is unknown (19). CPXV has the largest genome in the Orthopoxvirus genus and its host reservoir is the wild rodent population in Europe (10, 20-22). Since CPXV and the mouse have co-evolved, this makes host-pathogen interplay relevant to study in a mouse model. Another area of interest for research into CPXV biology is examination of

the large arsenal of potential host range and immunomodulatory open reading frames (ORFs) encoded by CPXV. Analysis of CPXV unique ORFs may highlight particularly important host immune responses for resistance to orthopoxviruses that cannot be studied using other orthopoxvirus genus members. Therefore, continued study of primary immune responses to orthopoxviruses in a matched host-pathogen relationship, such as mouse-CPXV, is of interest to provide additional insight into the host immune response which may lead to novel clinical advances to protect against emerging orthopoxvirus infections.

Viral Immune Evasion

Orthopoxvirus genome size varies greatly, from 130kb to 290kb, and many ORFs are highly conserved between genus members. The central coding region, encoding ORFs responsible for viral replication and life cycle, is highly conserved among all orthopoxvirus family members (22). The genetic termini are more variable among orthopoxviruses, and are where ORFs involved in host range and immunomodulation are located. Orthopoxviruses contain many virally encoded proteins that act in combination to subvert both intracellular and extracellular host immune responses (23, 24).

Intracellular inhibition by orthopoxviruses occurs through numerous viral proteins acting at different levels of respective anti-viral signaling pathways. Host recognition of orthopoxvirus infection is mediated by pattern recognition receptors (PRRs) such as toll-like receptors, NOD-like receptors and intracellular RNA sensors, including retinoic acid inducible receptors (RIG-I) and melanoma differentiation associated gene-5 (MDA5) (24-27). Orthopoxviruses encode inhibitory proteins that sequester double stranded RNA to evade recognition by RIG-I and MDA5. Also, numerous virally encoded proteins

interfere with signaling cascades downstream of PRRs to prevent host recognition. These mechanisms of inhibition have been well characterized and virally encoded regulators have been identified at most levels of signaling pathways (16, 23). In addition to inhibiting signaling pathways downstream of host recognition by PRR, several inhibitory proteins produced by orthopoxviruses have dual functions in inhibiting apoptotic signaling pathways (28). Orthopoxviruses also encode intracellular inhibitory proteins that prevent surface expression of major histocompatibility complex class I (MHC class I) to escape detection by the cytotoxic $CD8^+$ T cell response (29-32). Thus, orthopoxviruses encode numerous intracellular immune evasion proteins that interfere with multiple host responses.

Orthopoxvirus mediated control of the host response also occurs extracellularly through a number of mechanisms. These include expression of virally encoded binding proteins for cytokines, chemokines and complement proteins to inhibit the recruitment of lymphocytes and thus progression of the inflammatory response. There are numerous cytokines that orthopoxviruses target to prevent inflammation including type I interferons (IFNs), IFN-γ, tumor necrosis factor α (TNF-α), IL-1 and IL-18, with some orthopoxviruses encoding more than one ORF to target each cytokine (23, 33-35). Orthopoxviruses interfere with chemokine signaling and recruitment by encoding both chemokine binding proteins and proteins that can bind to and saturate glycosoaminoglycans on host surfaces where chemokines normally bind following secretion (36-38). Modulation of the inflammatory immune response by orthopoxviruses includes the induction of anti-inflammatory cytokines like IL-10 (39). Due to constant selective pressure from co-evolution with their hosts, orthopoxviruses have developed a number of strategies to subvert the host immune response.

Host Response to Orthopoxvirus Infection

Despite numerous immunomodulatory proteins encoded by orthopoxviruses, in general, a strong humoral and cellular immune response is elicited following infection, conferring lasting immunity including cross-species protection (14, 17, 40). Infection with orthopoxviruses leads to the generation of neutralizing antibodies against both the intracellular mature virion and the extracellular enveloped virus resulting in a long-lasting antibody-mediated protection. Generation of neutralizing antibodies requires $CD4^+$ T cells and is first detectable 14 days following vaccination and persists for decades. In the absence of B cells, but not $CD4^+$ or $CD8^+$ T cells, naïve hosts challenged with orthopoxvirus succumb to infection indicating that an antibody response is essential for survival. Although T cell responses are not required for survival, they prevent viral replication and spread immediately following inoculation (17). In contrast to $CD8^+$ T cells, whose function peaks 2 to 4 weeks post vaccination before primary responses decline, the $CD4^+$ T cell response is long lived (14, 40). Prophylactic treatment of naïve Rhesus macaques with human vaccinia immunoglobulin from vaccinated individuals is protective, even in the absence of memory $CD4^+$ or $CD8^+$ T cell responses (14). On the other hand, in the absence of B cells, $CD4^+$ and $CD8^+$ memory T cells can confer protection to VV(40). These strong cellular and humoral responses confer both resistance and long-lived cross-species protection against orthopoxvirus infection.

In addition to the requirement for a strong adaptive immune response, many elements of the innate immune system have been implicated in resistance to orthopoxvirus infection. These include induction of pro-inflammatory cytokines such as IL-12 and IL-18 that mediate T_H1 skewed adaptive immune priming and activation of

both NK cells and T cells (41, 42). Additionally, mice infected with VV that ectopically expresses IL-15 survive infection through the activation of NK cells (43). Dendritic cells (DCs) can sense infection through PRRs and secrete IL-12, IL-15 and IL-18 which stimulate activation of NK cells (44, 45). Despite several *in vitro* studies demonstrating inhibition of maturation and induction of apoptosis in DCs upon orthopoxvirus infection, *in vivo* infection results in up-regulation of co-stimuatory molecules and production of IL-12 (46-48). However, a requirement for DCs to mediate protection from orthopoxvirus infection has not been demonstrated *in vivo.* Similarly to orthopoxvirus infection of DCs, *in vitro* infection of macrophages results in apoptosis. However, *in vivo* macrophage depletion in an intranasal model of infection results in increased susceptibility (49, 50). These *in vivo* studies indicate that DCs and macrophages confer protection against orthopoxvirus infection. Thus redundancy in host immune responses to orthopoxvirus infection confers resistance and protection.

Natural Killer Cells

Natural killer (NK) cells are innate immune lymphocytes that play an important role in the response to tumors and infections by inducing lysis of transformed or infected cells and producing cytokines that help shape other immune responses. Activation of NK cell function is mediated through two distinct mechanisms: integration of signaling through inhibitory and activating receptors (51, 52) and cytokine stimulation (45, 53, 54). Down-regulation of MHC class I, which normally mediates strong inhibitory signaling in uninfected cells, renders cells sensitive to NK cell lysis (55). Ligands for activation receptors can either be pathogen-derived or host-derived and up-regulated upon cell stress (56, 57). While stimulation with cytokines, such as IL-12, IL-15 and IL-18, has

been shown to be effective at activating NK cells to produce other cytokines, NK cell effector functions are largely determined locally since cell-cell contact is required for NK cell-mediated lysis of infected cells. Ultimately, it is the integration of these signals that determines NK cell functionality.

Following activation, NK cells function by lysing target cells or secreting cytokines. Lysis of virally infected cells is mediated through granzyme B and perforin (58, 59). Activation of NK cells through cytokine signaling or activation receptor engagement results in cytokine production by NK cells including IFN-γ, TNF-α and granulocyte-macrophage stimulating colony factor (GMCSF) (60-62). Following stimulation, NK cells produce pro-inflammatory chemokines, including CCL3, CCL4 and CCL5, that recruit macrophages and other lymphocytes to the site of inflammation (63, 64). These coordinated actions of NK cells limit viral replication, induce inflammation and prime an adaptive immune response at early times following infection.

Chemokines and Chemokine Receptors

The immune response is marked by recruitment of innate and adaptive lymphocytes to the site of infection or inflammation and to secondary lymphoid organs. Recruitment of lymphocytes is mediated through multiple mechanisms, but one of the best characterized is chemokine-mediated trafficking. Chemokines have conserved cysteine residues and from which their nomenclature is derived (65). Some of these molecules are constitutively expressed, as is the case for CCL19 and CCL21 which recruit T and B cells into secondary lymphoid organs through high endothelial venues (66). During inflammation, there is induction of inflammatory chemokine expression that is responsible for recruiting innate and adaptive lymphocytes to the site of infection or

inflammation (67, 68). There is some suggestion that chemokines act not only in recruitment but also possess direct antimicrobial activity (69). Once chemokines are secreted, they bind to surface expressed glycosaminoglycans. Promiscuous binding occurs between inflammatory chemokines and their receptors, suggesting a need for redundancy in this recruitment system.

Chemokine receptors are G protein-coupled receptors (GPCRs) that contain seven transmembrane spanning regions (65, 70). As with other GPCRs, chemokine receptors signal via guanine nucleotide-binding proteins (G proteins) which become active when GDP is exchanged for GTP, activating downstream signaling cascades (70). It is well known that pertussis toxin blocks GPCRs by ribosylating the GDP on the G protein, locking it in an inactive state and preventing downstream signaling (71). Lymphocytes express an array of chemokine receptors, allowing trafficking during development, homeostatic conditions and to sites of inflammation.

The recruitment of NK cells in homeostatic and inflammatory conditions has been well studied in human systems, but many discrepancies exist in the murine model (72-74). Since infection with different pathogens stimulates and/or inhibits the production of different chemokines, NK cells must require the expression of several chemokine receptors for proper localization to control infection (75-79). However, many of these studies do not address murine pathogens, so conclusions about murine NK cell chemokine receptor requirements remain somewhat unclear.

A Protective Role for NK Cells Following Orthopoxvirus Infections

Our understanding of NK cells and their requirement for orthopoxvirus resistance is in the context of VV and ectromelia virus (ECTV) infection, although the endemic

hosts for these viruses remains obscure. In systems where NK cells are lacking, such as in genetic deficiency or following systemic antibody depletion, viral infection is uncontrolled and results in lethality (80-82). During ECTV infections, the NK cell receptors, CD94 and NKG2D, are required for protection and NK cells producing IFN-γ and granzyme B expand in the draining lymph node (81, 83). Additionally, the transfer of $Thy1^+$ memory NK cells is protective against lethal challenge with VV infection (84). These data indicate that NK cells are an important component of innate immunity-mediated resistance to ECTV and VV.

Since CPXV has co-evolved with its rodent hosts, CPXV infection of rodents is appropriate for the study of orthopoxvirus-host interactions. However, the role of NK cells in CPXV infection has not been investigated. CPXV has the largest genome in the orthopoxvirus genus (20) and contains several ORFs not found in either VV or ECTV genomes. This includes two ORFs, CPXV012 and CPXV203, that potently down-regulate the expression of MHC class I (29-32).While this might render the infected cell sensitive to NK cell-mediated lysis, CPXV also encodes another ORF, CPXV018, that binds *in vitro* with high affinity to the NKG2D activation receptor and blocks its recognition of ligands on target cells (85). Additionally, all orthopoxviruses encode a number of cytokine binding proteins which could also limit the activation of NK cells, such as one specifically targeting IL-18 (34), a well known mediator of NK cell activation. NK cell activation could also be non-specifically subverted through virally encoded chemokine binding proteins that may limit lymphocyte recruitment, including NK cells, to the site of infection (38, 86, 87). Thus the role of NK cells following CPXV infection was unclear.

In these studies, we developed a model of footpad inoculation using CPXV infection and demonstrated that it mimics the natural route of viral transmission both within the host population to zoonotic hosts. Using this model of inoculation, we determined that NK cells were required in response to CPXV infection. Furthermore, we investigated the mechanisms of NK cell recruitment to the draining LN following CPXV infection including examination of chemokine-mediated trafficking and up-stream signaling requirements. While NK cells were required for resistance to CPXV infection, we also observed that CPXV was inhibiting their function and further examined this inhibition by using CPXV deletion-mutant viruses in our footpad infection model. These studies extend the requirement of NK cells to CPXV infection and additionally provide novel insights into NK cell trafficking and stimulation following orthopoxvirus infection.

CHAPTER 2:

Materials and Methods

Mice

Mice were maintained according to institutional guidelines under specific pathogen free conditions. C57BL/6Ncr (CD45.1) mice and B6.LY5.2/Cr (CD45.2) mice were obtained from the National Cancer Institute (Fredrick, MD). $CCR7^{-/-}$, $CXCR3^{-/-}$, $CCR2^{-/-}$, $IFN\gamma R^{-/-}$ and CD11c-DTR transgenic mice were obtained from Jackson Laboratory (Bar Harbor, ME) and bred in our facility. $CCR5^{-/-}$ and C57BL/6 control mice were obtained from Taconic (Germantown, NY). $Batf3^{-/-}$ mice were a kind gift from the laboratory of Dr. Kenneth Murphy (Washington University, St Louis) and were also previously described(88). All mice were used between 6 and 12 weeks of age.

Cells and Viruses

CV-1 and Vero cells were obtained from the American Tissue Culture Center (ATCC, Manassas VA) and maintained in recommended media. BMDCs were generated by culturing bone marrow cells with Flt-3 ligand (200ng/mL) for 9 days at 37°C at 5% CO_2. Cowpox virus strain Brighton Red and Vaccinia virus strain Western Reserve were plaque purified three times from laboratory stocks initially obtained from the ATCC on CV-1 tissue culture cells. Viral stocks were amplified in Vero cells and isolated following cell lysis by centrifugation through 36% sucrose solution. Viral titers of these stocks were assessed by standard plaque assays on confluent CV-1 monolayers.

Infection

Mice under anesthesia were infected in the right rear footpad with $1.5x10^6$ pfu in 25μL volume of virus diluted in PBS. At 1, 2, 3, 6 or 9 dpi, LNs, spleen, kidneys, lungs, liver, feet, uterus and ovaries were isolated. Organs that were used to determine viral titers

were frozen at-80°C until processing and organs that were used to assess viral genome copies were frozen at -20°C until DNA extraction.

Flow Cytometry

For samples analyzed by flow cytometry, LNs and spleens were crushed in R10 (RPMI, 10% FCS, L-glutamine and pen-strep). When macrophages and DCs were stained, spleens and LNs were diced and incubated in liberase TL (Roche, Indianapolis, IN) for 45 minutes at 37°C in 5% CO_2 prior to being crushed. Red blood cells in splenocytes were lysed before staining for flow cytometry. For later experiments, prior to extracellular staining the cells were stained with cell fixable viabilty dye (eBioscience, San Diego, CA). Antibodies used for flow cytometry analysis were purchased from both BD Biosciences and ebiosciences: NK1.1 (PK136), NKp46 (29A1.4), CD3 (145-2C11), CD19 (1d3), CD11c (HL3), Ly6G (1A8), CD11b (M1/70), F4/80 (BM8), CD45.1 (Ly5.1, clone A20), CD45.2 (Ly5.2, clone104), CD49b (DX5), Ly49CIFH (14B11), Ly49AD (12A8), NKG2D (CX5), CD94 (18d3), CD62L (MEL-14), CD103 (2E7), CD-69 (H1.2F3), CD127 (A7R34), Siglec H (551), and Klrg1 (2F1). Surface staining of cells was performed on ice in staining buffer (3% FBS, 0.1% NaN_3 in PBS) with 2.4G2 (anti-FcγRII/III) to prevent non-specific antibody binding. When staining for IFN-γ and granzyme B, whole LNs or red blood cell lysed splenocytes were first incubation in R10 containing Brefeldin A (GolgiPlug, BD) for 20-30 minutes at 37°C in 5% CO_2 before extracellular staining. After surface staining, cells were fixed and permeablized using a Cytofix/Cytoperm kit (BD Pharmingen) or Mouse FoxP3 Buffer Set (BD Pharmingen) according to manufacturer's instructions. Antibodies used for intracellular staining were IFN–γ (XMG1.2), Ki67 (B56), FoxP3 (FJK-16s), and Granzyme B (clone GB-12,

caltag). Flow cytometry data were collected on BD FACSCanto™ using FACSDiva software (BD) and analyzed using FlowJo software (Tree Star, Ashland, OR).

Viral Titers

Traditional plaque assays were done using organ lysates generated by beat beading three times in 1mL of RPMI. Serial dilutions were plated in duplicate on confluent CV-1 monolayers grown using minimal FCS. Cells were stained 2dpi using a crystal violet solution and plaques were counted. Quantitative PCR was used as a more sensitive measurement of viral genome copy numbers. DNA was generated from organs and was then amplified using StepOnePlus (Applied Biosystems) in a 10μL volume containing 2x Universal PCR Master Mix, No AmpErase UNG (Roche). Quantitative PCR DNA probes are non-extendable oligonucleotides labeled with 5' 6-FAM reporter and 3' Zen / Iowa Black FQ quencher dyes. Primer/probe sets were obtained from IDT DNA and sequences are indicated in Table 1. Samples were run in duplicate, genome copy number was normalized to β-actin copy number and numerical values obtained were multiplied by 1000.

Depletion

To systemically deplete NK cells, 200μg of NK1.1 antibody (PK136) or control antibody (mAR) was injected IP 2 days prior to infection. For neutralization of IFN-γ, 250μg/mouse of H22 antibody or control PIP antibody, a kind gift from the Dr. Robert Schrieber laboratory (Washington University, St Louis), was injected 2 days prior to infection. In the CD11c-DTR mice, of diphtheria toxin (Sigma) diluted in PBS was first tested at 20, 10 and 5 ng/g body weight of the mouse to determine a dose that selectively

depleted DCs but not NK cells or macrophages in the draining lymph node when injected in the leg. For recruitment experiments, 5 ng/g body weight was administered in the hind leg 1 day prior to infection. To deplete macrophages, 50μL of commercially available liposomes that encapsulated clodronate or PBS were injected in the footpad in the foot 5 days prior to infection (Encapsula, Nashville, TN).

Chemokine RNA expression

Draining and non-draining LNs were isolated and RNA was extracted using Trizol following the manufacturer's instructions (Invitrogen, Carlsbad, California). cDNA was then generated using 500ng of the isolated RNA using Superscript III Reverse Transcriptase according to manufacturer's protocol (Invitrogen). Quantitative PCR was then performed as described for viral genome copies except values were only normalized to β-actin and were otherwise unmanipulated. Primer/probe set sequences are indicated in Table 1.

Adoptive Transfers

For adoptive transfer experiments, donor splenocytes were purified from C57BL/6 CD45.1, CCR7 (CD45.2) or CXCR3 (CD45.2) knockout mice and red-blood cells were lysed. For the pertussis toxin or PBS pre-treatment, cells were plated at a density of $3x10^7$/mL in R10 with either 100ng/mL pertussis toxin or PBS and incubated at 37°C in 5% CO_2 for 2 hours before cells were then washed 4 times with PBS. All transferred cells were labeled with 2.5μM CFSE (CellTrace, Invitrogen). The labeling reaction was quenched using 10% FCS in RPMI. Cells were then washed twice in PBS, passed through a 40μm cell strainer and resuspended in a volume such that animals could be

injected IV with 200μL volume. BMDCs were injected either into the top of the foot of the mouse in a volume of 20μL or intravenously injected in a volume of 100μL.

Multiplex Gene Expression Analysis

LNs from CPXV infected mice were isolated, homogenized in QuantiGene sample processing buffer (Affymetrix, Santa Clara, CA) and then incubated at 65°C for 30 minutes before being stored at -80°C. Samples were further processed and run using a custom multiplex set of beads (Affymetrix) for controls and all listed chemokines by the Genome Technology Access Center (Washington University, St Louis, MO). Chemokine expression was normalized first to *Hprt1* transcripts and fold change was assessed by normalizing to the appropriate non-draining LN control. Heat maps were generated using Jcolorgrid (UCSF, San Francisco, CA (89)).

Cytokine Bead Array

Organs were homogenized in 1mL RPMI and supernatants were used in the mouse inflammation kit (BD Bioscience) following the manufacturer's protocol. Data were collected using the BD FACSCalibur™ using CellQuest Pro Version 4.0 (Mac, BD Biosciences) and BD CBA Version 1.4 (Mac).

***Ex Vivo* Lymphocyte Stimulation**

Following infection, LNs were harvested and lymphocytes were isolated and incubated for 1 hour with with 0.5 μg phorbol myristate acetate (PMA, Sigma-Aldrich) and 4 μg ionomycin (Calbiochem) at 37°C in 5% CO_2. After 1 hour of incubation, Brefeldin A

(GolgiPlug, BD) was added and cells were incubated an additional 7 hours a 37°C in 5% CO_2 before staining as previously described.

Immunohistochemistry

LNs were harvested directly into PLP (0.05 M lysine phosphate buffer, pH 7.4, 0.05 % glutaraldehyde, 0.002 mg NaIO4 ml21, 0.5 % paraformaldehyde) with 0.1% Triton X-100 fixative for at least 8 hours then dehydrated in 30% sucrose overnight. Tissues were then embedded in OCT in Tissue-Tek (Sakura Finetek) and snap frozen in 2-methylbutane cooled over dry ice before being stored at -80C until use. Cryostat sections were cut 9μm thick before being rehydrated in PBS and blocked with 10% goat serum in 2.4G2 for 30 minutes. Sections were incubated with primary stain for 2 hours at room temperature, washed 3 times, and incubated in secondary stain for 1.5-2 hours. Primary antibodies used were anti-CD3 (FITC) and unconjugated anti-CD169 (AbD Serotec) and secondary antibody AlexaFluor594 (Molecular Probes). Sections were washed 3 more times in PBS and mounted in VectaShield mounting medium with DAPI (Vector Laboratories Inc, Burlingame, CA). Images were acquired using a Nikon Eclipse 80i microscope and processed using MetaMorph (Molecular Devices, Sunnyvale, CA).

Table 1: Quantitative PCR primer/probe sets.
Primer and probe sequences for RNA expression are shown in a 5' to 3' orientation.

Table 1: Primer and Probe Sequences

	Forward	Reverse	Probe
CPXV	5’-CGGCTAAGAGTTGCACATCCA-3’	5’-TCTGCTCCATTTAGTACCGATTCTAG-3’	5’-AGGACGTAGAATGATCTTGTA-3’
β-actin	5’-AGCTCATTGTAGAAGGTGTGG-3’	5’-GGTGGGAATGGGTCAGAAG-3’	5’-TTCAGGGTCAGGATACCTCTCTTGCT-3’
Chemokine Receptors			
CCL19	5'-CGCATCATCCGAAGACTGAAG-3'	5-TTTACTCAAGACACAGGGCTC-3'	5'-CCAAGAACAAAGGCAACAGCACCA-3'
CCL21	5'-GGGAACCTCTAAGTCTGGAAAG-3'	5'-TTGAGGGCTGTGTCTGTTC-3'	5'-AAGGAAAGGGCTCCAAGGGCT-3'
CXCL9	5'-CAAATCCCTCAAAGACCTCAAAC-3'	5'-GATCTCCGTTCTTCAGTGTAGC-3'	5'-CCCCAAGCCCCAATTGCAACAA-3'
CXCL10	5'-TCATCCCTGCGAGCCTAT-3'	5'-CTTGATGGTCTTAGATTCCGGAT-3'	5'-CCCACGTGTTGAGATCATTGCCAC-3'

CHAPTER 3:

Host Response to Cowpox Virus Footpad Infection

In vivo studies of CPXV are relatively rare and have typically utilized intranasal inoculation (30, 39, 90). These infections model the natural route of smallpox virus transmission and the proposed mechanism of dissemination by bioterrorists. However, the natural route of transmission for CPXV is contact-mediated both within the host reservoir during zoonotic spread to other species including humans (6, 8, 91). We have therefore examined CPXV infection using a footpad injection model in order to study the immediate host response to infection under normal physiological conditions. Only a few studies have employed CPXV footpad infection and there are no data available documenting the host response regarding this route of infection (92, 93). Therefore, we first sought to characterize the immediate immune response in the down-stream popliteal LN.

Determining Infectious Dose

In order to choose a dose to study a sublethal inoculation and infection that occurs following zoonotic transmission, we performed survival studies in C57BL/6 mice using an intraperitoneal (IP) route of inoculation which mimics systemic infection. We chose to perform survival studies with this route of infection because a previously published reports indicate that footpad infection with CPXV does not result in lethality (92, 93). C57BL/6 mice were inoculated with doses of CPXV ranging from $1.567x10^6$ pfu/mouse to $1.26x10^8$ pfu/mouse and mortality and morbidity were observed. This survival curve experiment indicated an LD_{50} of $1.155x10^7$ pfu/mouse during systemic infection. When mice were challenged IP with CPXV, all mice showed signs of illness including ruffled

fur and hunched posture. Additionally some, but not all mice developed lesions on their tails which resolved by 30 days post infection (dpi). Mice treated with higher doses of CPXV also lost of up to 10% of original weight before either succumbing to infection or recovering (Figure 1A). Following initial weight loss, surviving mice gained weight and, by 28 dpi, ranged from 100-125% of initial weight. At the lowest dose studied, $1.567x10^6$ pfu/mouse, all of the mice survived infection. Therefore, all subsequent experiments were carried out using a dose of $1.5x10^6$ pfu/mouse. By choosing this sublethal systemic dose of virus, we were then able to perform our studies in hosts with ensured survival.

Lymphocyte Expansion Following CPXV Infection

The LN plays a crucial role in immunosurveillance by collecting infectious antigens from the periphery in an environment that increases the likelihood of interaction between antigen presenting cells (APCs) and circulating naïve and memory T and B cells (94). One of the hallmarks of infections and inflammatory reactions is lymphadenopathy. This is the consequence of recruitment, expansion and retention of lymphocytes in the draining LN while an immune response is primed resulting in characteristically swollen LNs. Indeed, following footpad infection with CPXV, the draining popliteal LN was enlarged and many lymphocyte populations were expanded.

Innate lymphocytes including macrophages, neutrophils, and DCs, play a critical role in limiting viral replication and spread early following infection as well as simultaneously priming an appropriate adaptive immune response. These innate lymphocytes are characterized by their ability to phagocytose viral particles and recognize infection via PRRs which then stimulates an antiviral state (95, 96). Both macrophages and neutrophils function by producing inflammatory cytokines,

antimicrobial products, and reactive nitrogen and oxygen species that directly kill infected cells. Following CPXV infection, we have found that while macrophages were more quickly expanded, both macrophage and neutrophil populations were substantially increased by 3 dpi (Figure 2A, 2B). Pathogens are also phagocytosed and detected in the draining LN by resident DCs or at the site of infection, stimulating trafficking of migratory DCs to the draining LN (97, 98). The detection of most infections that occur in the periphery is mediated by a variety of migratory DC subsets, including dermal and Langerhan DCs. These migratory DCs are then thought to be responsible for stimulating the immune response in the draining LN either directly or indirectly by passing antigens to LN resident DCs. Surprisingly, the migratory DC population did not greatly expand at early time points following CPXV footpad infection in comparison to the homeostatic trafficking of this subset found in the non-draining LN (Figure 2C). In contrast, the LN resident DC population was significantly increased at 2 and 3 dpi, suggesting that this subset of DCs might play a more significant role following CPXV infection (Figure 2D). Whether LN resident DCs were expanded via *in situ* proliferation or recruitment and differentiation of blood monocytes was not determined at this time. All of these data demonstrated that innate immune cell populations are expanded in the draining LN following CPXV footpad infection.

The LN is an important site for priming an adaptive immune response as it provides a location for relatively rare naïve and memory T and B cells to interact with antigen bearing APCs. Under homeostatic conditions, T and B cells are recruited to the lymph node from circulation through high endothelial venules (99). If these cells do not encounter APCs displaying cognate antigens, they then either migrate out through the efferent lymph or are returned to circulation through the thoracic duct (94). When a T or

B cell recognizes its cognate antigen displayed on an APC, they are arrested in the LN where they undergo clonal expansion and acquire effector functions including cytolytic ability, antibody production and directional homing to the site of infection. Following CPXV infection, we found an increase in the total numbers of both T and B cells in the draining LN suggesting that there was an increased recruitment or retention of these cells to select CPXV-specific T and B cells (Figure 3A, 3B). When a marker of the cell cycle was examined in the T and B cell populations, we found that the majority of these cells were not replicating (Figure 3C, 3D). Therefore, as expected, T and B cells are recruited to and retained in the draining LN following CPXV infection.

Under homeostatic conditions in the mouse, NK cells are excluded from LNs as they do not express CCR7, which binds to CCL19 and CCL21 produced by cells in high endothelial venules (74). Following CPXV infection, we observed a statistically significant increase in the percent and total number of NK cells in the draining lymph node following infection beginning as early as 18 hours post infection (hpi) (Figure 4A, 4B). This expansion occurred quite rapidly and was maintained for up to 6 dpi before the NK cell population began to contract. These data indicated that the NK cell population is specifically expanded in the draining LN, suggesting a potential role following CPXV infection. Aside from the migratory DC population, all lymphocyte populations examined expanded following CPXV footpad inoculation in the C57BL/6 system.

CPXV Replication and Spread

Zoonotic CPXV disease in immunocompetent humans is often limited to the site of infection, with little to no spread of lesions from the site of inoculation (9). In order to determine if and where CPXV was able to spread and replicate following footpad

inoculation in mice, we measured viral titers in a variety of organs. First, traditional plaque assays were performed to assess viral titers in the draining LN, spleen, and liver. We found that CPXV was capable of infecting and replicating in the draining LN (Figure 5A) but that there was limited spread to the spleen where there appeared to be little to no replication of the virus, indicated by consistently low titers over time (Figure 5B). In contrast, in the liver no plaques were observed at any time, suggesting CPXV did not spread to this organ following footpad infection (data not shown). These data demonstrated that CPXV can spread from the site of inoculation and replicate to high titers in the draining lymph node.

Since qPCR provides a more sensitive measurement of viral replication, we used this method to further characterize viral spread by quantitating viral genome copy number in the draining LN, lungs, spleen, liver, kidney, uterus and ovaries. Viral genome copies again demonstrated that CPXV could infect and replicate in both the draining LN and to a high degree (Figure 6B). Meanwhile, minimal copy numbers were found in the lung and spleen (Figure 6C, 6D) while very few to no genome copies were found in the liver, kidney, uterus and ovaries at 3 dpi (Figure 6E, 6F, and 6G), but viral genome copies were elevated in all organs except the spleen at 6 dpi. The data obtained by qPCR from the LN and spleen showed a similar trend to the data obtained by traditional plaque assay, validating this technique. We were also able to detect some viral replication in the liver at 6 dpi, in contrast to traditional plaque assay, demonstrating the increased sensitivity of this system.

NK Cells Prevent Viral Replication

NK cells have been shown to be important for resistance to systemic infection with VV and footpad infection with ECTV (80-82). As the NK cell population was highly expanded in the draining lymph node following infection, we hypothesized that they were playing a role limiting CPXV infection. To investigate this hypothesis, we performed systemic antibody mediated depletion of NK cells prior to infection with CPXV (100). We found that following NK cell depletion (Figure 6A), viral replication in the draining LN was significantly increased in comparison to control antibody treated mice (Figure 6B). Additionally, there was a subtle trend toward increased viral spread in the spleen and more significantly in the lung when NK cells were not present at both 3 and 6 dpi (Figure 6C, 6D). The depletion of NK cells did not lead to an increased complete systemic spread at early times following infection, as viral replication in the liver, kidney, uterus and ovaries (Figure 6E, 6F and 6G) did not increase at 3 dpi. Lack of NK cells also did not affect secondary viremia in these organs at 6 dpi, suggesting NK independent that CPXV spread is. In addition to increased viral replication in the draining LN at 3 and 6 dpi, there was also a subtle delay in the clearance of CPXV from the LN and foot in NK cell depleted mice in comparison to control antibody treated mice at 12 dpi (Figure 7, 7B). Taken together, these data suggest that the expanded NK cell population is playing a role in limiting viral replication which prevents systemic viral spread.

Discussion:

Here we demonstrate that lymphocyte expansion in the draining LN in response to CPXV footpad infection does not appear to be impaired despite the expression of numerous virally encoded inhibitory proteins. Almost all populations of lymphocytes

examined were expanded in the draining LN except for migratory DCs. Additionally, we found a substantial increase in the NK cell population whose role in CPXV infection has not been previously studied. CPXV replication appears to be limited to the LN at early time points following infection, but can later spread to other organs. Following systemic depletion of NK cells, we found dramatic increases of viral burden in the draining LN. Also, spread to some but not all organs was affected in mice lacking NK cells, implying that NK cells prevent dissemination to distant sites.

Many *in vivo* studies of orthopoxvirus family members focus on routes of infection that model either systemic or aerosolized infections (30, 39, 90). Few studies exist that model a natural route of infection that mimics natural transmission both within the host reservoir and to zoonotic hosts. Rare studies have employ a footpad model of infection using CPXV, and these do not address the host response (10, 92, 93). Moreover, zoonotic infections have only been studied after development of symptoms leaving the immediate innate immune response to CPXV undocumented.

Zoonotic infections in immunocompetent humans are characterized by lesions that are limited to the site of inoculation, where it is thought that CPXV infects through abrasions in the skin. These lesions resolve in approximately two weeks. Other symptoms also include fever, myalgia, headache, nausea and lymphadenopathy (6, 8, 9). In the footpad model, mice also develop lymphadenopathy, do not develop lesions outside the region of inoculation and become disease free after 2-3 weeks. It appears that the footpad model in mice closely mimics the zoonotic infection of humans making it a relevant model system to study CPXV.

A previous study using CPXV footpad inoculation was performed in outbred mice and reported replication limited to the footpad and a lack viral spread and replication

(93). Further viral or host responses were not examined. We used the C57BL/6 strain of mice in these studies because many genetic knockouts have been developed this background including many host response factors which may play a role in the response to CPXV infection. In contrast to the previous study, when we examined titers in C57BL/6 after footpad inoculation, we found extensive replication in the draining LN and evidence of spread to the spleen by plaque assay. This discrepancy between this and previous studies is most likely due to the differences between strains of mice and the infectious dose. We were also able to detect viral genome copies not only in the LN and spleen but also in the lungs, kidney, liver, uterus and ovaries using a sensitive quantitative PCR method.

We next assessed the contribution of the innate immune response to lymphadenopathy by monitoring various lymphocyte populations in the draining LN over the course of infection. A detailed examination of lymphocyte populations following CPXV infection has, to our knowledge, not previously been undertaken. Lymphadenopathy resulted from an expansion of most lymphocyte populations examined, including both innate and adaptive lymphocyte populations. Lymphocyte populations appeared to expand normally following CPXV, with the potential exclusion of migratory DCs. An expansion of this population was never observed following CPXV infection in levels greater than the homeostatic migration in the non-draining LN. Whether the lack of migratory DC expansion is due to apoptosis at the site of infection following primary infection of the DCs or due to a specific inhibition of migratory DC recruitment to the draining LN is unknown. Following examination of the expansion of lymphocytes in the draining LN, we were most interested in the robust expansion of the relatively rare LN NK cell population. NK cells are known to be important not only for

lysis of infected cells, but also for priming a T_H1 adaptive immune response when recruited to draining LNs. We thus postulated that NK cells might be important for resistance to CPXV infection. In addition, a role for NK cells has also, to our knowledge, never been studied following CPXV infection but has been demonstrated to be important for resistance to other orthopoxviruses such as VV and ECTV.

CPXV has the largest genome in the orthopoxvirus genus (20) and contains several open reading frames not found in either VV or ECTV genomes. This includes two ORFs, CPXV012 and CPXV203, that potently down-regulate the expression of MHC class I (29-32).While this might render infected cells sensitive to NK cell-mediated lysis, CPXV also encodes another ORF, CPXV018, that binds *in vitro* with high affinity to the NKG2D activation receptor, blocks its recognition of ligands on target cells and prevents *in vitro* NKG2D mediated lysis (85). Additionally, all orthopoxviruses encode a number of cytokine binding proteins which may also limit the activation of NK cells, such as one specifically targeting IL-18 (34), a well known mediator of NK cell activation. It is therefore possible that NK cell populations may be expanded but effectively blocked from functioning by the immunomodulatory ORFs expressed by CPXV. In addition to these known potential modulators for NK cell function, additional unknown modulators may exist.

To investigate whether NK cells were playing a role in CPXV resistance, we performed systemic depletion of NK cells prior to footpad infection. The most striking increase in viral burden after depletion occurred in the draining LN, where we measured a two-log increase in viral replication. We also observed a more subtle increase in viral genome copy number in the lung and spleen at both 3 and 6 dpi, suggesting that NK cells prevent spread to these organs at these time points. Another subtle increase in viral

burden at later time points following infection was observed in the draining LN and in the foot, indicating that NK cells also play a role in viral clearance. Whether this was due to limiting initial viral burden shortly after infection or due to priming of the adaptive immune response is still unknown. This pattern of increased viral burden suggested to us that NK cells were playing an important role in the draining LN where viral replication was limited thus preventing viral spread.

It is important to note that when C57BL/6 mice were inoculated in the footpad, no mice succumbed to infection. This is in contrast to the increased mortality of mice following systemic depletion or genetic absence of NK cells during infection with either ECTV or VV (80-82). It is possible that NK cell depleted mice would succumb to infection following a larger dose of CPXV, but increased mortality was observed even with sub-lethal doses of ECTV and VV. Thus, while NK cells play an important role in resistance to CPXV, similar to ECTV and VV, they are not absolutely required for survival.

Also, despite viral dissemination at later time points after CPXV footpad infection, no lesions have been observed outside the site of inoculation. These data suggest that the primary site of early CPXV infection and replication is the foot and draining LN, from where it may rarely escape into the blood and be spread to the spleen and/or lungs. If CPXV replicates to sufficient titers in the draining LN and footpad, a secondary viremia may occur in other organs at later time points. In addition, this route of infection seems to mimic zoonotic infection where there is primary replication at the site of inoculation and systemic disease is not observed. This makes the footpad route of infection a relevant model to study both spread within the host reservoir, but also zoonotic spread in humans.

Figure 1: Morbidity and mortality following CPXV footpad infection.
Age and sex matched C57BL/6 mice were inoculated in the footpad with indicated doses of CPXV in 25μL volume. Mice were weighed every day for the first 11 days, then every other day for the next week and before sacrifice at the conclusion of the experiment. (A) Weight change and (B) mortality over time following CPXV infection are depicted. N=10 mice for $1.26x10^8$ pfu/mouse and $6.3x10^7$ pfu/mouse, n=8 mice for $1.4x10^7$ pfu/mouse, n=7 mice for $4.7x10^6$ pfu/mouse and n=6 mice for $1.567x10^6$ pfu/mouse.

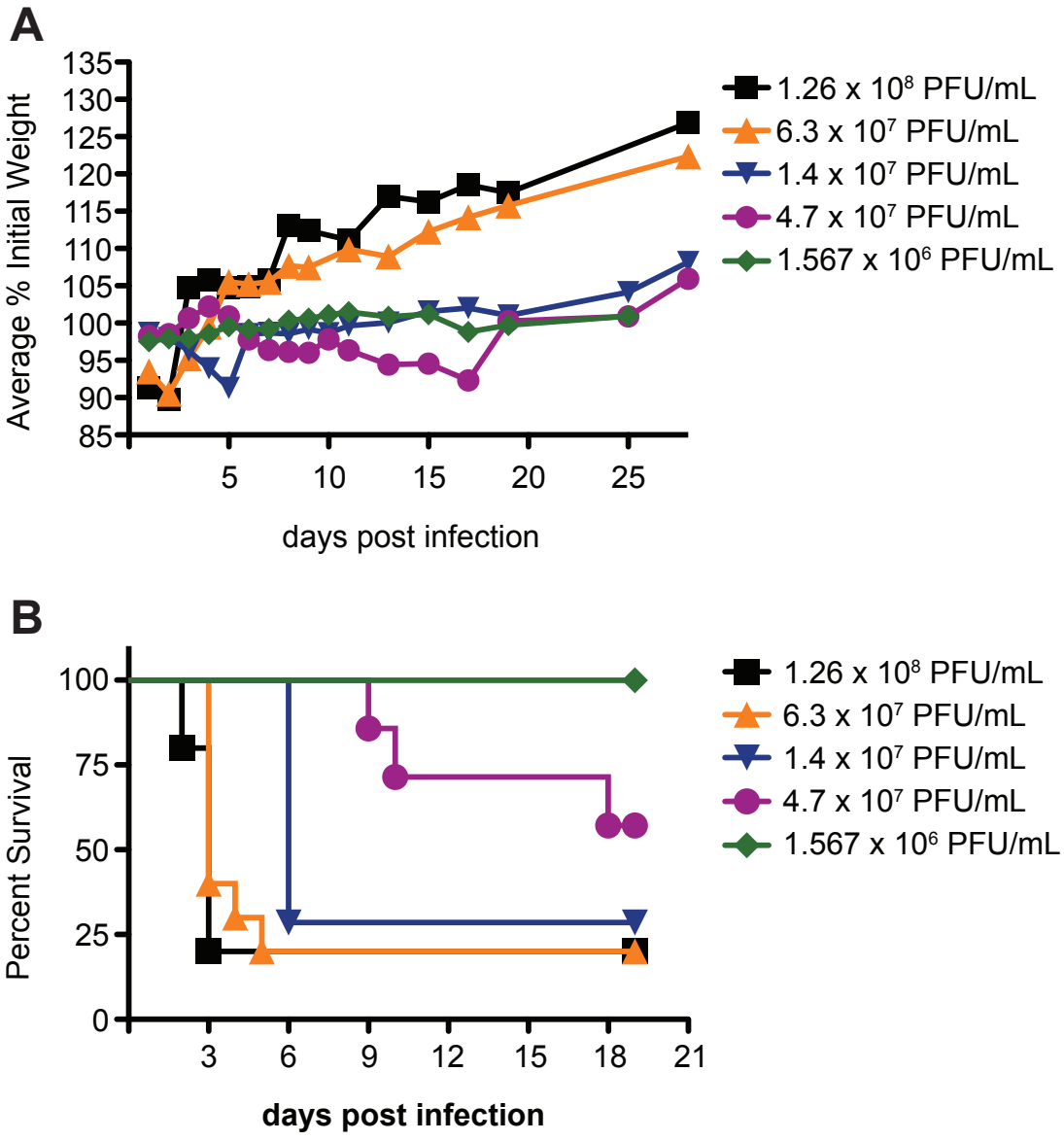
A
Average % Initial Weight
135
130
125
120
115
110
105
100
95
90
85
5
10
15
20
25
days post infection
1.26 x 10^8 PFU/mL
6.3 x 10^7 PFU/mL
1.4 x 10^7 PFU/mL
4.7 x 10^7 PFU/mL
1.567 x 10^6 PFU/mL
B
Percent Survival
100
75
50
25
0
3
6
9
12
15
18
21
days post infection
1.26 x 10^8 PFU/mL
6.3 x 10^7 PFU/mL
1.4 x 10^7 PFU/mL
4.7 x 10^7 PFU/mL
1.567 x 10^6 PFU/mL

Figure 2: Kinetics of innate lymphocyte expansion following CPXV footpad infection.
Age and sex matched C57BL/6 mice were inoculated in the footpad with$1.5x10^6$ pfu/mouse and at indicated times, lymphocytes from the non-draining and draining LNs were isolated, stained and analyzed by flow cytometry. Following exclusion of dead cells, total (A) macrophages ($F4/80^+CD11b^+$), (B) neutrophils ($Ly6G^+SSC^+$), (C) migratory DCs ($CD11c^+MHCII^{high}$) and (D) LN resident DCs ($CD11c^+MHCII^+$) were identified. Cell numbers were ascertained using trypan blue exclusion, then multiplied by the percentage of population found by FACS analysis. A graph depicting the average of 3 independent experiments is shown.

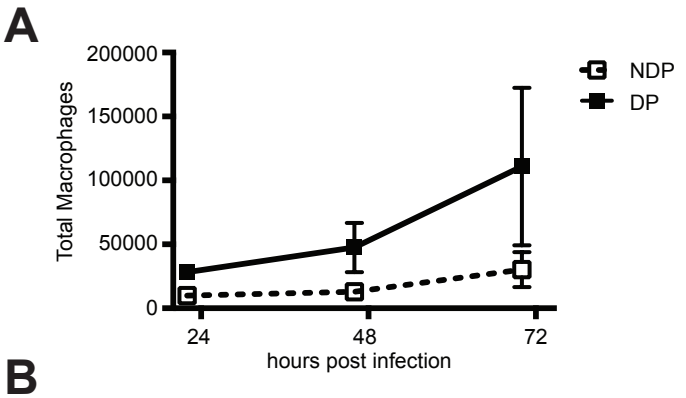
A
200000
150000
100000
50000
0
Total Macrophages
24
48
72
hours post infection
NDP
DP

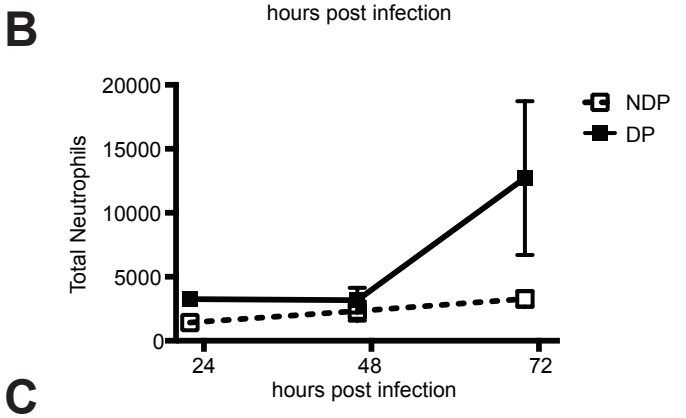
B
20000
15000
10000
5000
0
Total Neutrophils
24
48
72
hours post infection
NDP
DP

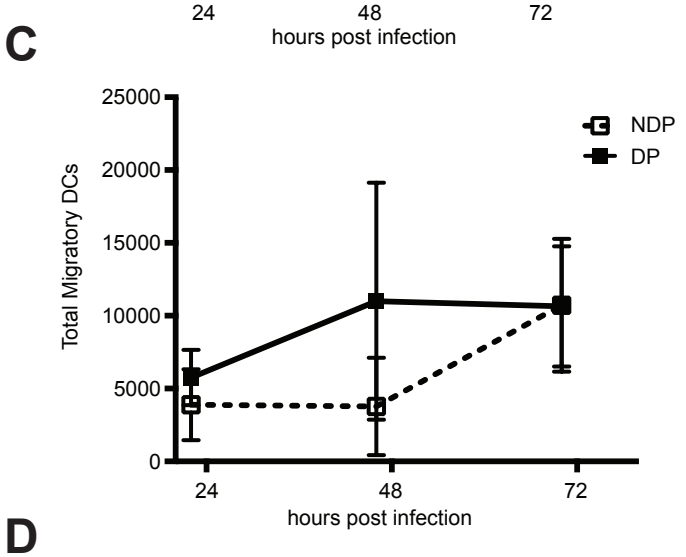
C
25000
20000
15000
10000
5000
0
Total Migratory DCs
24
48
72
hours post infection
NDP
DP

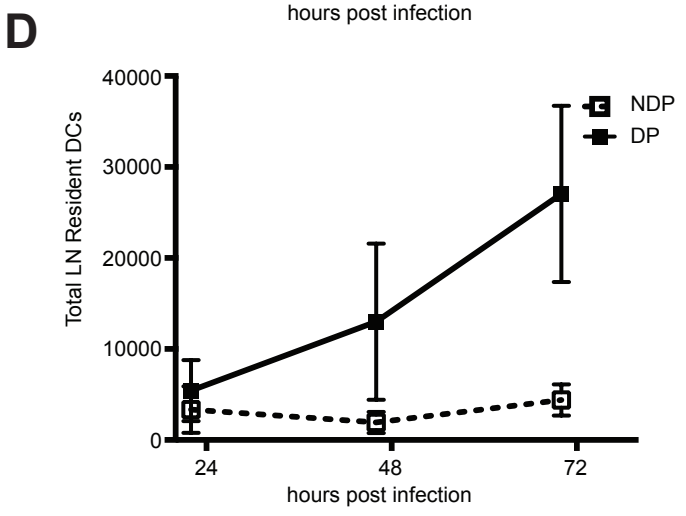
D
40000
30000
20000
10000
0
Total LN Resident DCs
24
48
72
hours post infection
NDP
DP

Figure 3: Kinetics of adaptive lymphocyte expansion following CPXV footpad infection.

Age and sex matched C57BL/6 mice were inoculated in the footpad with$1.5x10^6$ pfu/mouse and at indicated times, lymphocytes from the non-draining and draining LNs were isolated, stained and analyzed by flow cytometry. Total (A) T cells ($CD3^+CD19^-NK1.1^-$) and (B) B cells ($CD19^+CD3^-NK1.1^-$) were identified. Cell numbers were ascertained using trypan blue exclusion, then multiplied by the percentage of population found by FACS analysis. A graph depicting the average of 5 independent experiments is shown. Following extracellular staining, lymphocytes were fixed, permeablized and stained for Ki67. Total (C) T cells ($CD3^+CD19^-NK1.1^-Ki67^+$) and (D) B cells ($CD19^+CD3^-NK1.1^-Ki67^+$) were identified. A graph depicting the average of 3 independent experiments is shown.

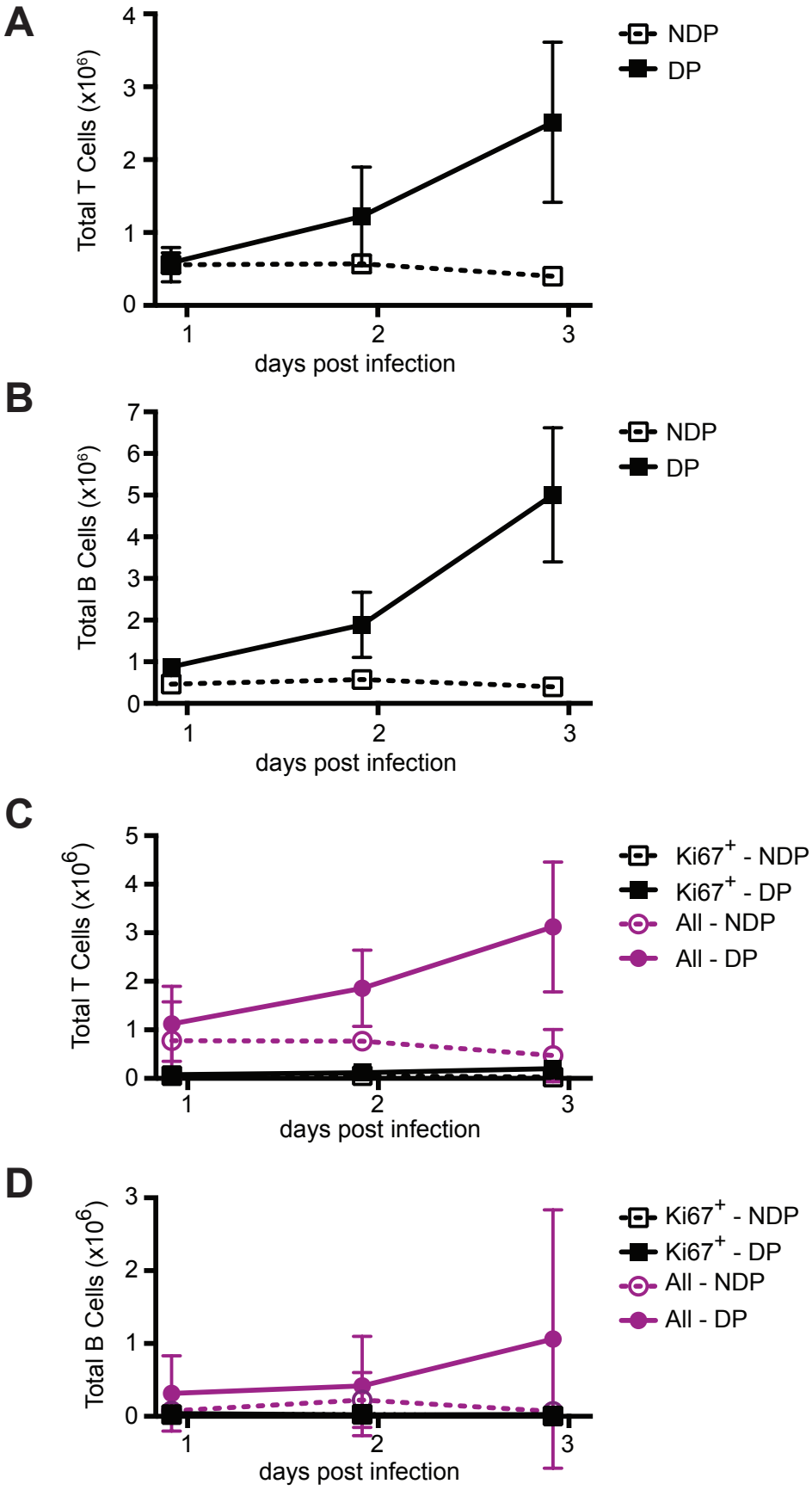
A
Total T Cells (x10^6)
days post infection
NDP
DP
B
Total B Cells (x10^6)
days post infection
NDP
DP
C
Total T Cells (x10^6)
days post infection
Ki67+ - NDP
Ki67+ - DP
All - NDP
All - DP
D
Total B Cells (x10^6)
days post infection
Ki67+ - NDP
Ki67+ - DP
All - NDP
All - DP

Figure 4: Kinetics of NK cell expansion following CPXV footpad infection.
Age and sex matched C57BL/6 mice were inoculated in the footpad with$1.5x10^6$ pfu/mouse and at indicated times, lymphocytes from the non-draining and draining LNs were isolated, stained and analyzed by flow cytometry. (A) Percent and (B) total NK cells ($NK1.1^+CD3^-CD19^-$) were identified. Cell numbers were ascertained using trypan blue exclusion, then multiplied by the percentage of population found by FACS analysis. The graphs depict average of n=6 independent experiments (18 hpi), n=14 independent experiments (1 dpi), n=3 independent experiments (36hpi), n=8 independent experiments (2 & 3 dpi), and n=2 independent experiments (6 & 9dpi). Paired Student's *t*-test: (*) = $p < 0.05$; (**) = $p < 0.005$; (***) = $p < 0.0005$.

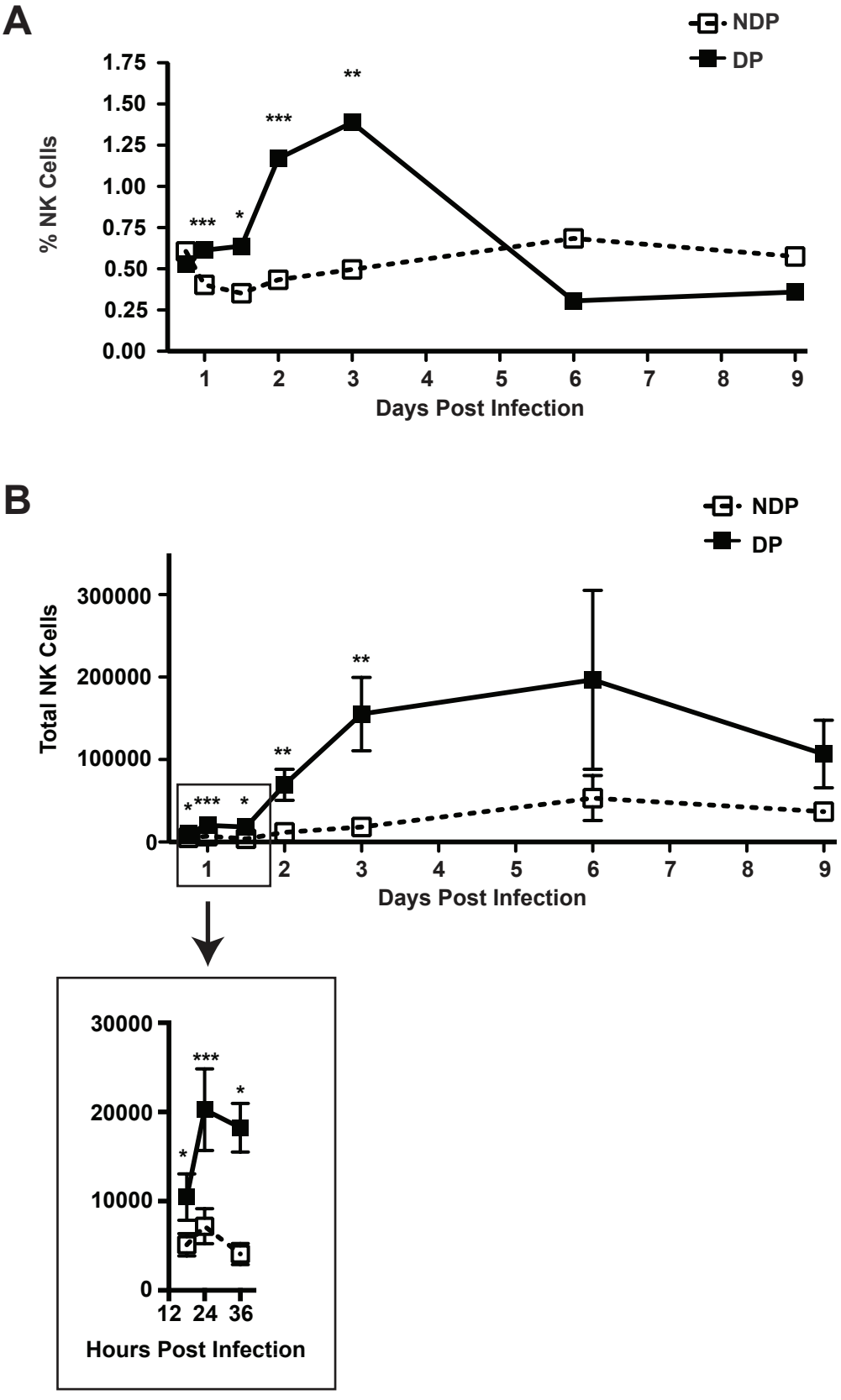
A
NDP
DP
% NK Cells
1.75
1.50
1.25
1.00
0.75
0.50
0.25
0.00
***
*
***
**
1
2
3
4
5
6
7
8
9
Days Post Infection
B
NDP
DP
Total NK Cells
300000
200000
100000
0
*
***
*
**
**
1
2
3
4
5
6
7
8
9
Days Post Infection
30000
20000
10000
0
*
***
*
12
24
36
Hours Post Infection

Figure 5: CPXV titers following footpad inoculation.
Age and sex matched C57BL/6 mice were infected with $1.5x10^6$ pfu of CPXV in the footpad and at indicated times, organs were removed and viral titers were assessed in the draining LN (A) and spleen (B) by plaque assay. Dotted lines indicate the limit of detection by the assay. Symbols indicate individual mice and the mean and SEM are depicted. N=4 to 5 mice/group were analyzed for each time point.

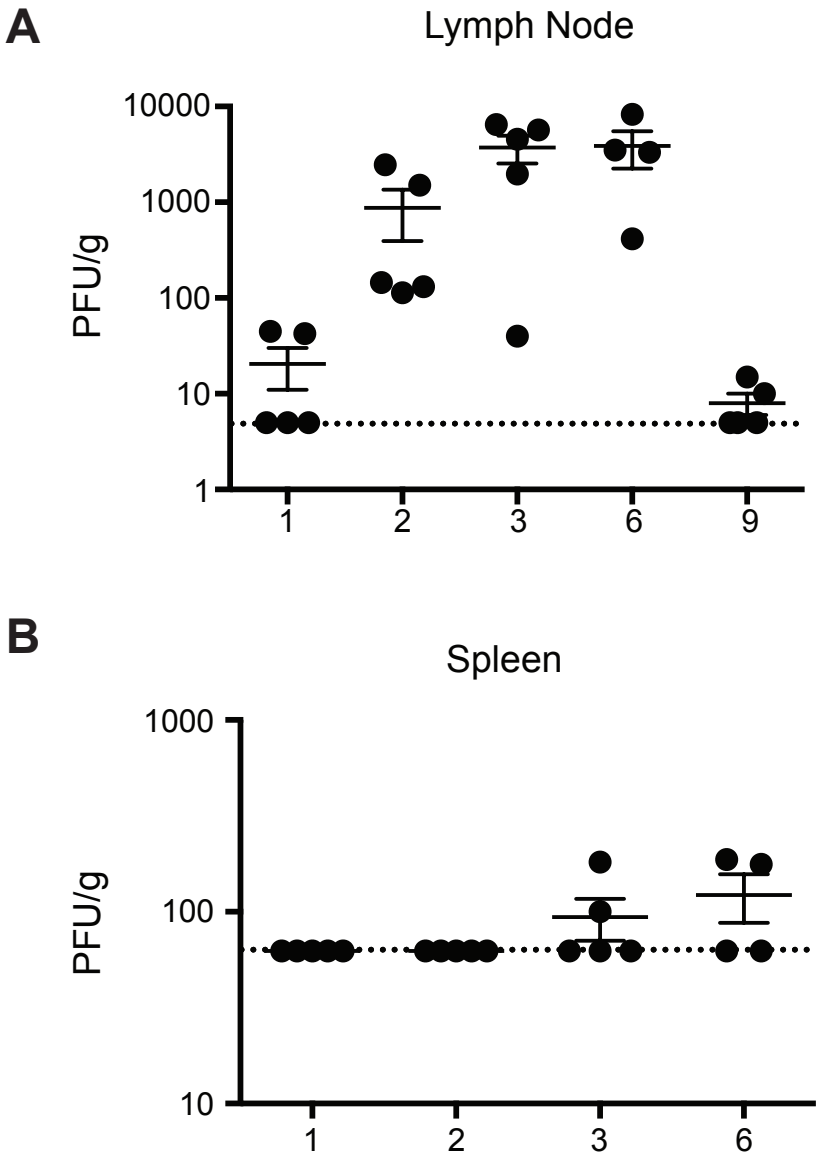
A
Lymph Node
10000
1000
100
10
1
PFU/g
1
2
3
6
9
B
Spleen
1000
100
10
PFU/g
1
2
3
6

Figure 6: Systemic NK cell depletion leads to increased viral burden in some but not all organs following early footpad inoculation.
Age and sex matched C57BL/6 mice were treated IP with 200μg control (mAR) or NK cell-depleting (anti-NK1.1, PK136) antibody 2 days prior to infection and 4 dpi. (A) NK cell depletion was assessed in the non-draining LN by staining lymphocytes and identifying NK cells ($NK1.1^{+}NKp46^{+}CD3^{-}CD19^{-}$) cells. Cell numbers were ascertained using trypan blue exclusion, then multiplied by the percentage of population found by FACS analysis. At indicated time points, organs were removed and viral titers were assessed by quantitative PCR in the (B) LN, (C) lungs, (D) spleens, (E) livers, (F) kidneys and (G) uterus and ovaries. CPXV copy number was normalized to β-actin copy numbers and then multiplying by 1000. Symbols indicate individual mice and lines indicate the mean. N=4 to 5 mice/group were analyzed for each time point. Data are representative of 2-3 independent experiments.

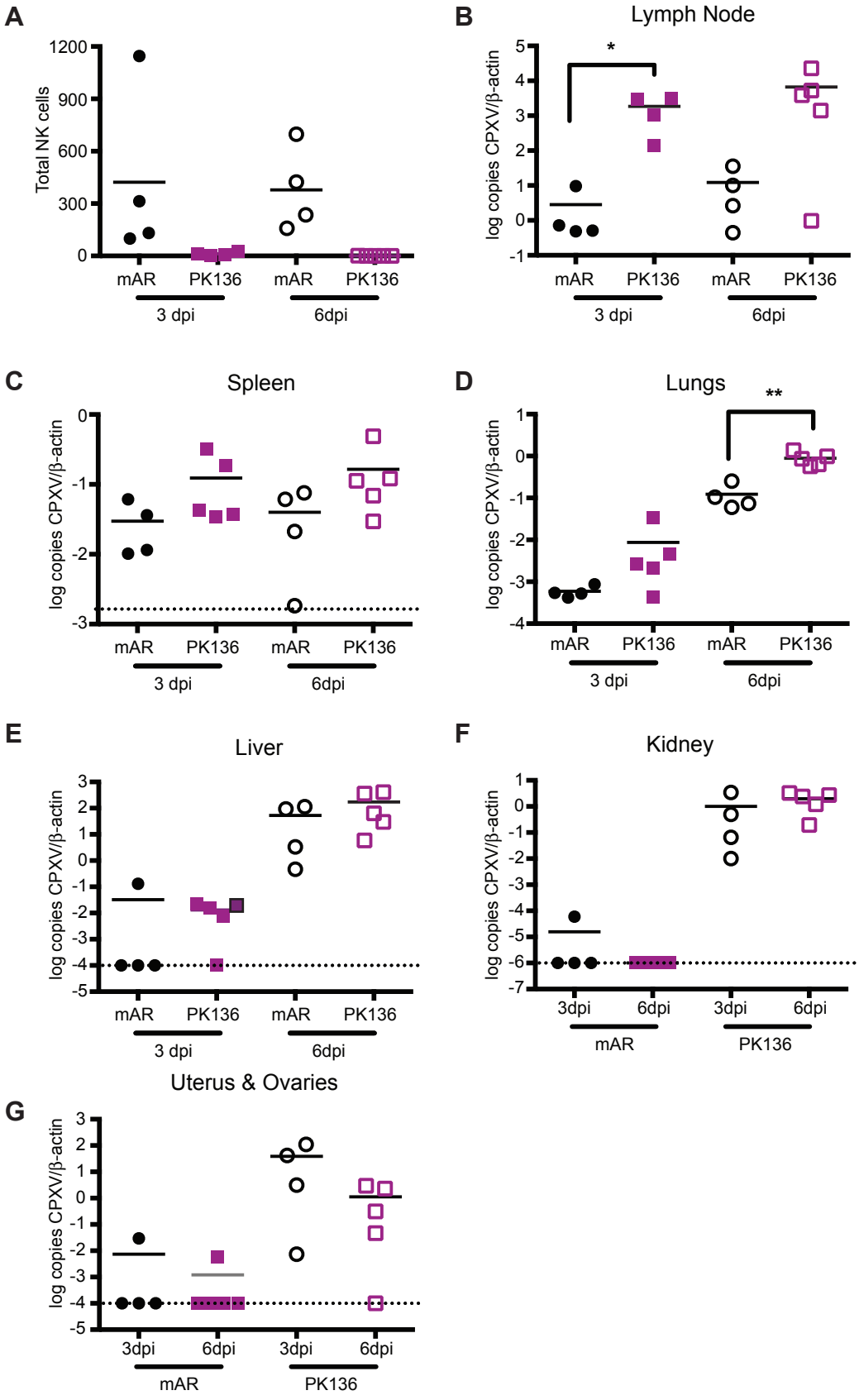
A
Total NK cells
1200
900
600
300
0
mAR
PK136
mAR
PK136
3 dpi
6dpi
B
Lymph Node
log copies CPXV/β-actin
*
5
4
3
2
1
0
-1
mAR
PK136
mAR
PK136
3 dpi
6dpi
C
Spleen
log copies CPXV/β-actin
0
-1
-2
-3
mAR
PK136
mAR
PK136
3 dpi
6dpi
D
Lungs
log copies CPXV/β-actin
**
1
0
-1
-2
-3
-4
mAR
PK136
mAR
PK136
3 dpi
6dpi
E
Liver
log copies CPXV/β-actin
3
2
1
0
-1
-2
-3
-4
-5
mAR
PK136
mAR
PK136
3 dpi
6dpi
F
Kidney
log copies CPXV/β-actin
1
0
-1
-2
-3
-4
-5
-6
-7
3dpi
6dpi
3dpi
6dpi
mAR
PK136
G
Uterus & Ovaries
log copies CPXV/β-actin
3
2
1
0
-1
-2
-3
-4
-5
3dpi
6dpi
3dpi
6dpi
mAR
PK136

Figure 7: CPXV persists longer in mice that were systemically depleted of NK cells. Age and sex matched C57BL/6 mice were injected IP with 200μg/mouse of control (mAR) or NK cell depleting (anti-NK1.1, PK136) antibody 2 days prior to infection, 4 and 10 dpi. At indicated time points, (A) LNs and (B) feet were isolated. DNA was generated and CPXV copy number was normalized to β-actin copy numbers and then multiplied by 1000. Symbols indicate individual mice and lines indicate the mean. N=4 to 5 mice/group were analyzed for each time point.

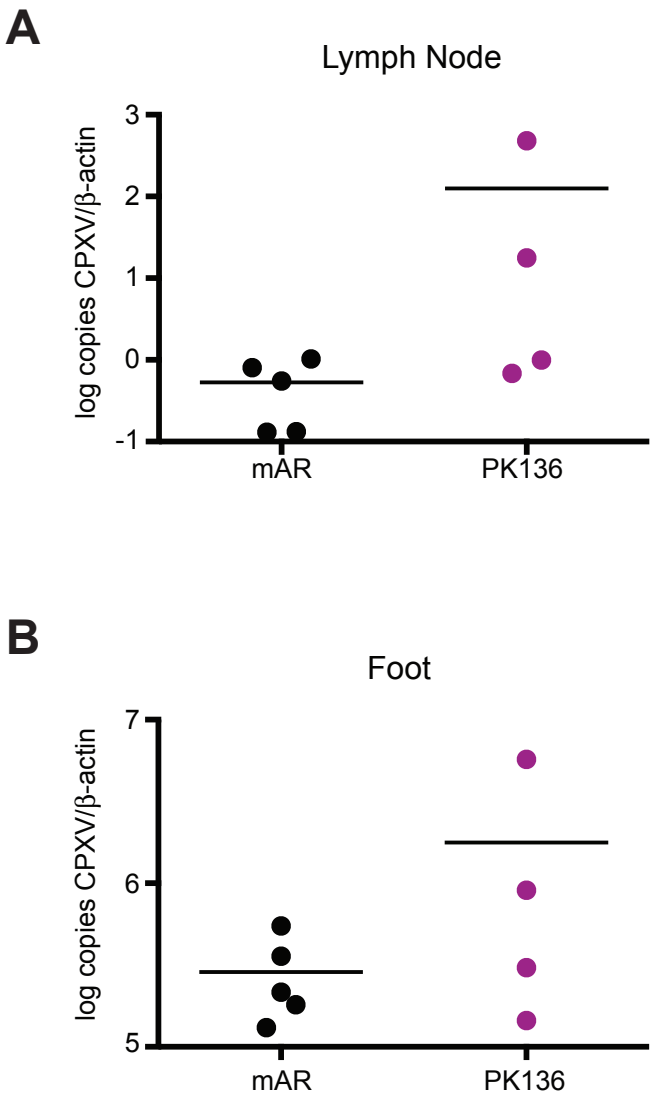
A
Lymph Node
log copies CPXV/β-actin
3
2
1
0
-1
mAR
PK136
B
Foot
log copies CPXV/β-actin
7
6
5
mAR
PK136

CHAPTER 4:

The Mechanism of NK Cell Recruitment

Following CPXV footpad infection we saw a dramatic and rapid expansion of NK cells in the draining LN. Murine NK cells are known to lack expression of CCR7, the homeostatic chemokine receptor responsible for T and B cell trafficking into secondary lymphoid organs in response to its ligands CCL19 and CCL21 (74). It is this lack of CCR7 expression that is thought to lead to the exclusion of murine NK cells from the LN. Therefore, it was of interest to determine the mechanism of NK cell population expansion following CPXV infection.

The Expansion of the NK Cell Population is Not Due to Proliferation

The rapid expansion of the NK cell population in the draining LN following CPXV could be the result of either *in situ* proliferation or the recruitment of NK cells from other areas. To determine if NK cells were undergoing proliferation, we isolated NK cells from the draining LN and co-stained them for Ki67, a cell cycle marker. While some NK cells isolated from the draining LN did stain positively for Ki67, the majority of NK cells did not express Ki67 (Figure 8). These data indicate that NK cell population expansion is mediated by active recruitment of NK cells to the draining LN following CPXV infection.

NK Cell Subset Surface Staining Profiles

There are several subsets of NK cells residing in different organs that have been characterized (101-103). Research has predominantly been performed with NK cells isolated from the spleen as it contains a large population of NK cells that is easy to isolate. Several groups, including our lab, have also characterized a rare alternatively matured subset of thymic NK cells. To determine if the expanded NK cell population

resulting from CPXV infection resembled either of these subsets, we analyzed NK cells isolated from the draining LN, non-draining LN, spleen and thymus for markers that can differentiate these populations.

Splenic NK cells have high expression of Mac-1 (CD11b), Ly49 family receptors, L-selectin (CD62L), DX5 (CD49b), CD94, and NKG2D (CX5) (102). NK cells isolated from the draining lymph node expressed identical surface levels of splenic markers as NK cells isolated from the spleen (Figure 9A-F). In contrast, NK cells isolated from the thymus expressed lower levels of splenic markers. Thymic NK cells have been shown to highly express the IL-7 receptor α (IL7Rα, CD127) and αE integrin (CD103) (102). When NK cells from the draining LN were examined, they did not express thymic surface markers (Figure 10A, 10B). Again, NK cells isolated from the spleen and the draining LN had identical expression profiles for these thymic surface markers. Additionally, when we examined the expression of splenic and thymic markers on NK cells isolated from the non-draining LN, we found intermediate expression of Mac-1, L-selectin and IL-7Rα. Taken together, these data show that NK cells expressing splenic markers are recruited to the draining LN.

NK Cell Expansion is Pertussis Toxin Sensitive

Given the rapid kinetics of the NK cell population increase, the minimal number of replicating NK cells, and the splenic surface marker profile of the NK cells isolated from the draining LN, we hypothesized that NK cells were being recruited to the draining LN. We isolated splenocytes from congenic mice and pre-treated them *in vitro* for 2 hours with either PBS or pertussis toxin. Following pre-treatment, the cells were washed extensively, labeled with CFSE and mixed together before adoptive transfer into

congenic C57BL/6 mice. We found that donor splenic NK cells treated with PBS specifically increased in the draining LN following adoptive transfer and CPXV infection (Figure 11A, 11B). The increase in the transferred PBS-treated NK cells was similar to the kinetics of host NK cell increase following CPXV infection, supporting the hypothesis that splenic NK cells are being recruited to the draining LN following CPXV infection.

These findings led us to consider chemokine receptor-dependent NK cell recruitment into the draining LN. As with other GPCRs, chemokine receptors signal via G proteins and these signals are blocked by pertussis toxin (70, 71). We thus used pertussis toxin to test whether chemokine receptors were important for the NK cell increase in the draining LN. Pertussis toxin pre-treated splenic NK cells were never found in the draining LN at any time point following CPXV infection (Figure 11B). Although it is difficult to fully control for off-target effects of petussis toxin treatment, these data further substantiate the possibility that splenic NK cells are being recruited to the draining LN following CPXV infection and additionally suggest that NK cell recruitment occurs via chemokine receptors.

CPXV Infection Specifically Up-regulates Inflammatory Chemokines in the Draining LN

As the data suggested a role for chemokines and chemokine receptor-mediated recruitment of NK cells following CPXV infection, we next determined specifically which of these were required. To examine chemokine expression in the draining LN, we assessed transcript levels over time following CPXV infection by use of a comprehensive bead-based array. In both draining and non-draining LNs over time, we examined 33

transcripts simultaneously: *Ccl1, Ccl2, Ccl3, Ccl4, Ccl5, Ccl6, Ccl7, Ccl8, Ccl9, Ccl11, Ccl12, Ccl17, Ccl19, Ccl20, Ccl21, Ccl22, Ccl24, Ccl25, Ccl27, Ccl28, Cxcl1, Cxcl2, Cxcl3, Cxcl5, Cxcl9, Cxcl10, Cxcl11, Cxcl12, Cxcl13, Cxcl14, Cxcl15, Cxcl16* and *Xcl1*.

Our analysis of these data was then informed by gene expression microarray data from a previously published study (59) and confirmed by our laboratory, indicating that NK cells express transcripts for *Ccr2, Ccr5, Cx3cr1, Cxcr3, Cxcr4* and *Cxcr6*. We found that transcripts of ligands for CCR2 and CCR5, including *Ccl2, 3,* and *7*, were up-regulated approximately 3- to 9-fold relative to the non-draining LN transcripts (Figure 12). Additionally, the ligands for CXCR3, namely IFN-γ inducible transcripts *Cxcl9, 10* and *11*, were up-regulated from 5 to 19-fold relative to transcript levels in the non-draining LN. While transcripts for *Cxcl11* were the most highly induced, CXCL11 protein is not expressed in C57BL/6 mice due to a point mutation (104). Finally, we did not find an increase in ligands for CXCR4 and CXCR6 (CXCL12 and CXCL16, respectively). Nonetheless, CPXV infection induces up-regulation of chemokine ligands for chemokine receptors expressed on NK cells.

CXCR3 but not CCR2 or CCR5 Is Required for Full NK Cell Recruitment

Our analysis of chemokine up-regulation following CPXV infection and NK cell expression of specific chemokine receptors suggested selective involvement of CCR2, CCR5 or CXCR3 in the recruitment of NK cells. To further analyze these possibilities, we examined NK cell recruitment in chemokine receptor-deficient mice. Despite up-regulation of transcripts for *Ccl2, Ccl3* and *Ccl7*, there were little to no defects in recruitment of NK cells in mice lacking either CCR2 or CCR5 (Figure 13A, 13B). Thus,

CCR2 and CCR5 individually do not contribute to NK cell recruitment following CPXV footpad infection.

We next studied NK cell trafficking to the draining LN in CXCR3-deficient mice. In these mice, we found that there was a substantial defect at 3 dpi, resulting in a marked decrease in trafficking of NK cells following CPXV infection, although NK cell recruitment at earlier times was relatively unaffected (Figure 13C). In order to determine whether these CXCR3-dependent trafficking defects were NK cell intrinsic or extrinsic, we adoptively transferred a mixture of enriched splenic NK cells from wild-type and CXCR3-deficient mice into congenic C57BL/6 mice (Figure 13D). We found that the fold change of recruited donor-derived NK cells for the adoptively transferred CXCR3-deficient NK cells was lower than for the adoptively transferred wild-type NK cells, especially at later time points as observed directly in the CXCR3-deficient mice (Figure 14C). These results indicate that NK cells intrinsically require CXCR3 expression for maximal recruitment.

Discussion

Two mechanisms could explain NK cell expansion in the draining LN following CPXV infection: either *in situ* proliferation of rare murine LN NK cells or recruitment from the blood and other organs. A specific cell cycle marker indicated that while some NK cells in the draining LN were proliferating, the majority of the expanding NK cell population were not. In support of these data, NK cells in the draining LN expressed splenic markers and recruitment of transferred splenic NK cells was pertussis toxin sensitive. Comprehensive analysis of chemokine receptor expression on NK cells in combination with chemokine expression following infection in the draining LN focused

our studies on CCR2, CCR5 and CXCR3. Although transcripts for ligands of these receptors were up-regulated, only CXCR3 was required on the NK cell for full recruitment following CPXV infection.

Productive interactions between NK cells and their targets require recruitment of NK cells to the relevant site. In non-infectious settings, several studies have implicated the requirement for CXCR3-mediated NK cell trafficking including following corneal epithelial injury (105), implantation of tumor cells that endogenously express IFN-γ (106), and LPS-matured dendritic cell footpad injection (107). In contrast, during parasitic and viral infections, NK cells have differential requirements for chemokine receptors, generally not including CXCR3. Following intratracheal inoculation of neutropenic mice with *Aspergillus fumigatus*, CCR2 is required (75) whereas CCR5 is required in *Toxoplasma gondii* (76) or Herpes Simplex Virus 2 (HSV2) (108) infections, with higher pathogen burden in CCR5-deficient mice. However, *Aspergillus* and HSV2 are not natural pathogens of rodents. For protection against MCMV, a natural pathogen of mice, recruitment of NK cells to the liver is mediated through CCR2 (68, 77). CXCR3 and CCR5 are also important for NK cell trafficking from the red pulp to the T cell zone in the spleen following injection of polyI:C and MCMV infection (109). Finally, CXCR6 is required for memory NK cells in the liver that respond to contact-mediated hypersensitivity or virus-like particles (79). Thus, several chemokine receptors are involved in recruitment of NK cells though little is known about NK cell recruitment to the draining LN in the context of natural rodent pathogens.

In contrast to other studies using other pathogens and NK cell recruitment to other organs (68, 75-77, 108), we found no role for CCR2 or CCR5 individually in recruitment of NK cells to the draining LN following CPXV inoculation. However, it is still possible

that they function redundantly in the individually deficient mice as CCR2 and CCR5 share several of the same ligands (70). To formally determine if CCR2 and CCR5 are required, a mouse lacking both CCR2 and CCR5 must be generated and tested. This would likely require the production of a single targeting construct containing deletions of both CCR2 and CCR5 since their genes are located within about 15 kb of each other (genome.ucsc.edu), making it unlikely that a double knockout can be readily generated by mating the CCR2- and CCR5-deficient mice. Additionally, since we analyzed chemokine transcript levels, not protein levels, is possible that actual chemokine proteins were not up-regulated following infection. Further complicating interpretation experiments in chemokine receptor deficient mice, CPXV encodes numerous chemokine binding proteins which may interfere with CCR2 or CCR5 function.

On the other hand, we found that CXCR3 was intrinsically required for full recruitment following CPXV infection. Expression of CXCR3 on NK cells has been shown to be important for the recruitment of NK cells to tumor sites (106) and to the draining LN following deliberate LPS-matured dendritic cell footpad injection (107). CXCR3 also plays a role in re-localization of NK cells from the red pulp to the T cell zone of the spleen during MCMV infection (109), another rodent specific virus. Therefore our data is in agreement with previously published data demonstrating the importance of CXCR3 in the recruitment of NK cells in the context of infection with natural rodent pathogens. These data suggest that CXCR3 mediates NK cell trafficking under both non-infectious and infectious inflammatory conditions.

Defective NK cell recruitment in CXCR3-deficient mice is most evident at 3 dpi when the largest increase in NK cells normally occurs. Earlier time points are less affected, suggesting that there is at least one other mechanism for NK cell recruitment

that is independent of CXCR3. There are several hypotheses that might explain this CXCR3-independent NK cell recruitment. One possibility is that CX3CL1, the ligand for CX3CR1, plays a role in NK cell recruitment. However, expression of CX3CL1 was not examined in the transcriptional chemokine expression array so the need for this receptor remains unknown. If expression of CX3CL1 was found in the draining LN relative to the non-draining LN, mice deficient for CX3CR1 are available and NK cell recruitment could easily be studied in them. Another possible mediator of recruitment may be up-regulation of another chemokine receptor on NK cells during active infection. We did not evaluate this possibility because of the low numbers of NK cells in the draining LN and the procedural concerns regarding FACS sorting of CPXV-infected samples. Taken together, these data suggest that in addition to CXCR3, at least one other chemokine and chemokine receptor pair may function to recruit NK cells to the draining LN.

Alternately, it is also possible that NK cells are being recruited in a non-chemokine receptor dependent manner. Other chemotactic compounds that are induced by inflammation also cause NK cells to traffic including lysophosphatidic acid (LPA), complement component C5a, *N*-formyl-methionyl-leucyl-phenylalanine and leukotrienes (74). LPA is involved in a variety of signaling pathways and interacts with GPCRs, conferring pertussis toxin sensitivity, but its role following any pathogenic infection has not been shown (110). In contrast, poxviruses are known to encode a number of complement control proteins that have been extensively studied using ECTV or VV but not CPXV (23, 24, 111). Meanwhile, the importance of leukotrienes for NK cell recruitment could be quite complicated. Orthopoxviruses, including CPXV, have an obligate requirement for arachidonic acid metabolites for replication both *in vitro* and *in vivo* (112, 113). However, arachodonic acid can be used as a precursor for pro-

inflammatory signaling molecules, including leukotrienes. To control the inflammatory response, CPXV encodes p38, which inhibits the synthesis of a specific intermediate that can be used in pro-inflammatory mediator synthesis. It is therefore possible that these alternate mediators of recruitment could also play a role in NK cell recruitment following CPXV infection.

NK cells also express sphingosine-1-phosophate 5, another GPCR, which senses a high concentration of sphingosine-1-phosphate in the blood. In mice deficient in $S1P_5$, it has been demonstrated that there is a decrease in the number of NK cells in the blood, lungs and spleen and increase in the LN and bone marrow, suggesting that it plays a role in NK cell egress (114). Following infection, it is possible that $S1P_5$ becomes depressed in the blood to allow for lymphocyte retention, including NK cells, in secondary lymphoid organs to prime an immune response. Thus it is possible that CXCR3-independent NK cell recruitment does not require another chemokine receptor, but does require another GPCR or pro-inflammatory mediator.

Here we demonstrate that NK cell expansion was not due to active replication of rare LN NK cells but was due to recruitment of splenic NK cells. This recruitment was chemokine receptor-dependent and we identified the NK cell intrinsic requirement for CXCR3. Deficiency of CXCR3 alone, however, does not abrogate the recruitment phenotype, suggesting requirement of additional chemokine receptors or other inflammatory mediators.

Figure 8: Expansion of the NK cell population cannot fully be explained by *in situ* proliferation.
Age and sex matched C57BL/6 mice were infected as before and at indicated time points, cells from the draining and non-draining LN were isolated and stained. Following extracellular staining, cells were fixed, permeablized and intracellularly stained for Ki67. Total Ki67 expressing NK cells were identified by gating on NK cells ($NK1.1^{+}CD3^{-}CD19^{-}$) then looking for those that expressed Ki67. Cell numbers were ascertained using trypan blue exclusion, then multiplied by the percentage of population found by FACS analysis. The graph depicts the average of 3 independent experiments.

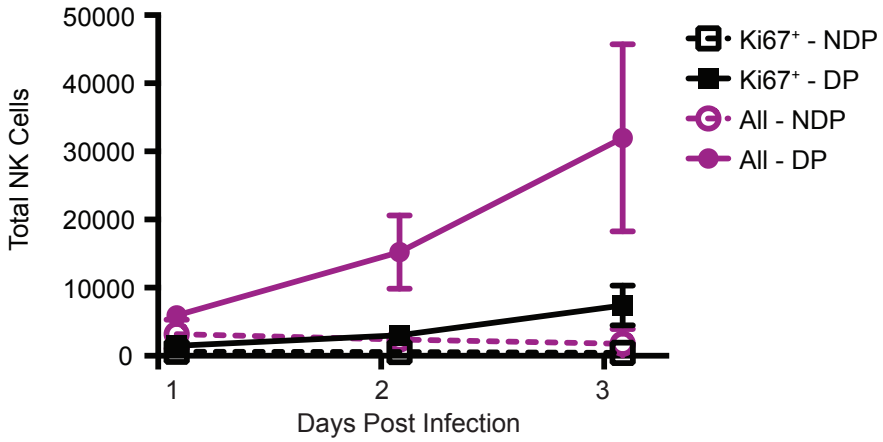
50000
40000
30000
20000
10000
0
Total NK Cells
1
2
3
Days Post Infection
Ki67+ - NDP
Ki67+ - DP
All - NDP
All - DP

Figure 9: NK cells isolated from the draining LN following CPXV infection phenocopy surface staining of splenically derived NK cells.
Age and sex matched C57BL/6 mice were infected as before and lymphocytes from the spleen, thymus, draining and non-draining LN were isolated 1 dpi and surface stained. Following identification of NK cells ($NK1.1^{+}CD3^{-}CD19^{-}$), expression of (A) Mac-1 (CD11b), (B) pan-Ly49 family receptors (Ly49ADCIFH), (C) L-selectin (CD62L), (D) DX5 (CX5), (E) CD94 and (F) NKG2D was determined. A representative result of 2 independent experiments is shown. Surface staining remained the same when observing NK cells isolated from these organs at 2 and 3 dpi.

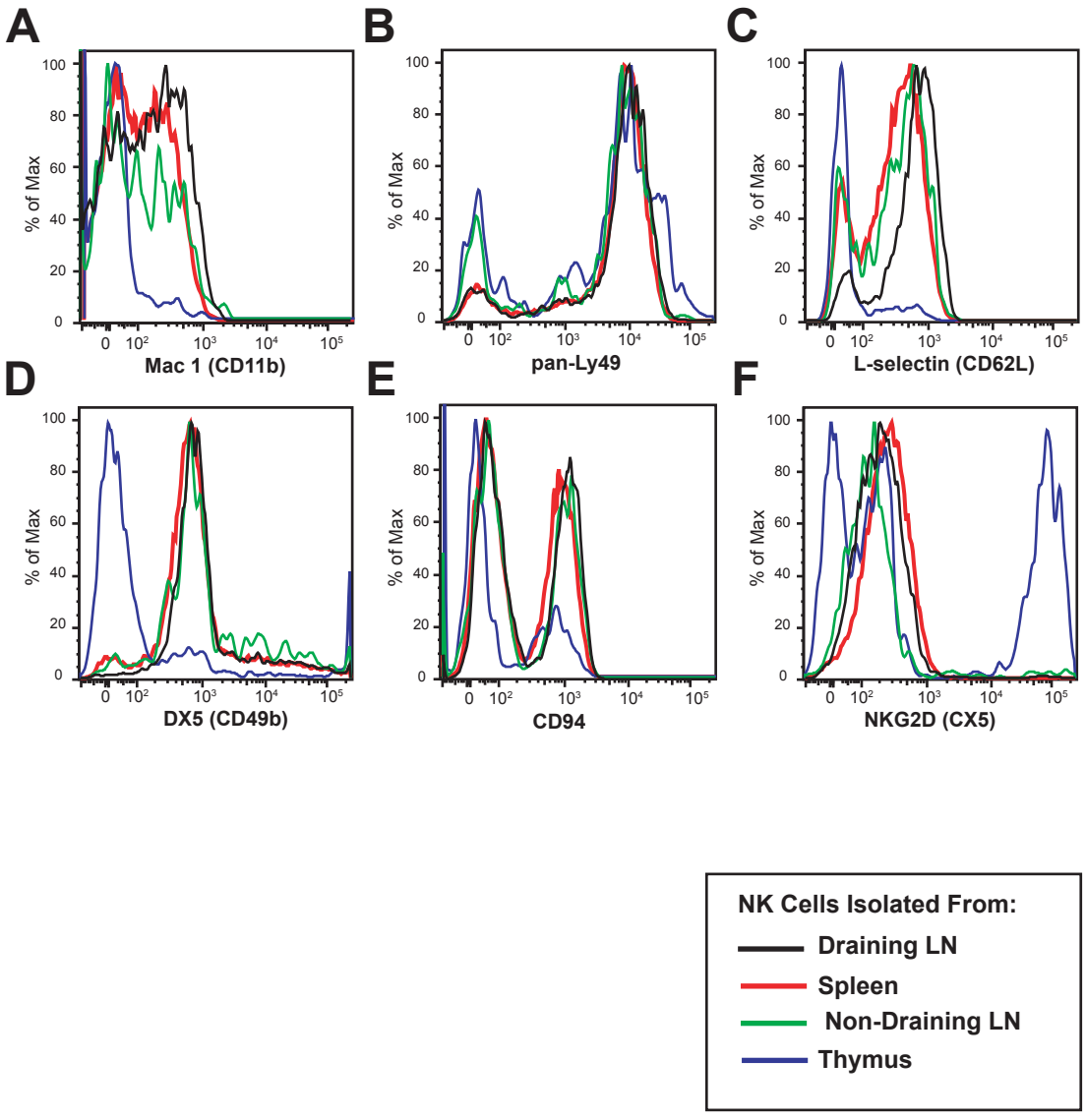
A
B
C
D
E
F
% of Max
Mac 1 (CD11b)
pan-Ly49
L-selectin (CD62L)
DX5 (CD49b)
CD94
NKG2D (CX5)
NK Cells Isolated From:
Draining LN
Spleen
Non-Draining LN
Thymus

Figure 10: Draining LN NK cells do not express markers of thymic NK cells.
Age and sex matched C57BL/6 mice were infected as before and lymphocytes from the spleen, thymus, draining and non-draining LN were isolated 1 dpi and surface stained. Following identification of NK cells ($NK1.1^{+}CD3^{-}CD19^{-}$), expression of (A) IL-7Rα (CD127) and (B) integrin αE (CD103) was determined. Representative results of 2 independent experiments are shown. Surface staining remained the same when observing NK cells isolated from these organs at 2 and 3 dpi.

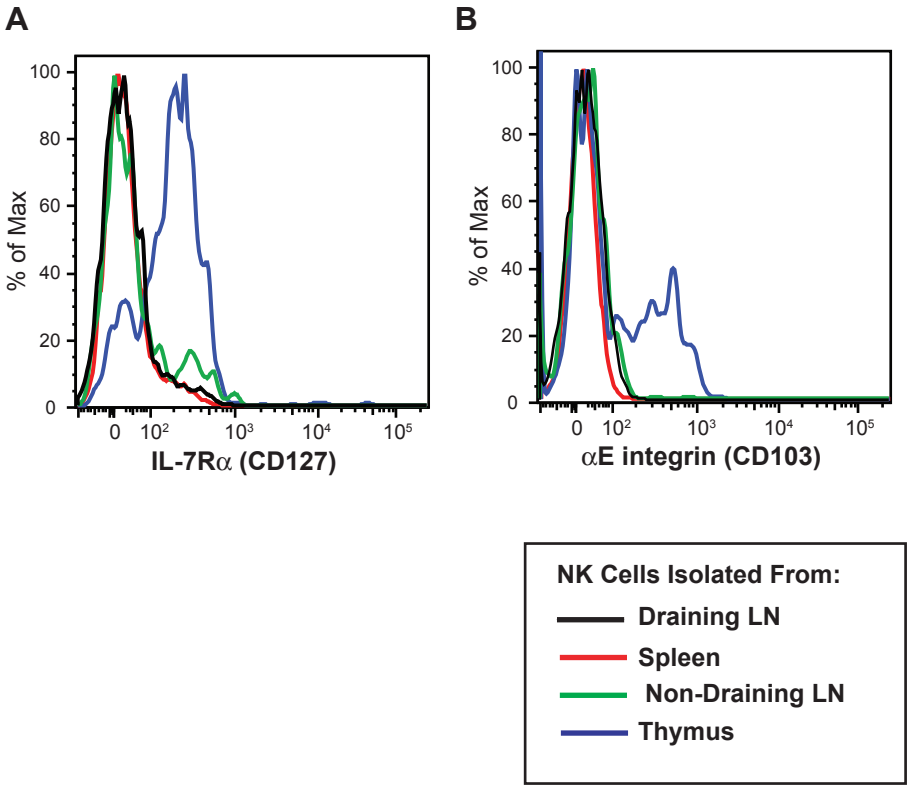
A
B
100
80
60
40
20
0
% of Max
0
10²
10³
10⁴
10⁵
IL-7Rα (CD127)
αE integrin (CD103)
NK Cells Isolated From:
Draining LN
Spleen
Non-Draining LN
Thymus

Figure 11: NK expansion in the draining LN is pertussis toxin sensitive following CPXV infection.
Splenocytes isolated from congenic C57BL/6 (CD45.2) and B6.LY5.2 (CD45.1) mice were pre-treated *in vivo* with PBS or pertussis toxin for 2 hours at 37°C, 5% CO_2 before being washed, CFSE labeled, mixed and co-injected IV into C57BL/6 mice. Immediately following adoptive transfer, the mice were infected with $1.5x10^6$ pfu of CPXV in the footpad. At the indicated time points, LNs were harvested and NK cells ($NK1.1^+CD3^-CD19^-$) were identified. Host NK cell recruitment ($CFSE^-$) (A) or donor NK cell recruitment ($CFSE^+$) (B) is shown over time. Data are representative of 2 independent experiments.

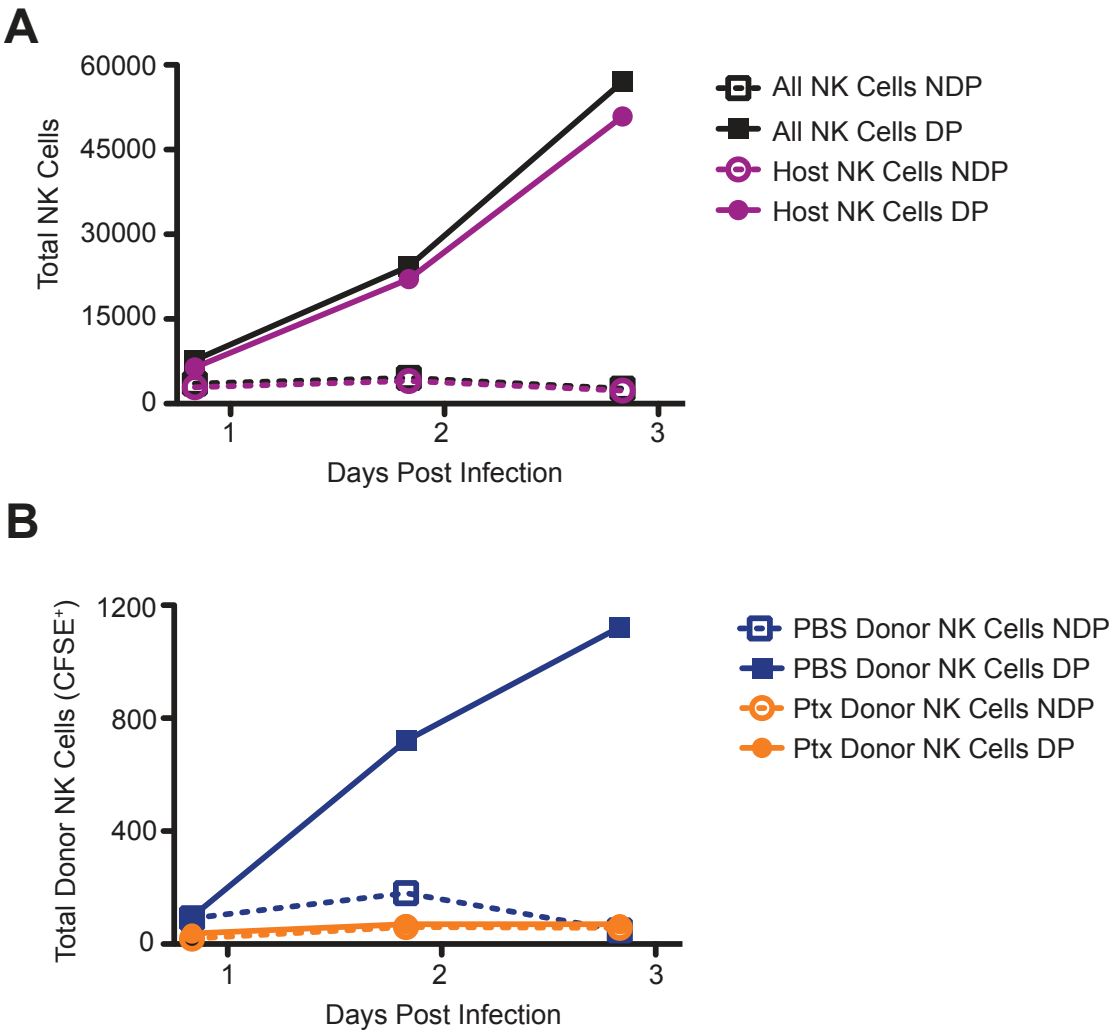
A
60000
45000
30000
15000
0
Total NK Cells
1
2
3
Days Post Infection
All NK Cells NDP
All NK Cells DP
Host NK Cells NDP
Host NK Cells DP
B
1200
800
400
0
Total Donor NK Cells (CFSE+)
1
2
3
Days Post Infection
PBS Donor NK Cells NDP
PBS Donor NK Cells DP
Ptx Donor NK Cells NDP
Ptx Donor NK Cells DP

Figure 12: Inflammatory chemokine transcripts are up-regulated following CPXV infection.
RNA transcript levels were assessed in age and sex matched C57BL/6 mice infected with $1.5x10^6$ pfu of CPXV in the footpad at indicated time points by multiplex gene expression analysis. LNs from 3 independently infected mice were isolated and lysates from either the non-draining or draining LN were generated, run in triplicate, and chemokine transcripts normalized to the control *Hprt1* transcript for each sample. The fold change indicated in each square depicts the average transcript level in the draining LN relative to the non-draining LN.

	1 dpi	2 dpi	3 dpi
Cxcl1 (Groα)	3.21	1.95	2.26
Cxcl2 (Groβ)	1.02	1.68	2.56
Cxcl3 (Groγ)	0.41	0.34	0.50
Cxcl5 (ENA-78)	1.39	1.00	2.44
Cxcl9 (Mig)	1.91	6.95	5.07
Cxcl10 (IP-10)	7.57	10.11	4.55
Cxcl11 (I-TAC)	2.06	7.16	19.57
Cxcl12 (SDF-1α/β)	0.85	0.24	0.25
Cxcl13 (BLC/BCA-1)	1.25	0.68	0.57
Cxcl14 (BRAK/bolekine)	1.28	2.85	1.51
Cxcl15 (Lungkine/WECHE)	0.20	1.67	2.47
Cxcl16 (None)	1.06	0.72	0.61
Xcl1 (Lymphotactin)	2.61	1.75	1.92

	1 dpi	2 dpi	3 dpi
Ccl1 (I-309)	1.58	0.52	0.45
Ccl2 (MCP-1)	5.62	6.57	8.03
Ccl3 (Mip-1a)	6.13	4.31	5.58
Ccl4 (Mip-1b)	9.49	6.33	6.07
Ccl5 (RANTES)	0.88	0.62	0.42
Ccl6 (C10/MRP1)	3.81	2.72	2.22
Ccl7 (MCP-3)	5.03	3.86	3.33
Ccl8 (MCP-2)	0.91	0.55	0.36
Ccl9 (MRP-2/MIP-1γ)	3.52	2.17	2.06
Ccl11 (Eotaxin)	1.41	0.89	0.77
Ccl12 (MCP-5)	3.28	1.41	1.58
Ccl17 (TARC)	0.34	0.24	0.17
Ccl19 (MIP3β/ELC)	1.23	0.72	0.53
Ccl20 (MIP-3α/LARC)	1.58	9.75	7.40
Ccl21a (6CKine/SLC)	1.19	0.46	0.36
Ccl22 (MDC)	0.50	0.31	0.21
Ccl24 (Eotaxin-2/MPIF-2)	1.06	12.98	10.68
Ccl25 (TECK)	0.82	0.71	0.84
Ccl27a (CTACK)	0.60	0.49	0.51
Ccl28 (MEC)	0.29	0.48	0.91

Figure 13: NK cell recruitment occurs in the absence of CCR2 and CCR5 but intrinsically requires CXCR3 expression following CPXV infection.
Age and sex matched C57BL/6 and (A) CCR2-deficient, (B) CCR5-deficient or (C) CXCR3-deficient mice were infected with $1.5x10^6$ pfu of CPXV. At indicated time points, lymphocytes from the non-draining and draining LNs were isolated, stained and analyzed by flow cytometry. Total NK cells ($NK1.1^+CD3^-CD19^-$) were identified. The graphs are the average of 3 independent experiments. (D) B5.LY5.2 (CD45.1) and $CXCR3^{-/-}$ (CD45.2) splenocytes were isolated and enriched by negative selection before being CFSE labeled, mixed and co-transferred IV into C57BL/6 mice. One day after transfer, mice were infected as before and NK cell populations were examined at indicated time points. To analyze the recruitment in this system, the total number of recruited wild-type or chemokine deficient NK cells at 2 and 3 dpi were compared relative to the initial time point at 1 dpi. A representative result of 3 independent experiments is shown.

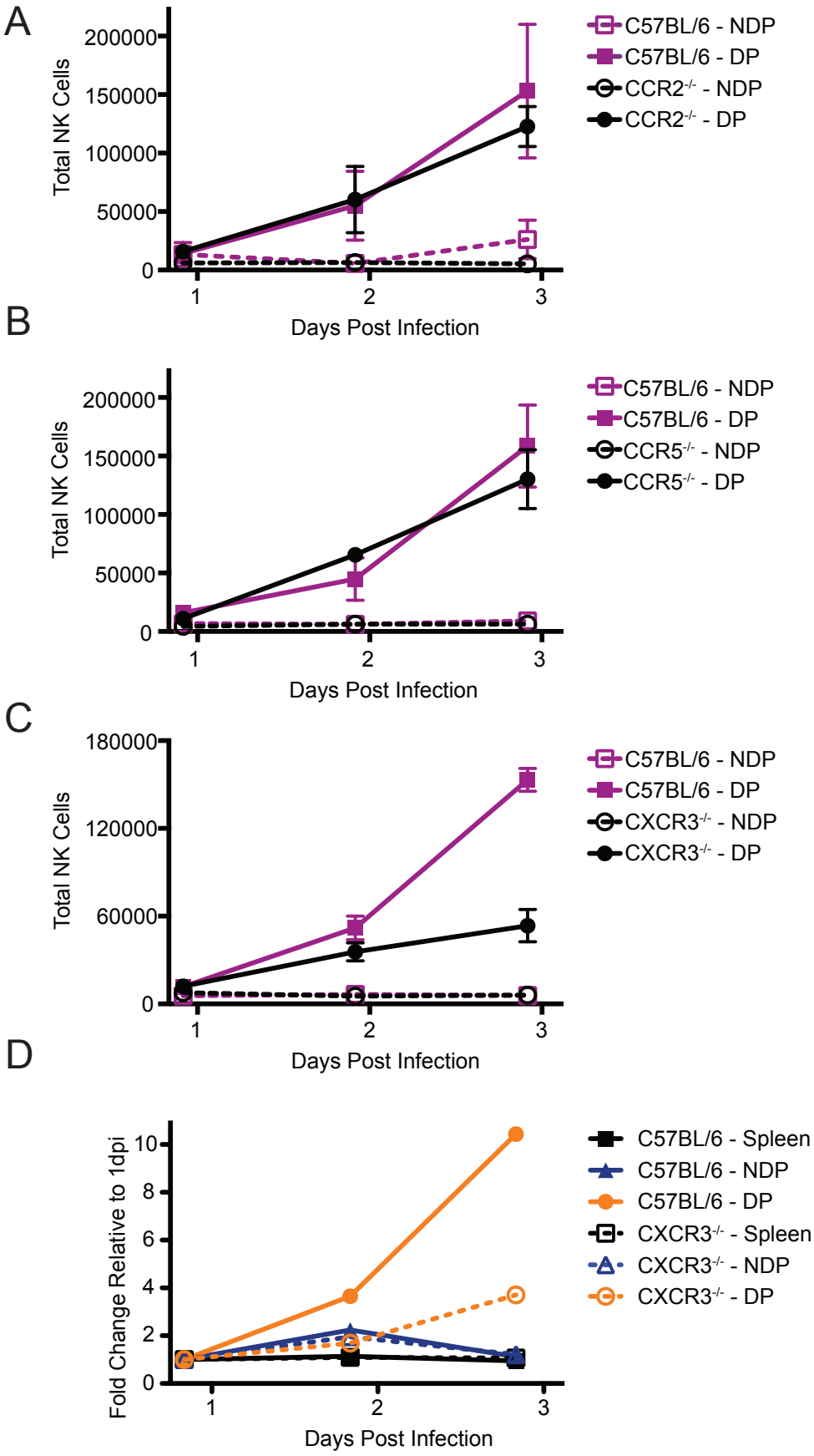
A
Total NK Cells
200000
150000
100000
50000
0
1
2
3
Days Post Infection
C57BL/6 - NDP
C57BL/6 - DP
CCR2-/- - NDP
CCR2-/- - DP
B
Total NK Cells
200000
150000
100000
50000
0
1
2
3
Days Post Infection
C57BL/6 - NDP
C57BL/6 - DP
CCR5-/- - NDP
CCR5-/- - DP
C
Total NK Cells
180000
120000
60000
0
1
2
3
Days Post Infection
C57BL/6 - NDP
C57BL/6 - DP
CXCR3-/- - NDP
CXCR3-/- - DP
D
Fold Change Relative to 1dpi
10
8
6
4
2
0
1
2
3
Days Post Infection
C57BL/6 - Spleen
C57BL/6 - NDP
C57BL/6 - DP
CXCR3-/- - Spleen
CXCR3-/- - NDP
CXCR3-/- - DP

CHAPTER 5:

Up-stream Requirements for NK Cell Recruitment and Viral Burden

NK cell recruitment to the draining LN is mediated through chemokine induction in the draining LN and at least one chemokine receptor on the NK cell. The induction of inflammatory chemokines indicated that there is viral recognition in the draining LN. This chapter explores the upstream requirements for NK cell recruitment, including the cells required and the signaling pathway leading to inflammatory chemokine induction.

IFN-γ is Required for NK Cell Recruitment

As discussed previously, ligands for CXCR3, including CXCL9 and CXCL10, are induced by IFN-γ. In order to further investigate the role that IFN-γ was playing upstream of NK cell recruitment, we examined mice that were deficient for IFN-γ receptor 1 (IFNγR1). These mice still produce IFN-γ but are unable to respond to its stimulus. Following CPXV infection, we observed a lack of recruitment of NK cells at both 2 and 3 dpi (Figure 14A). In fact, at these time points, levels of NK cell recruitment were lower in IFNγR1-deficient mice than in CXCR3-deficient mice, suggesting that other factors important for NK cell recruitment are also induced by IFN-γ.

Another method we employed to demonstrate the importance of IFN-γ was to observe NK cell recruitment in C57BL/6 mice given an injection of control or IFN-γ neutralizing antibody two days prior to infection. The lack of NK cell recruitment at 3 dpi in mice treated with neutralizing antibody recapitulated the results seen in IFNγR1-deficient mice (Figure 14B). In mice that received control antibody, the NK cell recruitment observed was similar to NK cell recruitment in CPXV infected unmanipulated mice. Interestingly, there did not appear to be a defect at 2 dpi. This could be explained by incomplete inhibition of IFN- γ signaling by neutralizing antibody or insufficient localization to the draining LN until later time points.

Supporting our hypothesis that IFN-γ is upstream of CXCR3 signaling required for NK cell recruitment, *Cxcl9* and *Cxcl10* transcripts were not induced in mice that were pre-treated with IFN-γ neutralizing antibody (Figure 14C, 14D). Meanwhile, CPXV infection in control antibody treated mice induced high levels of *Cxcl9* and *Cxcl10* transcripts at 3 dpi. The inhibition of *Cxcl9* and *Cxcl10* transcript induction was selective, as expression of control transcripts for homeostatic trafficking chemokines *Ccl19* and *Ccl21* showed little to no difference between control and IFN-γ neutralizing antibody treatment (Figure 14E, 14F). Taken together, these data indicated that IFN-γ is crucial for the selective induction of chemokines responsible for NK cell recruitment following CPXV infection.

CCR7 is Extrinsically Required for NK Cell Recruitment

Murine NK cells do not express transcripts or protein for CCR7, which leads to their exclusion from secondary lymphoid organs in mice (74). When analyzing the microarray data, we also confirmed a lack of *Ccr7* transcript expression in both resting and cytokine activated NK cells. Expression data published online also demonstrate low levels of *Ccr7* in NK cells relative to other lymphocytes such as T cells (immgen.com). During our analysis of the individual chemokine receptor deficient mice, as a control we also examined mice deficient for CCR7. Surprisingly, given the absence of expression of *Ccr7* transcripts in NK cells, mice lacking CCR7 had a complete reduction of NK cell recruitment at all time points observed following CPXV infection (Figure 15A).

The classical paradigm of pathogen sensing for peripheral DCs involves up-regulation CCR7 expression during the maturation process (115, 116). This up-regulation stimulates migration of DCs from the periphery to the draining LN where they directly

prime the immune response or pass antigens to other LN resident cells that prime the immune response (107). It is also well documented that after localization to the draining LN, DCs interact with NK cells inducing a positive feedback loop, where DCs produce IL-12, stimulating NK cells to produce IFN-γ and subsequently causing further maturation of the DCs and IL-12 production (44, 45, 53, 117).

It seemed a likely hypothesis that CCR7 was required for DC trafficking from the foot to the LN, where they stimulated the recruitment of NK cells as a consequence of this positive feedback loop. To verify the NK cell intrinsic or extrinsic requirement of CCR7, we isolated and enriched NK cells from wild-type or CCR7-deficient congenic mice, labeled the cells with CFSE and co-transferred them into congenic wild-type mice prior to CPXV infection. We found that the transferred NK cells deficient in CCR7 trafficked with similar kinetics to co-transferred wild-type NK cells (Figure 15B). These data indicated that the requirement for CCR7 was NK cell extrinsic as hypothesized.

Abolished Trafficking of NK Cells in Diphtheria Toxin Treated CD11c-DTR Mice

To test the potential requirement for DCs to induce recruitment of NK cells following CPXV infection, we employed CD11c-DTR transgenic mice. These transgenic mice encode the high affinity human diphtheria toxin receptor under control of the CD11c promoter (118, 119). This system allows for selective depletion of cells expressing CD11c when treated with diphtheria toxin. Given dosage variations found in the literature and NK cell expression of CD11c, we first performed a dose-response experiment with diphtheria toxin to determine the ideal concentration. Previously published studies that used models of peripheral depletion administered as much as 20ng/g body weight of diphtheria toxin, but when we tested that dose, we found that NK

cells and macrophage total cell numbers were also reduced (Figure 16A-D). Using a lower dose of 5 ng/g body weight of diphtheria toxin, there appeared to be little reduction of these cell types, but conventional DCs ($CD11c^{+}MHCII^{+}$) were still depleted (Figure 16E, 16F).

C57BL/6 or CD11c-DTR transgenic mice were treated with diphtheria toxin prior to inoculation with CPXV. Following verification that the CD11c expressing DCs were ablated in the diphtheria toxin treated transgenic mice but not in C57BL/6 mice, we next examined the NK cell population. NK cell recruitment was not affected in control mice treated with diphtheria toxin. In contrast, in the treated transgenic mice, we found that, similar to the CCR7-deficient mice, recruitment of NK cells did not occur in response to CPXV infection at either time point observed (Figure 16G). Taken together, these data suggested that a CD11c- and CCR7-expressing cell, potentially a migratory DC, was important for mediating NK cell recruitment following CPXV infection.

DCs Are Not Sufficient to Restore NK Cell Trafficking

Since depletion experiments indicated that DCs were involved upstream of NK cell recruitment following CPXV infection, we next addressed if DCs were sufficient to recruit NK cells. For these studies, we employed *in vitro* Flt3-matured BMDCs, which have a less mature and inflammatory phenotype (97, 120). We also wanted to spatially separate the injection sites of transferred BMDCs and virus since *in vitro* experiments have shown that infection of BMDCs prevents up-regulation of maturation markers and results in non-productive infection (47, 48, 121). Using the CCR7-deficient mice, we injected BMDCs on the top of foot opposite from where we normally inject the virus. Following transfer of BMDCs, we observed trafficking of transferred cells to the draining

LN as has been previously reported (Figure 17A) (116). However, when BMDCs were injected in the same foot as the virus, trafficking of BMDCs to the draining LN was highly diminished. It is possible that the amount of virus injected is so overwhelming that even a physical barrier does not prevent infection of the majority of the injected BMDCs leading to either a lack of maturation and subsequent up-regulation of CCR7 required for migration or apoptosis.

Additionally, in these experiments we began to encounter abnormalities in the CCR7-deficient mice, such as inconsistent and expanded NK cell populations in the draining LN following CPXV infection (Figure 17B). Further investigation of the literature revealed that CCR7-deficient mice develop several types of spontaneous autoimmune diseases, often resulting in lymphadenopathy (122, 123). Indeed, examination of CCR7-deficient mice in our colony showed that there was a broad range in the total number of cells in the draining LN, from 60,000 to 1,000,000 cells in unmanipulated mice regardless of the age of the mouse (Figure 17C). In comparison, total cells isolated from wild type mice were tightly grouped and fell around 500,000 cells per LN. This wide variation in total cell number in unmanipulated CCR7-deficient mice makes it impossible to study NK cell recruitment in these mice.

Next, we attempted to complement NK cell recruitment in CD11c-DTR transgenic mice that had been depleted of DCs prior to transfer of *in vitro* Flt3L-matured BMDCs and inoculation with CPXV. When examining lymphocytes isolated from the draining and non-draining LN, it was hard to detect transferred BMDCs in the CD11c-DTR mice because LNs were markedly smaller (Figure 18A, 18B). Additionally, even with very minimal numbers of BMDCs in the draining LN of mice deficient for DCs, NK cells were not observed to be recruited to the draining LN following BMDC

complementation (Figure 18C). Again, in control C57BL/6 mice, following footpad injection of only BMDCs, there was trafficking of the transferred cells from the foot to the draining LN which was diminished when CPXV was concurrently injected. These results suggested that while DCs may be involved in NK cell recruitment following CPXV infection, the minimal number that trafficked to the draining LN was not sufficient for recruitment of NK cells and that another cell might also be required.

Dermal DCs Do Not Appear to Play a Role in NK Cell Recruitment

In vitro infection of BMDCs with orthopoxviruses prevents maturation of BMDCs, demonstrated by the lack of up-regulation of MHC class II and co-stimulatory molecules (47, 48, 121). As previously discussed, CPXV is known to express two ORFs that potently down regulate expression of MHC class I on infected cells (29-32). However, our lab has also demonstrated that $CD8^+$ T cells are required for resistance to CPXV infection, as systemic depletion of $CD8^+$ T cells leads to decreased survival following infection with a mutant CPXV that cannot down-regulate MHC class I (30). If directly infected DCs cannot prime a $CD8^+$ T cell response, then it is likely that the $CD8^+$ T cell response is primed through cross presentation by a dermal DC subset that expresses CD103 (97, 124, 125). Additionally, previous investigations examining migratory DC trafficking from the periphery to the draining LN demonstrated that dermal DCs arrived earlier than langerin-expressing DCs in the draining LN (126-128). This earlier recruitment makes them likely candidate DC subset to stimulate early NK cell recruitment. Given the importance of cross-presenting DCs for viral resistance, we hypothesized that this dermal CD103 expressing DC subset was also responsible for NK cell recruitment.

We examined the role for cross presenting DCs by using BATF3-deficient mice, which have been shown to selectively lack the $CD103^+$ DC population (88). When we infected the BATF3-deficient mice with CPXV, we found that there was little to no difference in NK cell recruitment between the wild-type and BATF3-deficient mice at time points observed (Figure 19A, 19B). These results suggested that cross-presenting DCs were not essential for NK cell recruitment. Since we also did not observe increased migratory DC recruitment to the draining LN and were unable to complement NK cell recruitment with *in vitro* matured DCs, we hypothesized that another cell type was important for stimulating NK cell recruitment in response to CPXV infection. However, we remain unable to fully discount a possible contribution by a DC subset for NK cell recruitment following CPXV infection.

Macrophage Depletion Leads to Deficiency in NK Cell Recruitment

Macrophages have been shown to line the SCS of the LN, where they phagocytose and detect free viral particles that arrive from the periphery through the lymphatics (94, 129, 130). Additionally, previous data from our lab using an IP inoculation of CPXV that expresses GFP in the place of CPXV203 has demonstrate a preferential infection of $CD169^+$ macrophages in the draining mediastinal LN (78). In agreement with these findings, several other labs have recently shown $CD169^+$ macrophage co-localization with a number of pathogenic infections, including MVA and VV, in the draining LN following cutaneous inoculation (131, 132). Finally, it has also previously been demonstrated that the SCS macrophage population is sensitive to diphtheria toxin depletion in the CD11c-DTR transgenic mice (133). In light of DCs being necessary but not sufficient for the trafficking of NK cells to the draining LN

following infection, we decided to examine the role that macrophages play in NK cell recruitment.

To specifically deplete macrophages in the draining LN, five days prior to CPXV infection we subcutaneously injected liposomes encapsulating clodronate. When examined by immunohistochemistry and, as previously described, in mice were that treated with clodronate-loaded liposomes the SCS macrophage population that express CD169 was depleted in the LN (Figure 20A). Mice that received liposomes encapsulating PBS had an intact macrophage population and recruited NK cells when examined by flow cytometry 3 dpi (Figure 20B, 20C). In contrast, mice that were injected with clodronate-loaded liposomes had minimal numbers of classical macrophages when examined by flow cytometry and were not able to recruit NK cells. In fact, following macrophage depletion and subsequent CPXV infection, many of the lymphocyte populations we had previously examined showed decreased total cell numbers (Figure 20D-H). These data indicated that macrophages are responsible not only for the recruitment of NK cells but also other lymphocyte populations.

Macrophages and Chemokines Function Separately to Recruit NK Cells

Since macrophages produce many inflammatory cytokines and chemokines, including CXCL9 and CXCL10 (134, 135), it seemed likely that they were responsible for the CXCR3-mediated NK cell recruitment. Surprisingly, however, when we examined chemokine expression in the draining LNs of mice treated either with control liposomes containing PBS or liposomes containing clodronate, we found no decrease in transcripts for *Cxcl9* or *Cxcl10* (Figure 21A, 21B). As a control for liposome injection, we observed little to no difference in transcripts for *Ccl19* and *Ccl21* in the non-draining and draining

LNs (Figure 21C, 21D). These data suggest that NK cells are being recruited through two independent mechanisms and that chemokine-mediated recruitment may be necessary but not sufficient for NK cell recruitment following CPXV infection.

Control of Viral Replication in Depleted Systems

To assess the impact of decreased numbers of NK cells in the draining LN on control of CPXV infection, we again took advantage of CXCR3-deficient mice, where NK cell recruitment following CPXV infection is diminished but not eliminated. We also measured viral replication in CXCR3-deficient mice treated with control or NK cell depleting antibody (Figure 22A). When control antibody was administered to both wild-type and CXCR3-deficient mice, viral replication in the draining LNs was similar (Figure 22B). When these mice were systemically depleted of NK cells, the viral replication was increased in the draining LNs of both of these mice to similar extents. When examining viral replication in the lung and spleen, we did not see any significant difference between wild-type and CXCR3-deficient mice with or without NK cell neutralizing antibody (Figure 22C, 22D). These data suggest that even the decreased NK cell population such as that in CXCR3-deficient mice was sufficient to control local replication and prevent systemic dissemination.

Following clodronate-loaded liposome treatment and subsequent infection there were even fewer NK cells present in the draining LN than in the CXCR3-deficient mice. We also speculated that because macrophages are preferentially infected following cutaneous VV infection in the draining LN, that depletion of macrophages could lead to removal of the primary site of viral replication (132). To examine the impact of lack of these populations on viral control, we assessed whether there was a local decrease in viral

burden in the draining LN and increase in systemic spread following macrophage depletion. Even in the absence of macrophages and with minimal numbers of NK cells, viral burden in the draining LN was equivalent in mice pre-treated with either PBS- or clodronate-loaded liposomes (Figure 23A). These data indicated that replication of CPXV in the draining LN was unimpaired in the absence of macrophages suggesting an ability for CPXV to infect and replicate in another LN resident cell. Additionally, in contrast to our hypothesis that a lack of macrophages would result in systemic dissemination, there was no significant increase in viral burden in the lungs or spleens of macrophage depleted mice (Figure 23B, 23C). It seems then that removing the preferential target cell of CPXV did not impact viral replication or spread. Additionally, even the minimal number of NK cells present in the draining LN following macrophage depletion and CPXV infection was sufficient to control viral replication and spread.

Discussion

There are multiple factors required for NK cell recruitment to the draining lymph node following CPXV infection. Innate lymphocyte detection of infection results in cytokine induction, and we have dramatically demonstrated a lack of NK cell recruitment in IFNγR1-deficient mice. Mice that have selectively been depleted of DCs or macrophages demonstrate decreased NK cell recruitment indicating their importance for this process. Although it appears that NK recruitment requires both IFN-γ induced chemokine expression, including CXCL9 and CXCL10, and SCS macrophages, these pathways are not immediately linked. Finally, despite decreased NK cell recruitment, viral replication was still controlled by the minimal numbers of NK cells still founding in the draining LN following CPXV infection.

It is well known that there are multiple interactions between DCs and NK cells including DC mediated differentiation, maturation and activation of NK cells (44, 45, 53, 117, 136, 137). Recent studies also attempt to extend these interactions to include the requirement of DCs for NK cell recruitment. During MCMV infection, when NK cells trafficked into the white pulp of the spleen, they were preferentially associated with ERTR7 expressing cells that were also associated with DCs (109). A more direct study demonstrated that footpad injection of *in vitro* LPS matured DCs was sufficient to recruit NK cells to the draining LN (107). Therefore, as these studies indicate a role for DCs in NK cell recruitment, they appear to further contribute to the complex and established dynamic crosstalk between these two subsets.

To our surprise, evidence in support the importance of DCs upstream of NK cell recruitment appeared to be lacking following CPXV infection. Combining the results of the CD11c-DTR transgenic system and BMDC complementation, DCs appeared to be necessary but not sufficient for NK cell recruitment. However, these results remain confounded by the absence of a good model system of DC deficiency that could be complemented with an external source of DCs. While NK cells were not recruited in CCR7-deficient mice, the cell populations and architecture of the lymph node are highly distorted in these mice, leading to poor ability to prime a cellular immune response (99). Additionally, given the random induction of autoimmunity in these deficient mice and resultant lymphadenopathy, data collected in this system cannot be fully interpreted (99, 122, 123). There are also caveats when examining the diphtheria toxin treated CD11c-DTR transgenic mice. There is ectopic expression of CD11c expression on non-DC lymphocyte populations, leading to their ablation following diphtheria toxin treatment along with conventional DCs (133). Furthermore, depletion of DCs in this system is not

complete as only 85%-90% of DCs are depleted (138). Additionally, even at low doses of diphtheria toxin, mice became ill and died within 6 days of injection as has been reported in the literature (138). Attempts to restore NK cell recruitment by complementing DC deficiency in these mice, even when examining early time points, were ultimately unsuccessful in our hands. Given these off target effects of diphtheria toxin in CD11c-DTR mice, data collected in this background can be difficult to interpret.

With these results in mind, we re-examined previously collected data for further evidence that DCs might be involved in NK cell recruitment. We found that there was little to no increase in migratory DC populations in the draining LN of C56BL/6 CPXV infected mice. Additionally, we did not observe NK cell recruitment defects when examining BATF3-deficient mice, indicating the cross-presenting DC population was also not involved in recruitment. The only DC population in which we observed expansion in the draining LN following CPXV infection was the LN resident DC population. This population is seeded by the migration of monocytes into lymphoid organs and their differentiation into DCs (115). However, it remains unknown if there is a monocyte influx and differentiation into DCs in the draining LN following CPXV infection.

The role of macrophages in NK cell recruitment is a relatively new idea, which was published while we confirming our results. In several studies, macrophages were shown to be important for NK cell recruitment to the $CD169^+$ SCS macrophage area in response to both bacterial and viral pathogens (131, 139, 140). When liposomes encapsulating clodronate are injected in the footpad, NK cells no longer localize to the SCS region and are not activated in response to MVA (140). In agreement with these data, ablation of the $CD169^+$ macrophage population followed by CPXV footpad

infection resulted in decreased NK cell recruitment to the draining LN. These data suggest that macrophages are involved in important upstream events which lead to NK cell recruitment, including the detection of infection and direction of adaptive immune response priming.

A recently published report found that macrophages are important for inducing innate effector cell production of IFN-γ. These cells included "innate" $CD8^+$ T cells, NKT cells and γδ T cells. When the $CD169^+$ macrophages were depleted, the protective ability of these innate effector cells is reduced in response to *Pseudomonas aeruginosa* (131). The IFN-γ produced by these innate responders is important for controlling bacterial load in the draining LN and preventing spread to the blood. However, when we examined viral burden in mice that had been pre-treated with clodronate-loaded liposomes prior to CPXV infection, we did not see a substantial increase in draining LN titers, nor in titers at more distal sites in which we had previously seen spread following systemic NK cell depletion. These data indicate that there are differential responses to bacterial and viral infections by both NK cells and other innate immune lymphocytes.

There are several potential explanations as to why an increase in viral burden was not observed following macrophage depletion. It is possible that the minimal number of NK cells and the innate effector response were sufficient to suppress viral replication to a similar extent as in unmanipulated mice. In contrast to systemic NK cell depletion, where we did see an increase in viral burden both locally and distantly, NK cells in the draining LN were significantly reduced in comparison to macrophage depleted and infected mice. We have also observed this trend of viral control with minimal numbers of NK cells in CXCR3-deficient mice. Only after NK cell depletion in the CXCR3-deficient mice was there increased viral burden in the draining LN. While the CXCR3 draining LN did

contain a larger population of NK cells than the clodronate-loaded liposome treated LNs, it is possible that even the very small numbers of NK cells present in these conditions are sufficient for viral control. Alternately, as it appears that orthopoxviruses preferentially infect macrophages (132), it is possible that following macrophage depletion, viral particles traffic through the lymph to the next LN (the inguinal or thoractic LNs) instead of the blood. Future work to interrogate the mechanism of macrophage mediated NK cell recruitment could examine viral burden in these LNs. Given similar viral burdens in the draining LN after control- and clodronate-loaded liposome treatment, it appeared that another cell is infected in the absence of macrophages. Perhaps this alternately infected cell type does not raise a strong innate anti-viral immune response resulting in a diminished inflammatory response and lymphocyte recruitment.

Recognition of CPXV infection and induction of an inflammatory response including NK cell recruitment appears to be multifactorial and complex. Given the inability of BMDCs to restore NK cell recruitment and the depletion of SCS macrophages in diphtheria toxin treated CD11c-DTR transgenic mice, it appears that DCs are insufficient to induce NK cell recruitment following CPXV infection. While depletion of macrophages resulted in a decrease in the number of NK cells recruited, it did not result in a decrease of IFN-γ induced chemokine expression or increased local or systemic viral burden. These data suggest a two step model for NK cell recruitment, where chemokines are induced following infection and SCS macrophages provide an unknown second signal.

Figure 14: IFN-γ is required for NK cell recruitment and inflammatory chemokine expression.
(A) Age and sex matched IFNγR1-deficient and C57BL/6 mice were inoculated in the footpad with $1.5x10^6$ pfu/mouse and at indicated time points, lymphocytes from the non-draining and draining LNs were isolated, stained and analyzed by flow cytometry. Total NK cells ($NK1.1^+CD3^-CD19^-$) were identified. A representative result of 2 independent experiments is shown. (B-E) Age and sex matched C57BL/6 mice were treated 2 days prior to infection with 250μg of control (PIP) or IFN-γ neutralizing (H22) antibody. (B) Total NK cells ($NK1.1^+CD3^-CD19^-$) were identified. The graph depicts the average of 3 independent experiments. (C-F) Transcript analysis of *Cxcl9, Cxcl10, Ccl19* and *Ccl21* was analyzed by quantitative PCR. The graph represents the average of data from 2 mice/group from 3 independent experiments. Unpaired Student's *t*-test: (*) = $p < 0.05$; (**) = $p < 0.005$; (***) = $p < 0.0005$; (****) = $p < 0.0001$.

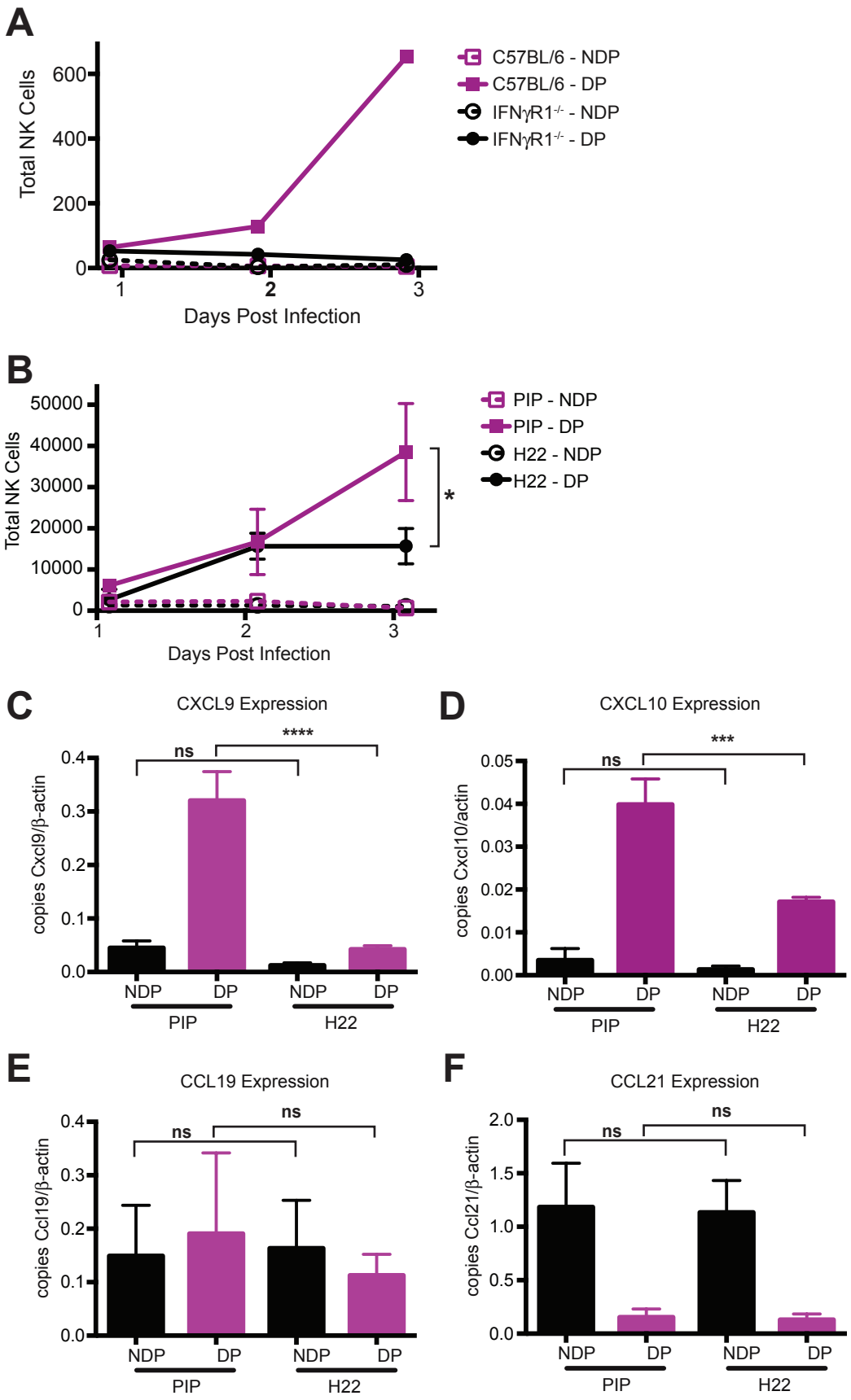
A
Total NK Cells
600
400
200
0
1
2
3
Days Post Infection
C57BL/6 - NDP
C57BL/6 - DP
IFNγR1-/- - NDP
IFNγR1-/- - DP
B
Total NK Cells
50000
40000
30000
20000
10000
0
1
2
3
Days Post Infection
*
PIP - NDP
PIP - DP
H22 - NDP
H22 - DP
C
CXCL9 Expression
copies Cxcl9/β-actin
0.4
0.3
0.2
0.1
0.0
ns
****
NDP
DP
NDP
DP
PIP
H22
D
CXCL10 Expression
copies Cxcl10/actin
0.05
0.04
0.03
0.02
0.01
0.00
ns
***
NDP
DP
NDP
DP
PIP
H22
E
CCL19 Expression
copies Ccl19/β-actin
0.4
0.3
0.2
0.1
0.0
ns
ns
NDP
DP
NDP
DP
PIP
H22
F
CCL21 Expression
copies Ccl21/β-actin
2.0
1.5
1.0
0.5
0.0
ns
ns
NDP
DP
NDP
DP
PIP
H22

Figure 15: CCR7 is extrinsically required for NK cell recruitment to the draining LN following CPXV infection.
(A) Age and sex matched CCR7-deficient and C57BL/6 mice were infected with CPXV and NK cell recruitment was monitored as before. The graph depicts the average of 3 independent experiments. (B) C57BL/6 (CD45.1) and $CCR7^{-/-}$ (CD45.2) splenocytes were isolated and enriched by negative selection before being CFSE labeled, mixed and co-transferred intravenously into C57BL/6 mice. One day after transfer, mice were infected as before and NK cell ($NK1.1^{+}CD3^{-}CD19^{-}$) populations were examined at indicated time points. To analyze the recruitment in this system, the total number of recruited wild-type or chemokine knockout NK cells at 2 and 3 dpi were compared relative to the initial time point at 1 dpi. A representative result of 3 independent experiments is shown.

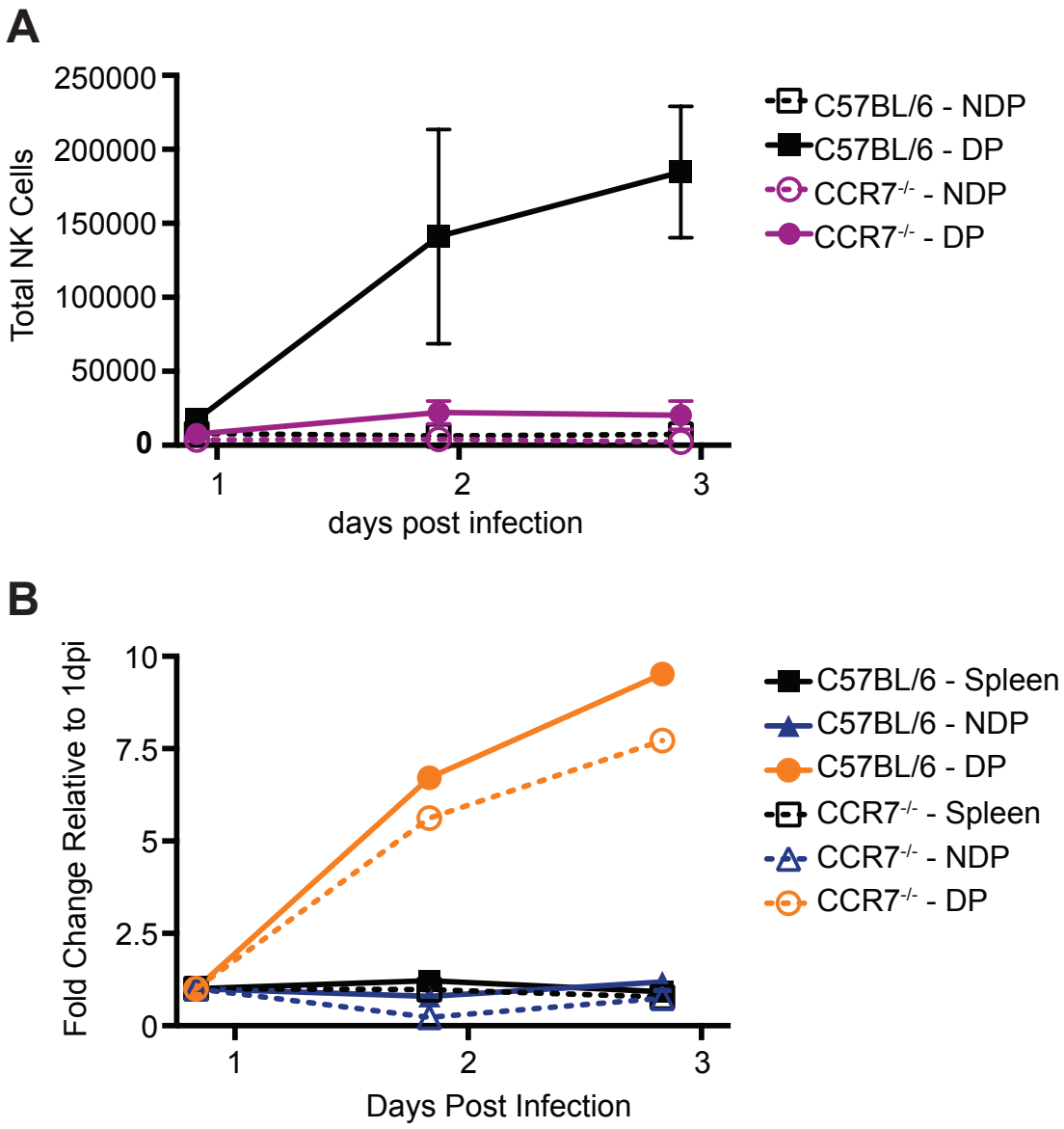
A
250000
200000
150000
100000
50000
0
Total NK Cells
1
2
3
days post infection
C57BL/6 - NDP
C57BL/6 - DP
CCR7-/- - NDP
CCR7-/- - DP
B
10
7.5
5
2.5
0
Fold Change Relative to 1dpi
1
2
3
Days Post Infection
C57BL/6 - Spleen
C57BL/6 - NDP
C57BL/6 - DP
CCR7-/- - Spleen
CCR7-/- - NDP
CCR7-/- - DP

Figure 16: NK cell recruitment is defective in CPXV infected CD11c-DTR transgenic mice.
(A) Age and sex matched CD11c-DTR$^{+/-}$ and C57BL/6 mice were treated with 20, 10 and 5 ng/g body weight of diphtheria toxin. Lymphoid (A, C, E) and splenic (B, D, F) total NK cells (A, B), total macrophages (C, D) and total conventional DCs (E, F) were analyzed by flow cytometry. (G) For NK cell recruitment, a dose of 5 ng/g body weight was chosen and administered 1 day prior to infection with CPXV. At 1 and 2 dpi, LNs were harvested, treated with Liberase TL, and lymphocytes were isolated, stained and analyzed by flow cytometry. The graph depicts the average of 3 independent experiments.

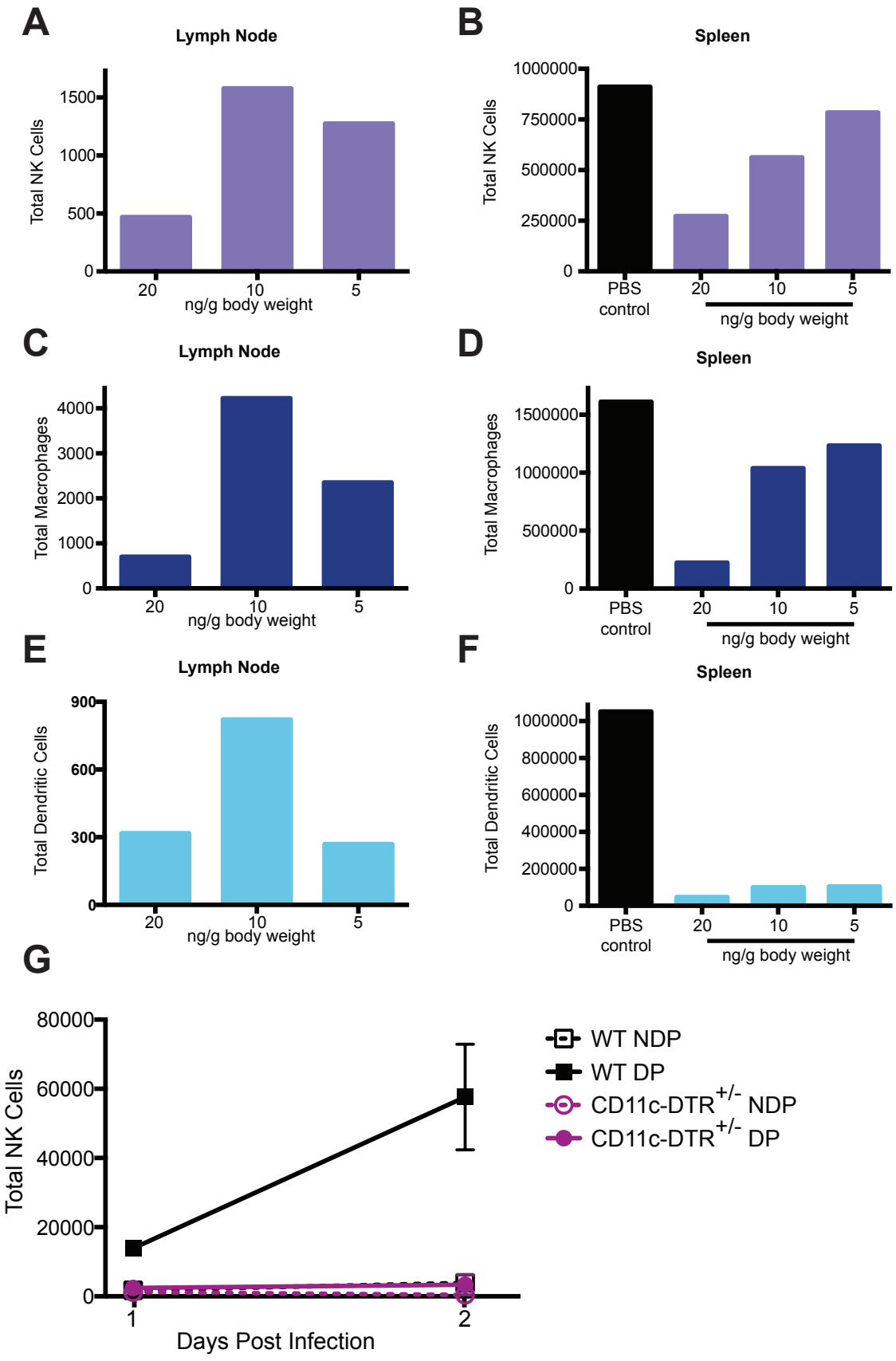
A
Lymph Node
Total NK Cells
1500
1000
500
0
20
10
5
ng/g body weight
B
Spleen
Total NK Cells
1000000
750000
500000
250000
0
PBS control
20
10
5
ng/g body weight
C
Lymph Node
Total Macrophages
4000
3000
2000
1000
0
20
10
5
ng/g body weight
D
Spleen
Total Macrophages
1500000
1000000
500000
0
PBS control
20
10
5
ng/g body weight
E
Lymph Node
Total Dendritic Cells
900
600
300
0
20
10
5
ng/g body weight
F
Spleen
Total Dendritic Cells
1000000
800000
600000
400000
200000
0
PBS control
20
10
5
ng/g body weight
G
Total NK Cells
80000
60000
40000
20000
0
1
2
Days Post Infection
WT NDP
WT DP
CD11c-DTR+/- NDP
CD11c-DTR+/- DP

Figure 17: Inconsistencies in CCR7-deficient mice.
(A) Flt3L BMDCs were generated *in vitro*, labeled with CFSE and injected into the top of the foot of CCR7-deficient mice. LNs were isolated 1 day later and treated with Liberase TL following which lymphocytes were isolated, stained and analyzed by flow cytometry. (B) Age and sex matched CCR7-deficient and C57BL/6 mice were infected and NK cell recruitment was monitored as before. The graph depicts the average of 2 independent experiments. (C) Total cells from the popliteal LNs from 3-4 unmanipulated CCR7-deficient mice per age group and 1 unmanipulated C57BL/6 mouse were counted using trypan blue exclusion. CCR7-deficient mice were examined at 2, 3 and 4 months of age and from C57BL/6 mice at 2 months of age. Each symbol represents 1 popliteal LN from a mouse, with both popliteal LNs represented on the graph.

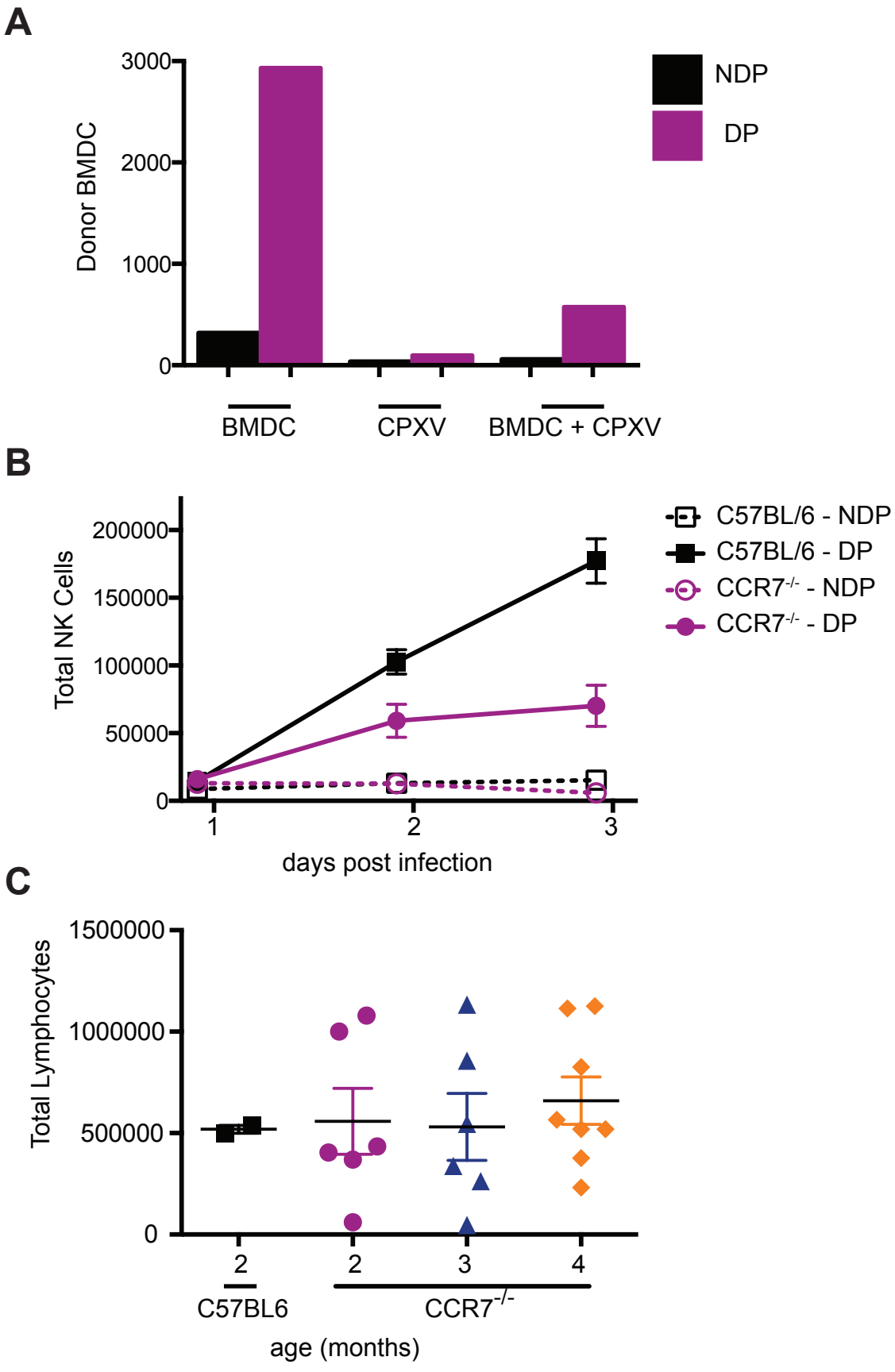
A
3000
2000
1000
0
Donor BMDC
NDP
DP
BMDC
CPXV
BMDC + CPXV
B
200000
150000
100000
50000
0
Total NK Cells
1
2
3
days post infection
C57BL/6 - NDP
C57BL/6 - DP
CCR7-/- - NDP
CCR7-/- - DP
C
1500000
1000000
500000
0
Total Lymphocytes
2
2
3
4
C57BL6
CCR7-/-
age (months)

Figure 18: BMDCs do not complement NK cell recruitment defects seen in CD11c-DTR transgenic mice following CPXV infection.
C57BL/6 and CD11c-DTR transgenic mice were age and sex matched and treated with 5 ng/g body weight of diphtheria toxin 1 day prior to injection of BMDCs and CPXV infection. Flt3L BMDCs were generated *in vitro*, labeled with CFSE and injected into the top of the foot while CPXV was injected in the bottom of the footpad of diphtheria toxin treated CD11c-DTR mice and C57Bl/6 mice. LNs were isolated 1 day later and treated with Liberase TL following which lymphocytes were isolated, stained and analyzed by flow cytometry. (A) Percent and (B) total donor derived BMDCs ($CD11c^{+}MHCII^{high}CFSE^{+}$) and (C) total NK cells ($NK1.1^{+}CD3^{-}CD19^{-}$) were assessed and graphed. The graph represents 1 mouse for BMDC injected alone and CXPV injected alone while BMDC and CPXV injected in the same foot represent the average 2 mice for both CD11c-DTR and C57BL/6 mice.

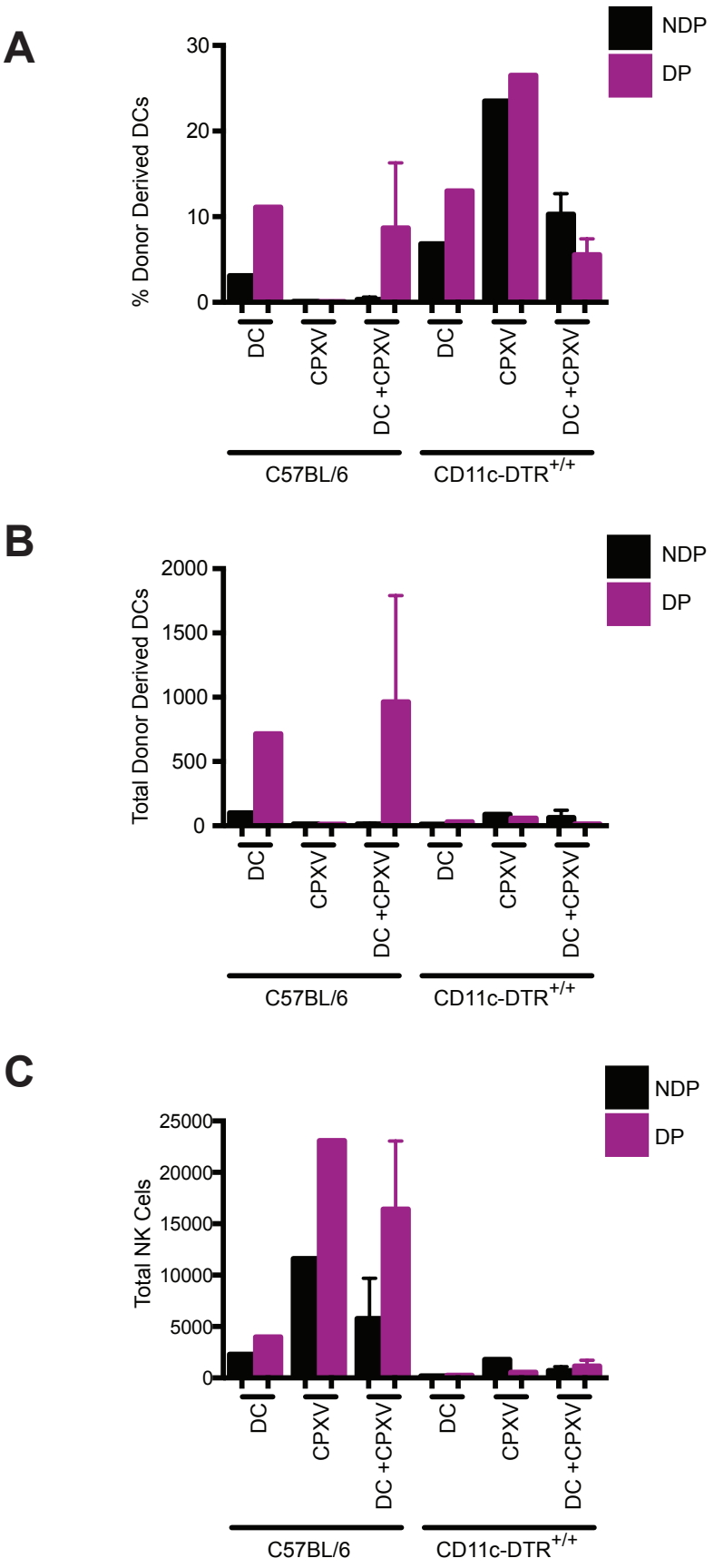
A
NDP
DP
% Donor Derived DCs
30
20
10
0
DC
CPXV
DC +CPXV
DC
CPXV
DC +CPXV
C57BL/6
CD11c-DTR+/+
B
NDP
DP
Total Donor Derived DCs
2000
1500
1000
500
0
DC
CPXV
DC +CPXV
DC
CPXV
DC +CPXV
C57BL/6
CD11c-DTR+/+
C
NDP
DP
Total NK Cels
25000
20000
15000
10000
5000
0
DC
CPXV
DC +CPXV
DC
CPXV
DC +CPXV
C57BL/6
CD11c-DTR+/+

Figure 19: BATF3 deficiency does not affect NK cell trafficking following CPXV infection.
Age and sex matched BATF3-deficient mice on a 129S6/SVEV background and 129S6/SVEV control mice were infected as previously described. Draining and non-draining LNs were isolated at 2 and 3 dpi and lymphocytes were isolated, stained and assessed by flow cytometry for (A) percent and (B) total NK cells ($NK1.1^{+}CD3^{-}CD19^{-}$) as before. The graph depicts the average of 2 independent mice.

A

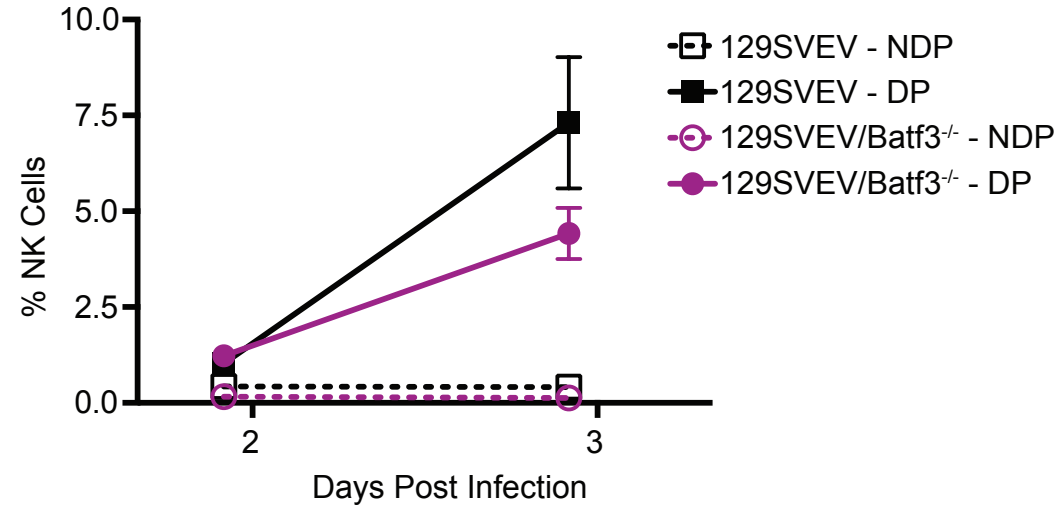
10.0
7.5
5.0
2.5
0.0
% NK Cells
2
3
Days Post Infection
129SVEV - NDP
129SVEV - DP
129SVEV/Batf3-/- - NDP
129SVEV/Batf3-/- - DP

B

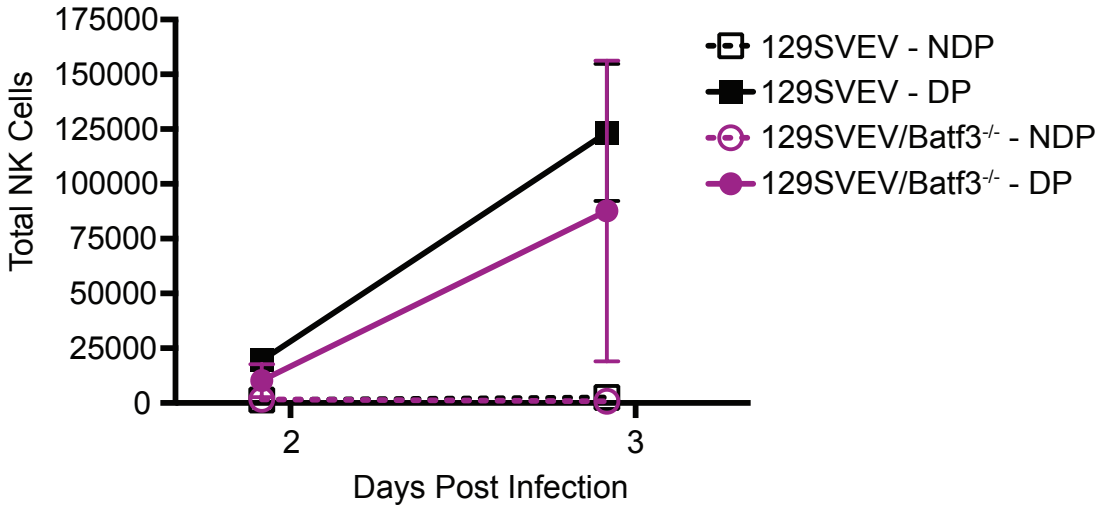
175000
150000
125000
100000
75000
50000
25000
0
Total NK Cells
2
3
Days Post Infection
129SVEV - NDP
129SVEV - DP
129SVEV/Batf3-/- - NDP
129SVEV/Batf3-/- - DP

Figure 20: Macrophage depletion leads to decreased lymphocyte recruitment. Five days prior to infection, C57BL/6 mice were treated in both rear footpads with 50μL of either PBS- or clodronate-loaded liposomes. (A) A representative section of a macrophage depleted draining LNs isolated 3 hpi following CPXV infection is shown following staining with $CD169^+$ (PE), $CD3^+$ (FITC) and DAPI. The (B) total macrophage population ($F4/80^+CD11b^+$), (C) total NK cell population ($NK1.1^+CD3^-CD19^-$), (D) total neutrophil population ($Ly6G^+SSC^+$), (E) total migratory DC population ($CD11c^+MHCII^{high}$), (F) total LN resident DC population ($CD11c^+MHCII^+$), (G) total T cell population ($CD3^+CD19^-NK1.1^-$) and (H) total B cell population ($CD19^+CD3^-NK1.1^-$) were observed by flow cytometry 3 dpi. The graph depicts the average of 2 mice from 2 independent experiments. Figure 1A was contributed by Dorothy Sojka.

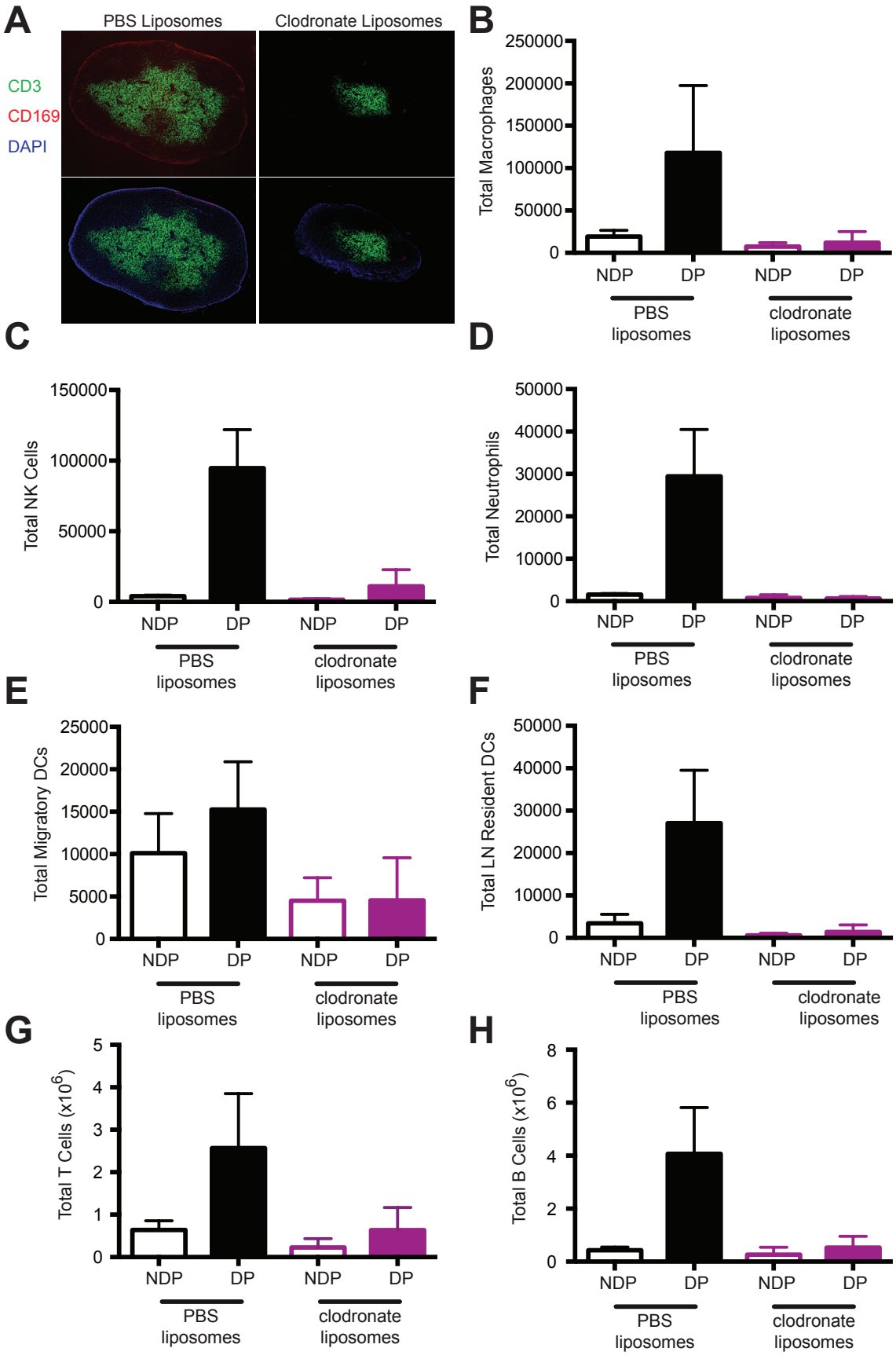
A
PBS Liposomes
Clodronate Liposomes
CD3
CD169
DAPI
B
Total Macrophages
250000
200000
150000
100000
50000
0
NDP
DP
NDP
DP
PBS liposomes
clodronate liposomes
C
Total NK Cells
150000
100000
50000
0
D
Total Neutrophils
50000
40000
30000
20000
10000
0
E
Total Migratory DCs
25000
20000
15000
10000
5000
0
F
Total LN Resident DCs
50000
40000
30000
20000
10000
0
G
Total T Cells (x10^6)
5
4
3
2
1
0
H
Total B Cells (x10^6)
8
6
4
2
0

Figure 21: Inflammatory chemokine transcripts are unaffected by macrophage depletion.
Five days prior to infection, C57BL/6 mice were treated in both rear footpads with 50μL of either PBS- or clodronate-loaded liposomes. Transcript analysis of (A) *Cxcl9,* (B) *Cxcl10*, (C) *Ccl19* and (D) *Ccl21* was analyzed by quantitative PCR. The graph represents the average of data from 2 independent experiments with 3 mice/group for each experiment. Unpaired Student's *t*-test: (*) = $p < 0.05$.

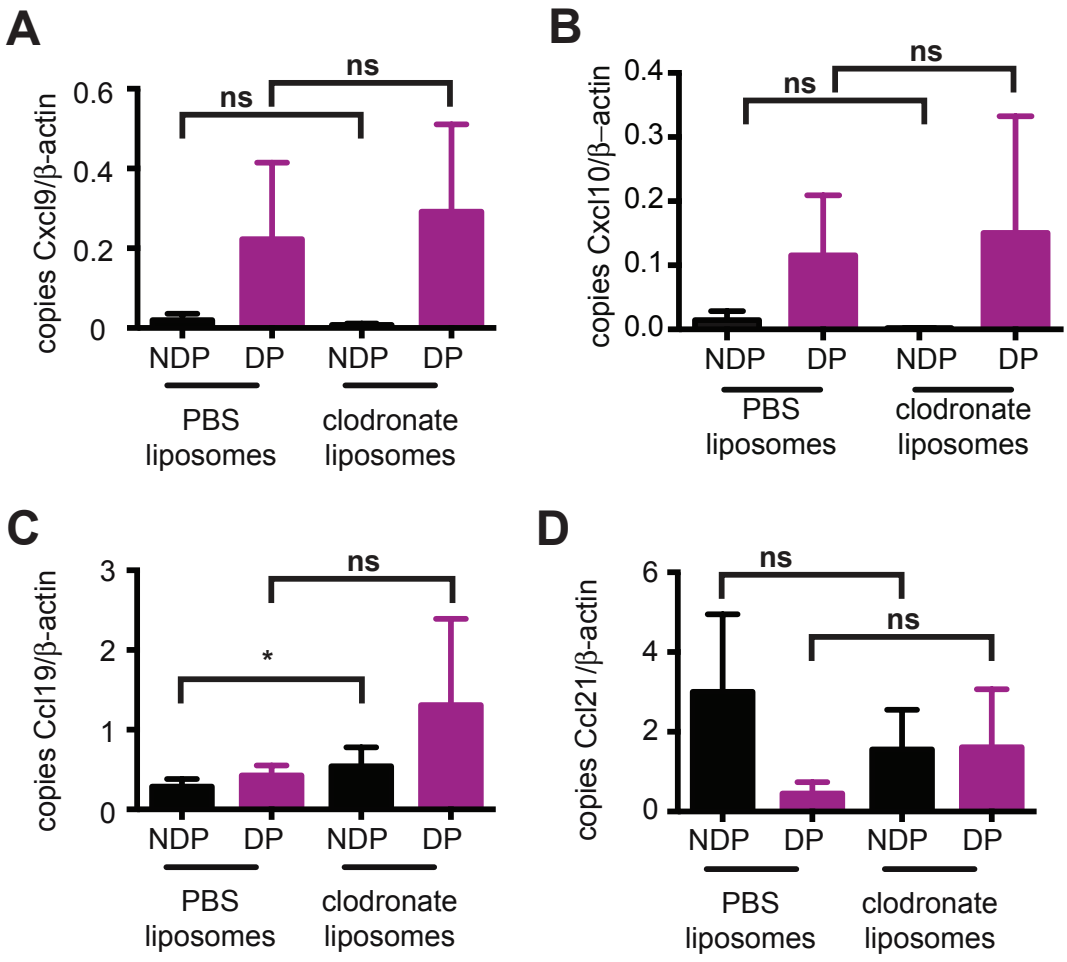
A
copies Cxcl9/β-actin
0.6
0.4
0.2
0
ns
ns
NDP
DP
NDP
DP
PBS liposomes
clodronate liposomes
B
copies Cxcl10/β–actin
0.4
0.3
0.2
0.1
0.0
ns
ns
NDP
DP
NDP
DP
PBS liposomes
clodronate liposomes
C
copies Ccl19/β-actin
3
2
1
0
ns
*
NDP
DP
NDP
DP
PBS liposomes
clodronate liposomes
D
copies Ccl21/β-actin
6
4
2
0
ns
ns
NDP
DP
NDP
DP
PBS liposomes
clodronate liposomes

Figure 22: NK cells control CPXV replication in CXCR3-deficient mice.
Age and sex matched CXCR3-deficient and C57BL/6 mice were injected IP with 200μg control (mAR) or PK136 antibody 2 days prior to infection. (A) NK cell depletion was confirmed in the non-draining LN at 3 dpi. Quantitative PCR was used to assess viral burden in the (B) LNs, (C) lungs (D) and spleens. CPXV copy number was normalized to β-actin copy numbers and then multiplied by 1000. Symbols indicate individual mice and lines indicate the mean. N= 4 to 7 mice/group were analyzed for each time point.

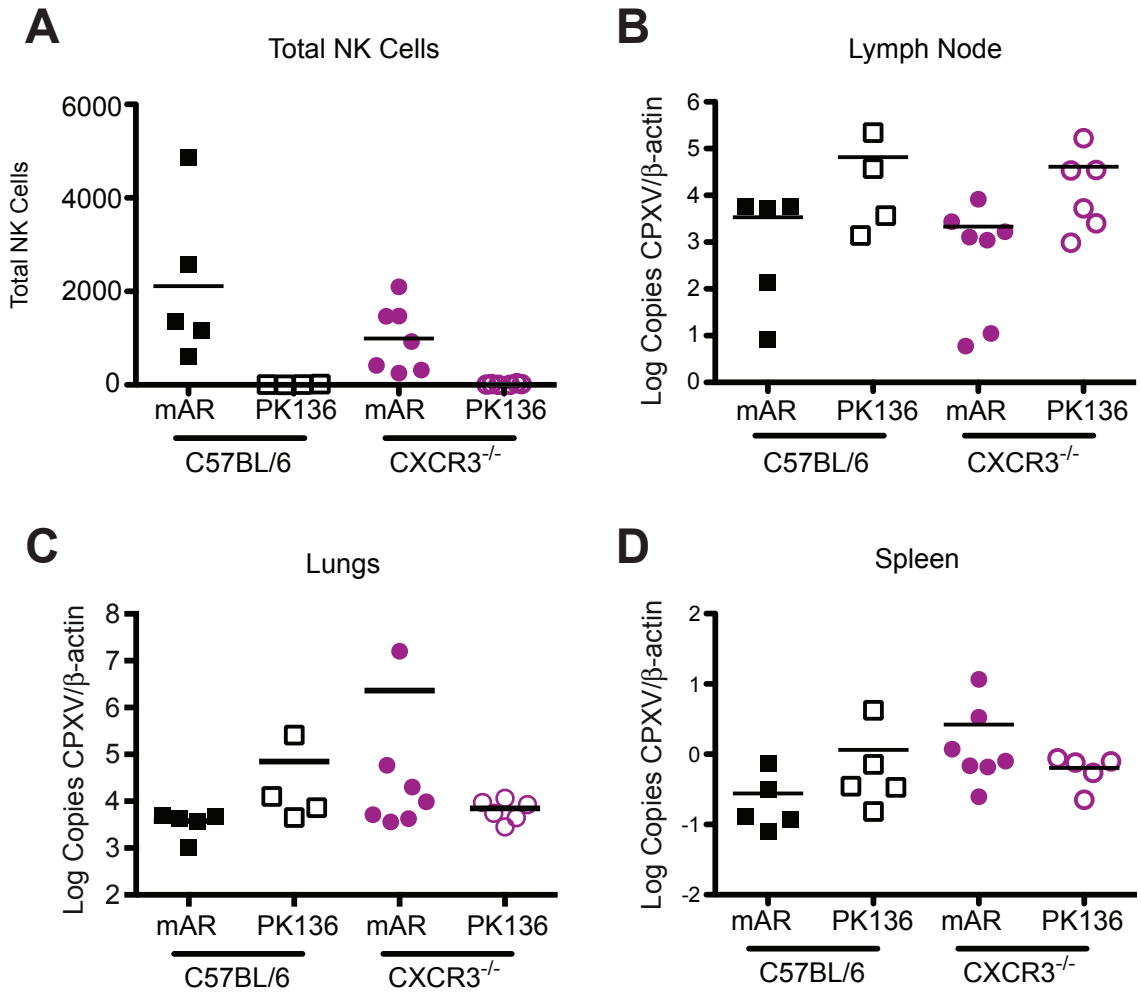
A
Total NK Cells
Total NK Cells
6000
4000
2000
0
mAR
PK136
mAR
PK136
C57BL/6
CXCR3-/-
B
Lymph Node
Log Copies CPXV/β-actin
6
5
4
3
2
1
0
mAR
PK136
mAR
PK136
C57BL/6
CXCR3-/-
C
Lungs
Log Copies CPXV/β-actin
8
7
6
5
4
3
2
mAR
PK136
mAR
PK136
C57BL/6
CXCR3-/-
D
Spleen
Log Copies CPXV/β-actin
2
1
0
-1
-2
mAR
PK136
mAR
PK136
C57BL/6
CXCR3-/-

Figure 23: Macrophage depletion does not impact CPXV replication.
Five days prior to infection, C57BL/6 mice were treated in both rear footpads with 50μL of either PBS- or clodronate-loaded liposomes. Quantitative PCR was used to assess viral burden in the (A) LNs, (B) lungs (C) and spleens at 3 dpi. CPXV copy number was normalized to β-actin copy numbers and then multiplied by 1000. Symbols indicate individual mice and lines indicate the mean. N= 5 mice/group were analyzed for each time point.

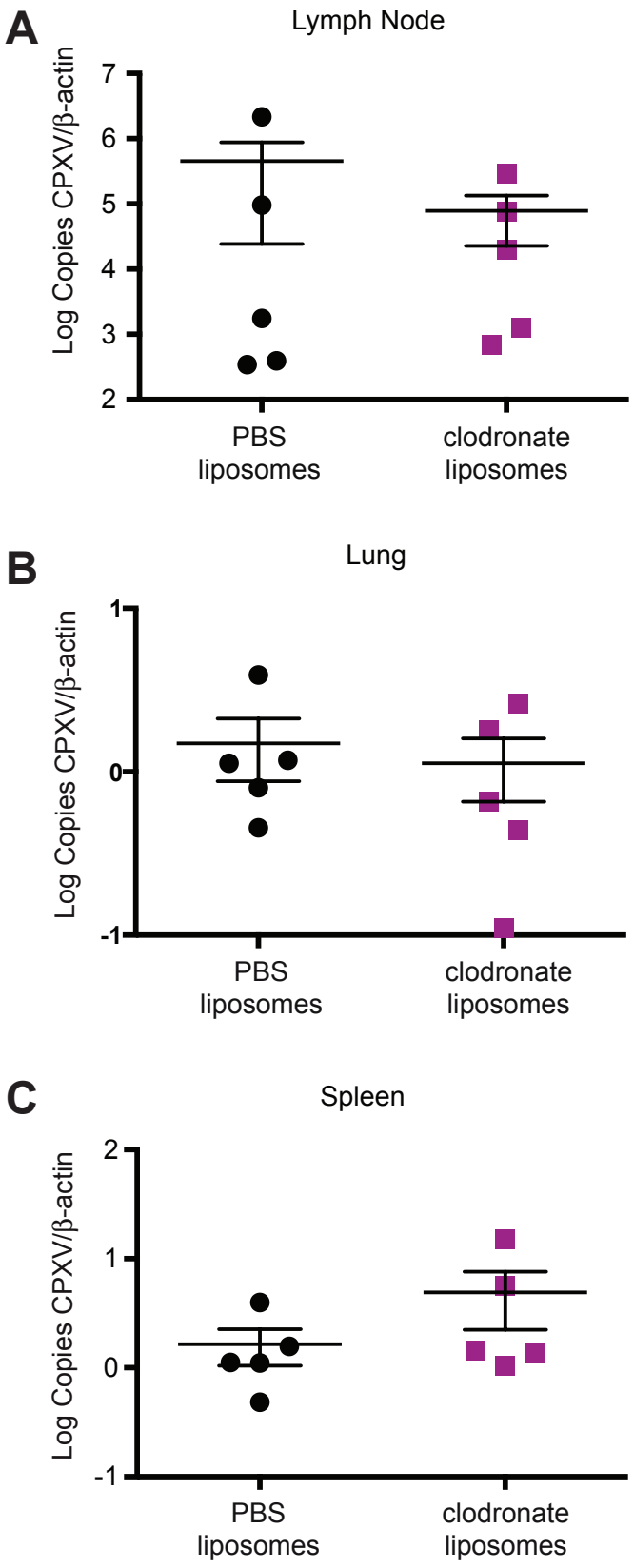
A
Lymph Node
Log Copies CPXV/β-actin
7
6
5
4
3
2
PBS liposomes
clodronate liposomes
B
Lung
Log Copies CPXV/β-actin
1
0
-1
PBS liposomes
clodronate liposomes
C
Spleen
Log Copies CPXV/β-actin
2
1
0
-1
PBS liposomes
clodronate liposomes

CHAPTER 6:

Comparison of Cowpox Virus and Vaccinia Virus Footpad Infection

Vaccinia virus has been used extensively as a prototypical model for orthopoxviral infection in both *in vitro* and *in vivo* studies. To better understand whether CPXV acts like a typical or abnormal orthopoxvirus for NK cell recruitment studies, we used VV as a control. This chapter describes the host response to VV footpad infection, with particular regard to NK cell recruitment.

Vaccinia Virus Effectively Infects Both the Draining LN and Spleen Following Footpad Inoculation.

Viral spread and replication following CPXV or VV infection was similar, but had distinct differences. When VV was inoculated in the footpads of C57BL/6 mice using the same dose used for CPXV infections, VV spread to and replicated in the draining LN. Titers for both viruses increased with similar kinetics between 1 and 3 dpi (Figure 24A). However, following VV infection LN titers did not reach the same levels and resolved faster than titers following CPXV inoculation. Titers were reduced to the limit of detection by 6 dpi following VV infection whereas CPXV titers were not resolved until 9dpi. Thus CPXV was capable of surviving and replicating longer in the draining LN than VV. Additionally, no titers were found for either virus in the liver by traditional plaque assays (data not shown).

While productive infection of the draining LN appeared to be similar when comparing the two viruses, the same was not true for spread to the spleen. Following VV inoculation, titers were found above the limit of detection in the spleen 2 dpi whereas titers were barely above or were at the limit of detection following CPXV inoculation (Figure 24B). In addition, VV replicated in the spleen, peaking somewhere between 3 and 6 dpi reaching titers 2-logs greater than the limit of detection. Titers were decreased at 6

dpi but we did not determine the day at which VV infection resolved. Taken together, these data show that CPXV and VV replicate similarly, though with different kinetics, in the draining LN and that VV, but not CPXV, is capable of spreading to and replicating within the spleen.

CPXV and VV Cause Similar Lymphocyte Population Expansion in the Draining LN

Cowpox and Vaccina virus infection caused lymphadenopathy resulting from an expansion of the same lymphocyte populations in the draining LNs following footpad infection. Both macrophage and neutrophil populations were increased at early times following VV and CPXV inoculation (Figure 25A, 25B). The total neutrophil population expansion was equivalent following either orthopoxviral infection but increase in the macrophage population was slightly greater following VV inoculation at all time points observed. In agreement with data generated following CPXV infection, following VV infection we found little to no increase in the migratory DC population but an expanded LN resident DC population (Figure 25C, 25D). We also observed large increases in both T and B cell numbers, again with the total populations being larger following VV inoculation (Figure 25E, 25F). Most importantly, we determined that there was a large increase in the NK cell population following VV inoculation, which occurred with slightly faster kinetics and persisted for a similar length of time following CPXV infection (Figure 25G). All together, these data suggest that CPXV and VV prime similar recruitment responses of lymphocytic populations, though VV may less efficiently inhibit recruitment of lymphocyte populations resulting in a faster and more robust expansion of macrophages, NK and T cells.

When we examined the surface phenotype of NK cells found in the draining LN following VV footpad inoculation, we found that they expressed markers typical of splenic but not thymic NK cells. NK cells isolated from the spleen and draining LN displayed identical expression of Mac-1 (CD11b), DX5, L-selectin (CD62L), NKG2D, the Ly49 family (ADCIFH) and CD94 (Figure 26A-F). Similar to following CPXV infection, expression of Mac-1 (CD11b) and L-selectin (CD62L) was different on NK cells isolated from the non-draining and draining LN. Again, markers of thymic NK cells were not found on NK cells isolated from the draining LN following VV infection (Figure 26G, 27H). NK cells isolated from the draining LN following either CPXV or VV infection expressed the same markers with the same intensity as NK cells derived from the spleen, suggesting that the same subset of NK cells are being recruited following either infection. These data suggest that the NK cell population in the draining LN was recruited rather than the result of *in situ* proliferation.

NK Cells Are Recruited by the Same Mechanism Following Infection With Either CPXV or VV

In agreement with the data generated following CPXV inoculation, VV also induced NK cell expansion in a pertussis toxin sensitive manner. When we transferred NK cells pre-treated with PBS *in vitro* into congenic mice, we found that these cells were again accumulated over time in the draining LN following VV inoculation. Recruitment of PBS pre-treated adoptively transferred NK cells appeared stronger following VV infection than CPXV infection, as total cell numbers of these transferred NK cells were greater at both 2 and 3 dpi following VV infection (Figure 27A, 27B). When NK cells that had been pre-treated *in vitro* with pertussis toxin were co-transferred at the same

time, they did not accumulate in the draining LN. Taken together, these data indicate that NK cells recruitment was pertussis toxin sensitive and therefore required GPCRs following both CPXV and VV infection.

When examining chemokine transcripts in the draining LN following VV infection, we observed differential upregulation of some chemokine transcripts. Some transcripts we observed to be up-regulated following VV but not CPXV inoculation including *Cxcl1, Cxcl2* and *Cxcl5* at 1 dpi (Figure 28). These chemokines have been implicated to affect neutrophils trafficking (141-143). It also appeared that *Ccl24,* which has been shown to be important in eosinophils, basophils, and T cells (144), was expressed earlier and then diminished more immediately following VV infection, whereas CPXV induced prolonged expression of this transcript. There were also differences in the abundance of transcripts for *Ccl20*, which has been shown to be important a variety of lymphocytes including T cells, NKT cells and activated B cells, which appeared to have a delay in expression following VV infection. These data indicate that there is up-regulation of additional chemokines during VV infection that were not observed following infection with CPXV.

Expression of chemokine transcripts up-regulated during VV infection was fairly similar to that following CPXV infection. However, there were several important differences in the intensity of chemokine up-regulation following CPXV and VV infection. When examining transcripts for *Ccl2* and *Ccl7,* we observed more abundant transcripts following VV infection at all time points observed in comparison to CPXV infection. Also, the IFN-γ induced transcripts *Cxcl9, Cxcl10*, and *Cxcl11* were more highly induced and with faster kinetics following VV inoculation. Meanwhile, some transcripts, such as those for *Ccl3* and *Ccl4,* were nearly identical following either

infection. The inflammatory chemokine transcript expression profile corresponded highly with the larger increase in lymphocyte populations following VV infection in the draining LN. These data again suggest that CPXV better inhibits the inflammatory response including inflammatory chemokine expression than VV. This may permit a faster and more robust accumulation of lymphocytes in the draining LN following VV inoculation.

To determine whether recruitment of NK cells following VV infection required the same chemokine receptors as following CPXV infection, we examined NK cell recruitment in chemokine receptor-deficient mice. In mice deficient for either CCR2 or CCR5, there was a slight defect at 2 dpi but at 3 dpi NK cell recruitment was equivalent in wild-type and chemokine receptor-deficient mice following VV infection (Figure 29A, 29B). These data were comparable to the requirement for CCR2 and CCR5 following CPXV infection at 3 dpi. Mice that were deficient for CXCR3 showed a defect in NK cell recruitment at both 2 and 3 dpi following both CPXV and VV infection (Figure 29C). As expected, NK cell recruitment following VV, like CPXV infection, required NK cell intrinsic expression of CXCR3 during adoptive transfer experiments (Figure 29D). These data suggest that NK cells required similar chemokine receptors for recruitment following infection with either CPXV or VV, providing further evidence that the same NK cell population is recruited using related mechanisms following infection with either orthopoxvirus.

Upstream Signaling Appears to Be Comparable Following Either CPXV or VV Infection

As discussed in Chapter 5, we initially hypothesized that DCs were important for NK cell recruitment following orthopoxviral infection. It appeared that DC populations

were fairly equivalently following either CPXV or VV infection, with a slight elevation in total resident DC numbers following VV infection at 6 dpi. However, this time point is well beyond the peak of NK cell expansion in the draining LN. Concurrent to testing the requirement for DCs upstream of CPXV infection, we also examined if DCs could complement NK cell trafficking defects following VV infection in DC depleted mice. Again we saw a defect in trafficking of injected BMDCs when VV concurrently injected in the CD11c-DTR depleted mice (Figure 30A, 30B). Interestingly, the defect in DC trafficking in the presence of VV was not observed in the C57BL/6 mice. Additionally, even with some DCs trafficking to the draining LN, recruitment of NK cells was not observed when BMDCs were co-injected in the CD11c-DTR mice (Figure 30C). These data further indicate that DCs are not sufficient for recruitment of NK cells following both CPXV and VV infection.

Discussion

Here we demonstrate that similar lymphocyte populations accumulate in the draining LN during both CPXV and VV infection. There was a trend towards a more robust recruitment of some but not all lymphocytes following VV infection suggesting that CPXV inhibits lymphocyte recruitment more than VV. This increased lymphocyte recruitment correlated with the induction of more inflammatory chemokine transcripts during VV infection. The NK cell population expanded with faster kinetics following VV infection, but the mechanism of recruitment and origin of recruited cells was the same.

Although, it has been well established that VV can subvert the immune system, immunocompetent hosts routinely clear infection. While VV has been used extensively to study immunomodulation of the host immune system by orthopoxviruses, it does not

contain the extensive range of immunomodulatory ORFs found in CPXV (16, 23, 24). While CPXV and VV share many homologous ORFs responsible for the viral life cycle and immunomodulation, CPXV encodes many completely unique ORFs, mostly in regions of its genome associated with immunomodulation and host adaptation. Therefore, it was important to determine if the immune response to both viruses was similar or if CPXV was more immunosuppressive as a consequence of these unique ORFs. We assessed viral titers, viral spread and lymphocyte recruitment to the draining LN following infection of mice with both viruses. Our data thus far indicate that CPXV and VV very similarly recruited lymphocytes and replicated to similar titers following infection.

In contrast to CPXV footpad infection, VV was capable of spreading to and replicating within the spleen. This raises the possibility that VV may spread to other distant sites from the draining LN, but a systematic survey of other organs has not been performed. The increased viral spread of VV was surprising given the induction of a more robust recruitment of lymphocytes following VV infection and because viral titers in the LN did not reach the same levels as titers following CPXV infection. Secondary viral spread is thought to follow sufficient replication in a primary organ, therefore although viral burden in the draining LN following VV infection did not reach levels found following CPXV infection, it was sufficient for viral spread. One possible explanation for increased viral dissemination is that VV may have a broader cellular tropism than CPXV. Once a few viral particles enter the circulation or the lymph, they could establish productive foci of infection elsewhere, such as the spleen. However, this hypothesis seems unlikely as CPXV has been shown to have one of the broadest host ranges of the orthopoxviruses and therefore the ability to infect many different host cells

(145). An alternate hypothesis is that VV recruits a lymphocyte population that is not recruited following CPXV that traffics from the infected LN to the spleen. It is currently unclear why VV, but not CPXV, is able to spread to and replicate within the spleen.

Although both CPXV and VV caused lymphadenopathy and influxes of the same types of lymphocytes, VV stimulated an earlier and sometimes greater expansion of some lymphocytes, including macrophages, NK cells and T cells. These results suggest that CPXV more strongly attenuated inflammatory lymphocyte recruitment than VV, particularly at early times following infection. Again, transcriptional profiles of inflammatory chemokines lend support to this hypothesis, including expression of *Ccl24, Cxcl1, Cxcl2,* and *Cxcl5* that was only seen following VV infection. CXCL1, CXCL2 and CXCL5 all bind only CXCR2, which has been implicated in neutrophil recruitment following infection with several bacterial pathogens (141-143). Additionally, as macrophages and neutrophils secrete CXCL1 and CXCL2, the expression of these chemokines and subsequent recruitment of additional macrophages and neutrophils could be acting in a positive feedback loop. Eosinophils express CCR3 (144), the receptor for CCL24. However we did not examine this population so it is unknown whether it is differentially recruited. While CCL24 is important during parasitic infections and renders $CD4^+$ T cells more sensitive to human immunodeficiency virus infection, its role following orthopoxvirus infection has not been determined (146, 147). In addition, chemokine transcripts that have been previously implicated in NK cell recruitment following CPXV and other bacterial and viral pathogens, including *Ccl2, Ccl7, Cxcl9, Cxcl10,* and *Cxcl11,* also had higher induction following VV infection of the draining LN.

Despite these slight differences, it appeared that the course of infection following either CPXV or VV was very similar. There was a notably slight delay in NK cell recruitment at early times following CPXV infection. NK cells isolated from the draining LN following infection with CPXV and VV had identical expression of NK cell surface markers which were typical of splenic NK cells. We observed a slight defect at 2 dpi in the CCR2 and CCR5 defect following VV infection, which may be linked to the high levels of *Ccl2* induction. Again, NK cell recruitment did not appear to occur in a CCR2- or CCR5-dependent manner at 3 dpi, but in a CXCR3 cell intrinsic manner for both viruses. Overall, it appears that though VV recruitment of lymphocytes was more robust and faster, CPXV infection was similar to the prototypical model of orthopoxviral infections. We can therefore conclude that NK cell recruitment following infection with orthopoxvirus family members is likely to be mediated by similar or identical mechanisms.

After footpad inoculation with either CPXV or VV, lymphadenopathy resulted from similar recruitment of lymphocyte populations. These data also indicated that recruitment of the splenic NK cells to the draining LN is mediated by same chemokines and chemokine receptors. Additionally, DC complementation was also insufficient to restore NK cell trafficking suggesting an upstream requirement for macrophages in NK cell trafficking following VV infection. Taken together, these data indicated that CPXV and VV induce a very similar host response following footpad infection.

Figure 24: VV establishes infection in the draining LN and spleen following footpad inoculation.
Age and sex matched C57BL/6 mice were infected with $1.5x10^6$ pfu of VV in the footpad and at indicated time points, organs were removed and viral titers were assessed in the draining LN (A) and spleen (B) by plaque assay. Dotted lines indicate the limit of detection by the assay. Symbols indicate individual mice and the mean and SEM are depicted. N= 4 to 5 mice/group were analyzed for each time point.

A

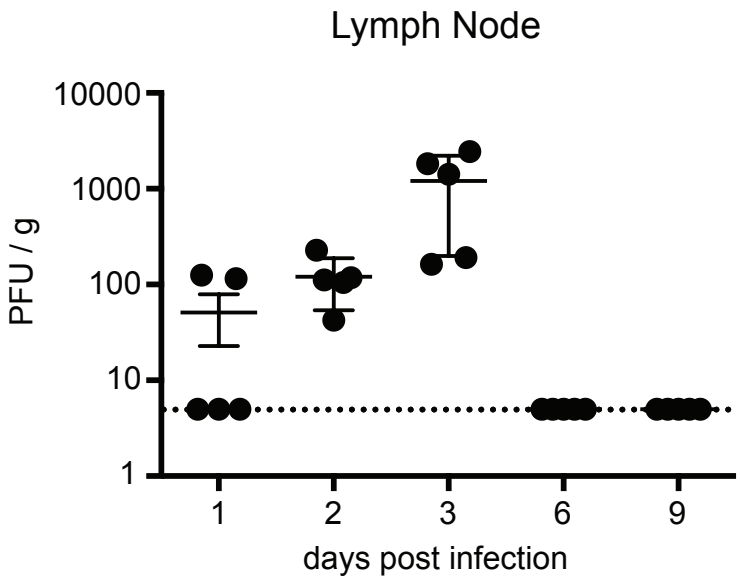
Lymph Node
10000
1000
100
10
1
PFU / g
1
2
3
6
9
days post infection

B

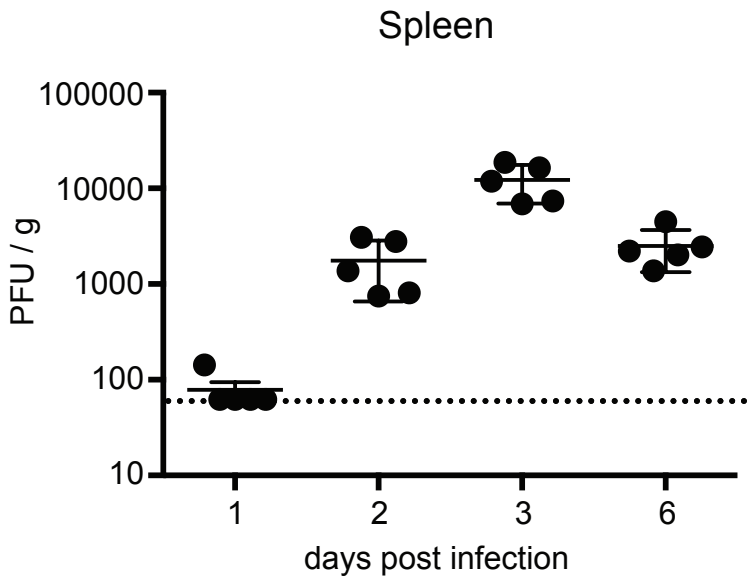
Spleen
100000
10000
1000
100
10
PFU / g
1
2
3
6
days post infection

Figure 25: Comparative kinetics of innate and adaptive lymphocyte expansion following CPXV or VV footpad infection.
Age and sex matched C57BL/6 mice were inoculated in the footpad with$1.5x10^6$ pfu/mouse of VV and at indicated time points, lymphocytes from the non-draining and draining LNs were isolated. (A-D) LNs were diced and incubated in Liberase TL before lymphocytes were isolated, stained and analyzed by flow cytometry. (E-G) Lymphocytes were isolated, stained and analyzed by flow cytometry and (A) total macrophages ($F4/80^+CD11b^+$), (B) total neutrophils ($Ly6G^+SSC^+$), (C) total migratory DCs ($CD11c^+MHCII^{high}$), (D) total LN resident DCs ($CD11c^+MHCII^+$), (E) total T cells ($CD3^+CD19^-NK1.1^-$), (F) total B cells ($CD19^+CD3^-NK1.1^-$) and (G) total NK cells ($NK1.1^+CD3^-CD19^-$) were identified. (A-F) Graphs depicting the average of 3 independent experiments are shown. (G) The graphs depict average of n=6 independent experiments (18 hpi), n=14 independent experiments (1 dpi), n=3 independent experiments (36hpi), n=8 independent experiments (2 & 3 dpi), and n=2 independent experiments (6 & 9dpi).

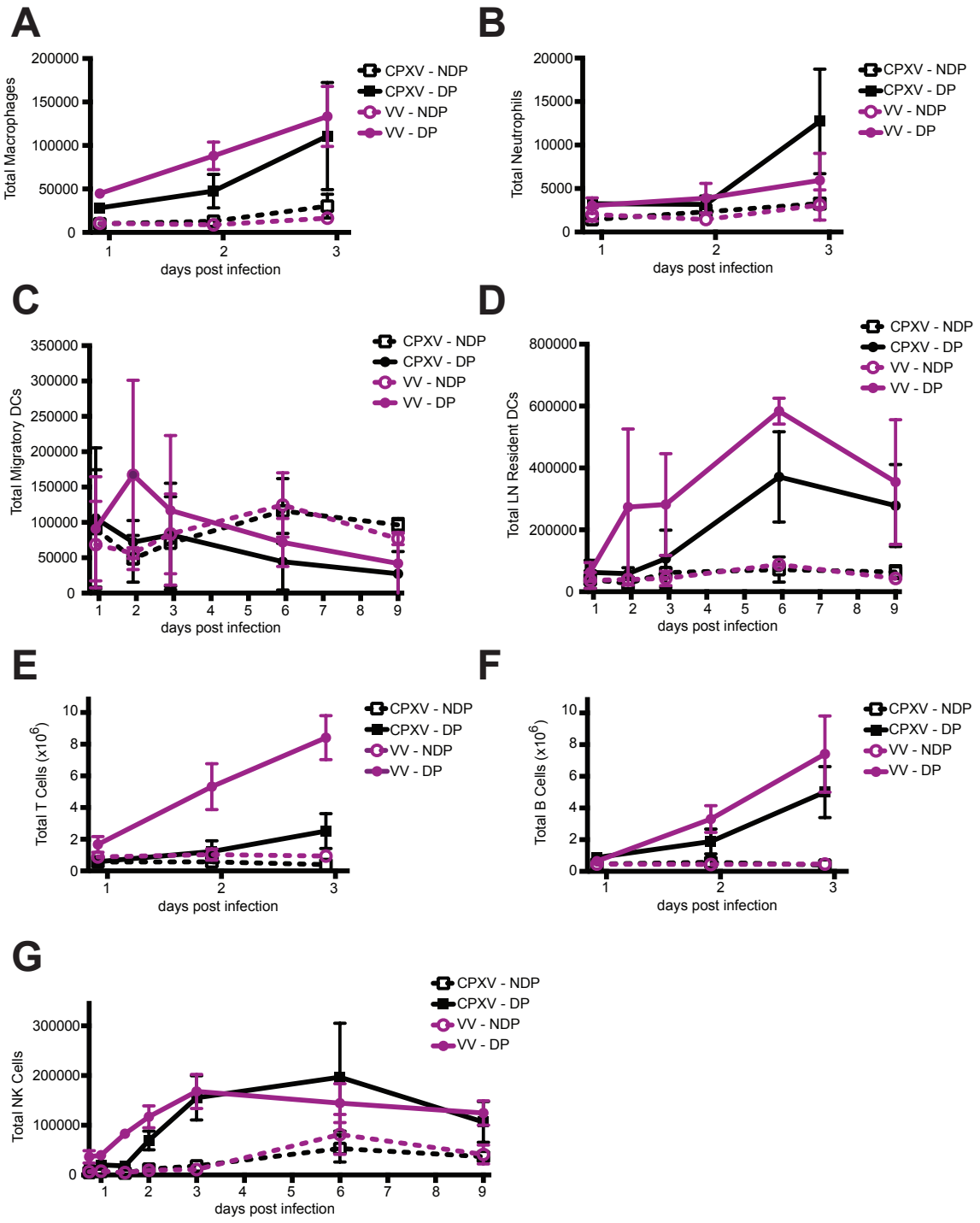
A
Total Macrophages
200000
150000
100000
50000
0
1
2
3
days post infection
CPXV - NDP
CPXV - DP
VV - NDP
VV - DP
B
Total Neutrophils
20000
15000
10000
5000
0
1
2
3
days post infection
CPXV - NDP
CPXV - DP
VV - NDP
VV - DP
C
Total Migratory DCs
350000
300000
250000
200000
150000
100000
50000
0
1
2
3
4
5
6
7
8
9
days post infection
CPXV - NDP
CPXV - DP
VV - NDP
VV - DP
D
Total LN Resident DCs
800000
600000
400000
200000
0
1
2
3
4
5
6
7
8
9
days post infection
CPXV - NDP
CPXV - DP
VV - NDP
VV - DP
E
Total T Cells (x10^6)
10
8
6
4
2
0
1
2
3
days post infection
CPXV - NDP
CPXV - DP
VV - NDP
VV - DP
F
Total B Cells (x10^6)
10
8
6
4
2
0
1
2
3
days post infection
CPXV - NDP
CPXV - DP
VV - NDP
VV - DP
G
Total NK Cells
300000
200000
100000
0
1
2
3
4
5
6
7
8
9
days post infection
CPXV - NDP
CPXV - DP
VV - NDP
VV - DP

Figure 26: NK cells isolated from the draining LN following VV infection express markers of splenic but not thymic NK cell subsets.
Age and sex matched C57BL/6 mice were infected as before and lymphocytes from the spleen, thymus, draining and non-draining LN were isolated 1 dpi and surface stained. Following identification of NK cells ($NK1.1^{+}CD3^{-}CD19^{-}$), expression of (A) Mac-1 (CD11b) (B) pan-Ly49 family receptors (Ly49ADCIFH), (C) L-selectin (CD62L), (D) DX5 (CX5), (E) CD94, (F) NKG2D, (G) IL-7Rα (CD127) and (H) integrin αE (CD103) was determined. Surface staining remained the same when observing NK cells isolated from these organs at 2 and 3 dpi.

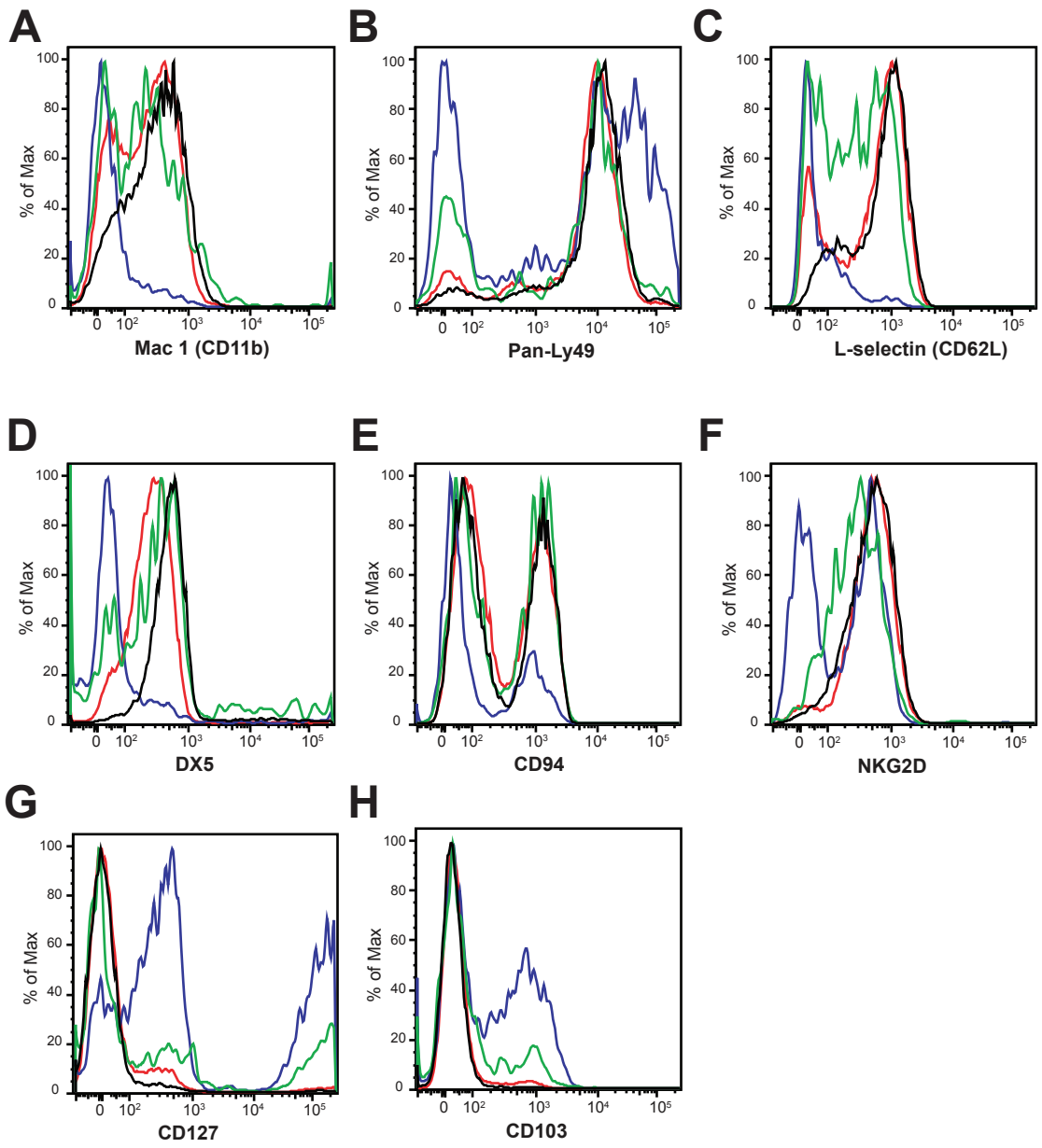
A
B
C
D
E
F
G
H
% of Max
Mac 1 (CD11b)
Pan-Ly49
L-selectin (CD62L)
DX5
CD94
NKG2D
CD127
CD103
NK Cells Isolated From:
Draining LN
Spleen
Non-Draining LN
Thymus

Figure 27: NK expansion in the draining LN is pertussis toxin sensitive following VV infection.
Splenocytes isolated from congenic C57BL/6 (CD45.2) and B6.LY5.2 (CD45.1) mice were pre-treated *in vivo* with PBS or pertussis toxin for 2 hours at 37°C, 5% CO_2 before being washed, CFSE labeled, mixed and co-injected IV into C57BL/6 mice. Immediately following adoptive transfer, the mice were infected with $1.5x10^6$ pfu of VV in the footpad. At the indicated time points, LNs were harvested and NK cells ($NK1.1^+CD3^-CD19^-$) were identified. Host NK cell recruitment ($CFSE^-$) (A) or donor NK cell recruitment ($CFSE^+$) (B) is shown over time. Data are representative of 2 independent experiments.

A

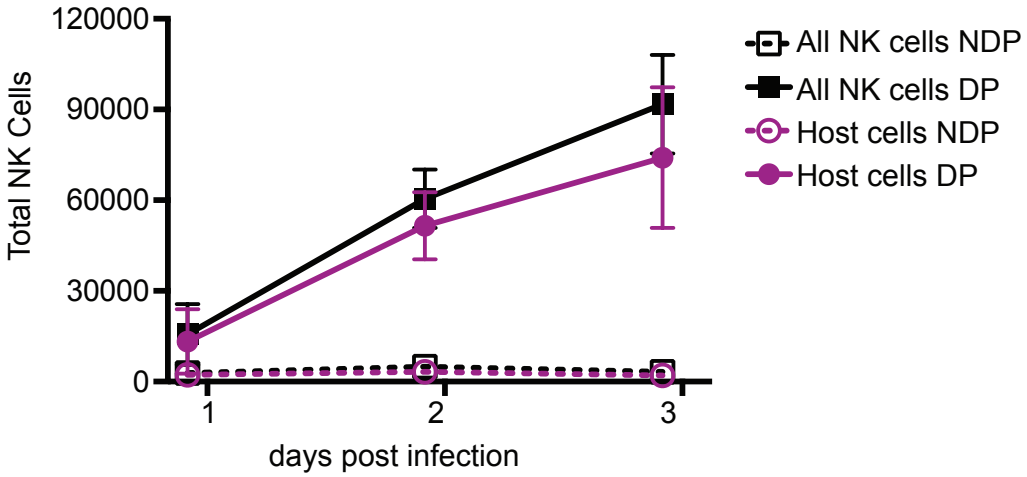
120000
90000
60000
30000
0
Total NK Cells
1
2
3
days post infection
All NK cells NDP
All NK cells DP
Host cells NDP
Host cells DP

B

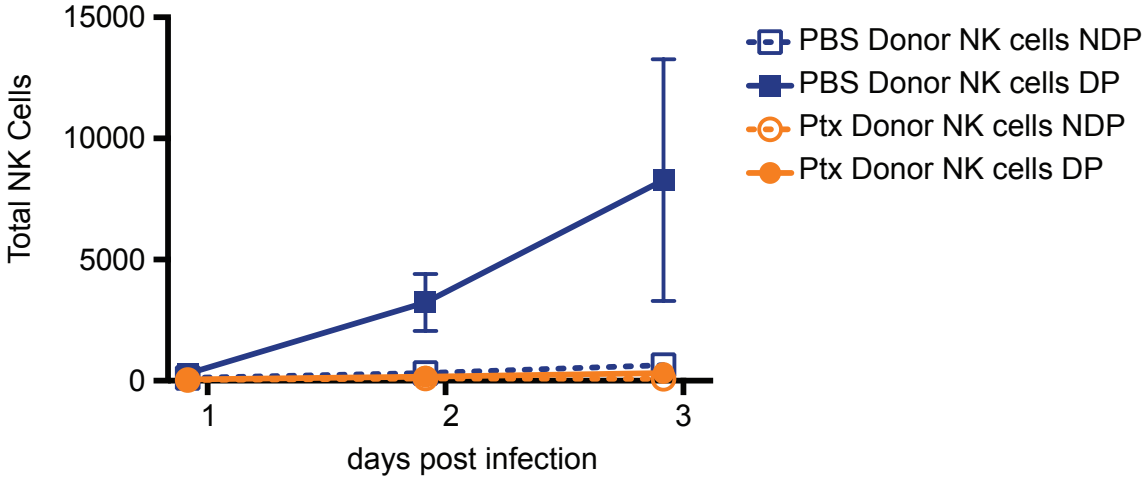
15000
10000
5000
0
Total NK Cells
1
2
3
days post infection
PBS Donor NK cells NDP
PBS Donor NK cells DP
Ptx Donor NK cells NDP
Ptx Donor NK cells DP

Figure 28: Inflammatory chemokine transcripts are up-regulated following VV infection.
RNA transcript levels were assessed in C57BL/6 mice infected with $1.5x10^6$ pfu of VV in the footpad at indicated time points by multiplex gene expression analysis. LNs from 3 independently infected mice were isolated and lysates from either the non-draining or draining LN were generated, run in triplicate, and chemokine transcripts normalized to the control *Hprt1* transcript for each sample. The fold change indicated in each square depicts the average transcript level in the draining LN relative to the non-draining LN.

	1 dpi	2 dpi	3 dpi
Cxcl1 (Groα)	9.67	2.89	1.40
Cxcl2 (Groβ)	17.38	0.85	1.10
Cxcl3 (Groγ)	1.02	0.30	0.31
Cxcl5 (ENA-78)	11.31	2.22	2.9
Cxcl9 (Mig)	12.95	6.26	3.72
Cxcl10 (IP-10)	19.72	19.24	10.81
Cxcl11 (I-TAC)	35.24	18.9	39.54
Cxcl12 (SDF-1α/β)	0.21	0.23	0.08
Cxcl13 (BLC/BCA-1)	0.58	0.59	0.47
Cxcl14 (BRAK/bolekine)	1.95	0.42	0.87
Cxcl15 (Lungkine/WECHE)	0.16	0.10	0.15
Cxcl16 (None)	0.75	0.59	0.41
Xcl1 (Lymphotactin)	5.07	3.96	2.30

	1 dpi	2 dpi	3 dpi
Ccl1 (I-309)	0.33	0.26	0.59
Ccl2 (MCP-1)	18.94	9.09	11.44
Ccl3 (Mip-1a)	5.16	4.06	6.01
Ccl4 (Mip-1b)	7.97	5.86	4.74
Ccl5 (RANTES)	0.58	0.70	0.39
Ccl6 (C10/MRP1)	2.88	1.19	1.10
Ccl7 (MCP-3)	14.56	5.45	6.86
Ccl8 (MCP-2)	0.47	0.84	0.18
Ccl9 (MRP-2/MIP-1γ)	1.92	1.85	1.64
Ccl11 (Eotaxin)	3.17	0.94	0.95
Ccl12 (MCP-5)	1.99	1.46	0.82
Ccl17 (TARC)	0.99	0.28	0.16
Ccl19 (MIP3β/ELC)	1.30	0.59	0.27
Ccl20 (MIP-3α/LARC)	1.38	5.90	12.77
Ccl21a (6CKine/SLC)	0.31	0.28	0.10
Ccl22 (MDC)	0.88	0.37	0.25
Ccl24 (Eotaxin-2/MPIF-2)	11.77	0.83	0.97
Ccl25 (TECK)	0.88	0.72	0.58
Ccl27a (CTACK)	0.78	0.44	0.44
Ccl28 (MEC)	2.02	0.70	1.30

Figure 29: NK cell recruitment occurs in the absence of CCR2 and CCR5 but intrinsically requires CXCR3 expression following VV infection.
Age and sex matched C57BL/6 and (A) CCR2-deficient, (B) CCR5-deficient or (C) CXCR3-deficient mice were infected with $1.5x10^6$ pfu of VV. At indicated time points, lymphocytes from the non-draining and draining LNs were isolated, stained and analyzed by flow cytometry. Total NK cells ($NK1.1^+CD3^-CD19^-$) were identified. The graph depicts the average of 3 independent experiments. (D) C57BL/6 (CD45.1) and $CXCR3^{-/-}$ (CD45.2) splenocytes were isolated and enriched by negative selection before being CFSE labeled, mixed and co-transferred intravenously into C57BL/6 mice. 1 day after the transfer, mice were infected as before and NK cell populations were examined at indicated time points. To analyze the recruitment in this system, the total number of recruited wild-type or chemokine knockout NK cells at 2 and 3 dpi were compared relative to the initial time point at 1 dpi. A representative result of 3 independent experiments is shown.

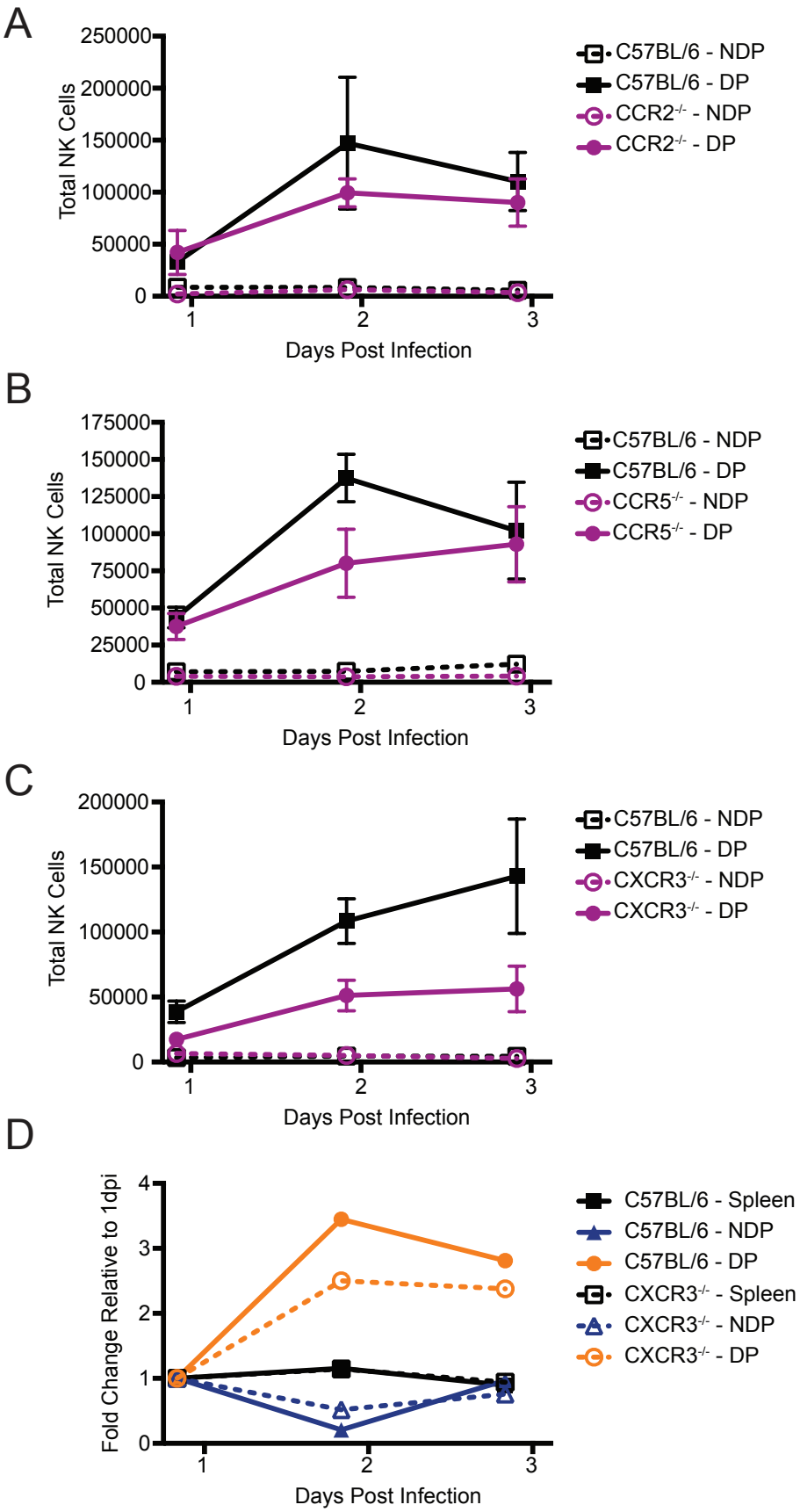
A
250000
200000
150000
100000
50000
0
Total NK Cells
1
2
3
Days Post Infection
C57BL/6 - NDP
C57BL/6 - DP
CCR2-/- - NDP
CCR2-/- - DP
B
175000
150000
125000
100000
75000
50000
25000
0
Total NK Cells
1
2
3
Days Post Infection
C57BL/6 - NDP
C57BL/6 - DP
CCR5-/- - NDP
CCR5-/- - DP
C
200000
150000
100000
50000
0
Total NK Cells
1
2
3
Days Post Infection
C57BL/6 - NDP
C57BL/6 - DP
CXCR3-/- - NDP
CXCR3-/- - DP
D
4
3
2
1
0
Fold Change Relative to 1dpi
1
2
3
Days Post Infection
C57BL/6 - Spleen
C57BL/6 - NDP
C57BL/6 - DP
CXCR3-/- - Spleen
CXCR3-/- - NDP
CXCR3-/- - DP

Figure 30: BMDCs do not complement NK cell recruitment defects seen in CD11c-DTR transgenic mice following VV infection.
Age and sex matched C57BL/6 and CD11c-DTR transgenic mice were treated with 5 ng/g body weight of diphtheria toxin 1 day prior to injection of BMDCs and VV infection. Flt3L BMDCs were generated *in vitro*, labeled with CFSE and injected into the top of the foot while CPXV was injected in the bottom of the footpad of diphtheria toxin treated CD11c-DTR mice and C57Bl/6 mice. LNs were isolated 1 day later and treated with Liberase TL following which lymphocytes were isolated, stained and analyzed by flow cytometry. (A) Percent and (B) total donor derived BMDCs ($CD11c^{+}MHCII^{high}CFSE^{+}$) and (C) total NK cells ($NK1.1^{+}CD3^{-}CD19^{-}$) were assessed and graphed. The graph represents 1 mouse for BMDC injected alone and CXPV injected alone while BMDC and CPXV injected in the same foot represent the average 2 mice for both CD11c-DTR and C57BL/6 mice.

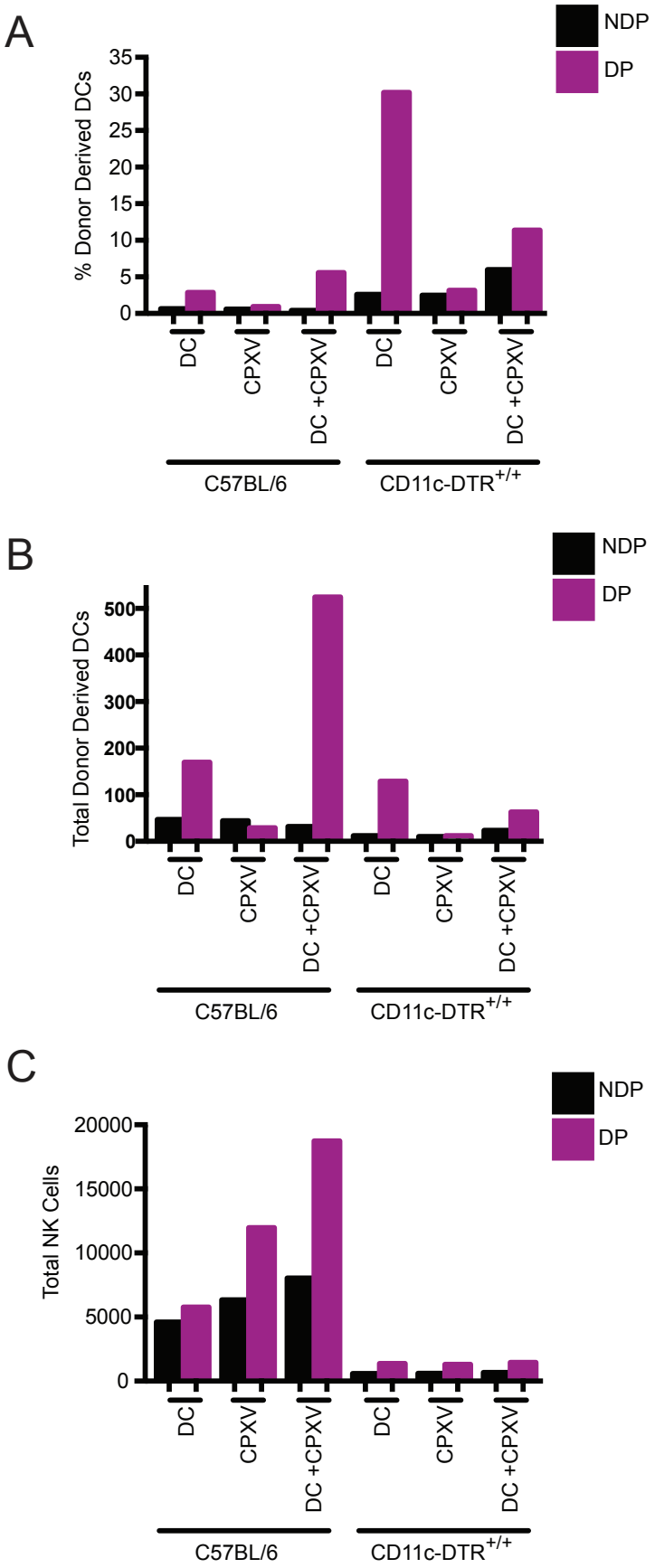
A
NDP
DP
% Donor Derived DCs
35
30
25
20
15
10
5
0
DC
CPXV
DC +CPXV
DC
CPXV
DC +CPXV
C57BL/6
CD11c-DTR+/+
B
NDP
DP
Total Donor Derived DCs
500
400
300
200
100
0
DC
CPXV
DC +CPXV
DC
CPXV
DC +CPXV
C57BL/6
CD11c-DTR+/+
C
NDP
DP
Total NK Cells
20000
15000
10000
5000
0
DC
CPXV
DC +CPXV
DC
CPXV
DC +CPXV
C57BL/6
CD11c-DTR+/+

CHAPTER 7:

Cowpox Virus Mediated-Inhibition of NK Cell Activation

During the initial analysis of NK cell recruitment, it became apparent that NK cells recruited to the draining LN following CPXV infection were not producing IFN-γ. This cytokine is an important mediator of the inflammatory response and contributes to priming of a T_H1 adaptive immune response (54, 107, 131, 137, 148). NK cells are one of the major producers of IFN-γ at early times following infection. This chapter describes the inhibition of NK cells by CPXV in a footpad model of infection.

NK Cells Recruited by CPXV Do Not Produce IFN-γ

One of the primary functions of NK cells aside from target cell lysis is production of cytokines, including IFN-γ which primes a T_H1 T cell response (54, 107, 148). It was demonstrated that following ECTV infection, NK cells producing IFN-γ were recruited to the draining LN at early times following infection (80, 81). With these studies informing our experiments, NK cells recruited to the draining LN were examined for IFN-γ following CPXV footpad inoculation. Surprisingly, at no time point studied did we observe NK cells producing IFN-γ (Figure 31A). In contrast to this CPXV specific finding, C57BL/6 mice inoculated with either VV or MCMV recruited IFN-γ producing NK cells in the draining LN (Figure 31A, 31B). Production of IFN-γ peaked between 1 and 2 dpi for MCMV and between 2 and 3 dpi for VV, time points where there was no IFN-γ observed following CPXV infection.

Since it was possible that the lack of IFN-γ production by NK cells following CPXV infection may have been a consequence of insufficient infectious dose, we examined a range of CPXV doses to determine if it was possible to induce IFN-γ production under any circumstances. However, IFN-γ production by NK cells did not

occur when mice were inoculated with a wide range of doses, from 3.75 x 10^3 pfu/mouse to 3.75 x 10^6 pfu/mouse (Figure 32A). In contrast, we observed IFN-γ producing NK cells following infection with VV beginning at 3.75 x 10^4 pfu/mouse, with increased IFN-γ production directly correlating with increased infectious dose (Figure 32B). In order to simultaneously study both NK cell recruitment and IFN-γ inhibition by CPXV, all subsequent experiments were performed using a dose of 1.5 x10^6 pfu/mouse.

Cytokine Production in the Draining LN Following CPXV and VV Infection

NK cells are one of the primary sources of early IFN-γ production following infection by a variety of pathogens. As IFN-γ induced chemokines were found to be responsible for NK cell recruitment at 2 and 3 dpi following CPXV infection, we measured cytokine protein levels in the draining LN by cytometric bead array. We found that following infection with VV, IFN-γ was produced at constant levels between 1 and 3 dpi in the draining LN and diminished between 3 and 6 dpi (Figure 33A). In contrast, CPXV did not stimulate production of IFN-γ to the same extent as VV until 3 dpi. However, CPXV induced higher levels of IFN-γ than VV at 6 dpi. IFN-γ was reduced by 9 dpi infection for both viruses and only following CPXV infection did we see minimal levels of IFN-γ in the draining LN at 12 dpi. These data indicate that infection with VV induced a lower IFN-γ response at early times following infection that contracted more quickly, coinciding with earlier resolution of VV titers in the draining LN. Meanwhile, CPXV induced a greater but delayed IFN-γ response that was sustained longer and also corresponded with resolution of CPXV titers.

Following CPXV and VV infection, cytokine production closely correlated with the course of infection by either virus. Levels of IL-6, an inflammatory cytokine (149),

were similar following infection with either virus at 1 dpi, but differed at subsequent time points (Figure 33B, 33C). Levels of IL-6 increased following CPXV infection beginning at 2 dpi and peaking between 6 and 9 dpi. In contrast, following VV infection, levels of IL-6 remained fairly constant at all time points observed. CPXV *in vivo* infection induces of high levels of IL-10, an anti-inflammatory cytokine (39, 150). Following CPXV footpad infection, we observed sustained high levels of IL-10 through 6 dpi. In comparison, IL-10 levels following VV were lower at most time points observed, peaking at 1 dpi and not detected at 6 dpi. Protein production of MCP-1, otherwise known as CCL2, was also measured following infection with CPXV and VV. VV induced high CCL2 protein levels at 1 through 6 dpi while CCL2 protein levels were minimal following CPXV infections at these times (Figure 33D). Detection of high levels of CCL2 did not occur until 9 dpi following CPXV, a time point where CCL2 production was declining following VV infection. Taken together, these data suggest that infection with CPXV leads to expression of anti-inflammatory cytokines at early times following infection, lending further evidence in support of our hypothesis that CPXV more completely inhibits the immune response than VV.

Activation of NK Cells is Incomplete Following CPXV Infection

The lack of IFN-γ production by NK cells suggested that CPXV subverted NK cell function. Seemingly in contrast to these findings, we observed an increased viral burden in the draining LN in the absence of NK cells, suggesting anti-viral NK cell functionality in spite of IFN-γ inhibition. We therefore examined whether recruited NK cells were activated following infection with CPXV. Examining the surface expression of several activation markers, we observed that NK cells isolated from the draining LN had

little to no expression of CD69 or CD25 (Figure 34). When examining NK cells isolated from the draining LN following VV infection, we observed differential expression of surface activation markers. At 1 dpi, CD69 was up-regulated but surface expression decreased over time while the inverse was observed for CD25 (Figure 34). These results suggested CPXV infection inhibited the activation of NK cells in the draining LN.

Despite this lower expression of activation markers on NK cells following CPXV, systemic depletion of NK cells resulted in increased viral burden. In order to measure NK cell function, we examined the induction of granzyme B, an effector molecule in targeted cell lysis. In contrast to IFN-γ production, NK cells isolated from the draining LN following both CPXV and VV infection produced higher levels of granzyme B than NK cells isolated from the non-draining LN when examined by flow cytometry (Figure 35). These data suggest that since NK cells produced granzyme B, resistance to CPXV infection may be mediated through cell lysis.

NK cell Production of IFN-γ is Inhibited by CPXV Infection

We had several hypotheses regarding the differential ability of NK cells to produce IFN-γ following CPXV or VV infection. The first hypothesis was that VV but not CPXV encoded a molecule that was recognized by an activating NK cell receptor, akin to m157 mediated activation following MCMV infection (57). Alternately, it was also possible that CPXV, having a larger genome than VV and therefore a greater number of potentially inhibitory ORFs, contained one or more unique ORFs that inhibited IFN-γ production by NK cells. Additionally, neither of these hypotheses is mutually exclusive, and it was possible that VV produced an activating molecule and CPXV produced an inhibitory molecule.

To determine if CPXV was inhibiting IFN-γ production by NK cells, we employed a co-infection model where C57BL/6 mice were injected with either CPXV or VV or a mixture of CPXV and VV at a 1:1 ratio. NK cells isolated from the draining LNs of co-infected mice did not produce IFN-γ, similar to following CPXV infection (Figure 36A, 36B). These data indicated that NK cell production of IFN-γ was being inhibited by CPXV infection. To ensure that VV was replicating following co-infection, we used CPXVΔ203-GFP, where GFP has been inserted in the place of CPXV203. Following co-infection, LNs were titered and plaques that expressed GFP, indicating CPXV replication, were counted prior to fixing and staining all plaques on the monolayer allowing differentiation between CPXV and VV plaques. At early time points, we observed that most plaques were GFP positive, indicating mostly CPXV replication (Figure 36C). However, 2 and 3 dpi, we observed plaques that did not express GFP indicating active VV replication at later times following co-infection. These data indicate that NK cells production of IFN-γ is actively inhibited by CPXV infection, even during co-infection with VV.

Next we examined the effect of varying the co-infection ratio to determine whether CPXV mediated inhibition of IFN-γ production by NK cells could be overcome. When the amount of CPXV in the co-infection was lowered, there was an intermediate restoration of IFN-γ production by recruited NK cells (Figure 37A, 37B). However, when the amount of CPXV was maintained at the normal dose and the dose of VV was increased, recruited NK cells were not capable of producing IFN-γ (Figure 37A, 37B). These data suggest that CPXV is producing an inhibitory molecule that at $1.5x10^6$ pfu/mouse is sufficient to inhibit NK cell production of IFN-γ, even in the presence of overwhelming VV infection. However, since IFN-γ production was less inhibited when

using a decreased dose of CPXV during the co-infection, it appears that the putative CPXV inhibitory molecule can be titrated. As these data suggested that CPXV inhibition could be overcome *in vivo*, we attempted to stimulate NK cells *ex vivo* with PMA and ionomycin. Treatment with this strong stimulus resulted in production of IFN-γ by NK cells (Figure 37C). These data indicated that CPXV inhibition can be overcome both *in vivo* by limiting the CPXV infectious dose in a co-infection model and *ex vivo* with a strong stimulus.

Inhibition of IFN-γ Production in NK Cells is Complex and Multifactorial

Next, we performed genomic comparisons between CPXV Brighton Red, ECTV Moscow, and VV Western Reserve to identify likely candidate ORFs in CPXV which might be responsible for the inhibition of IFN-γ production by NK cells. Since footpad infection with VV and ECTV induces the recruitment of IFN-γ producing NK cells (80, 81), we chose to exclude CPXV ORFs with homologues in VV or ECTV. Based on a nucleotide sequence identity threshold of 80%, we determined that there were 36 unique CPXV specific ORFs (Table 2). The identification of CPXV012, CPXV018 and CPXV203 in our screen, which have previously been demonstrated to be unique CPXV ORFs (29, 30, 85) supported the validity of our screen.

To rule out ORFs not involved in inhibition of IFN-γ by NK cells, we first tested viruses deficient for ORFs that had previously been implicated in the down-regulation of MHC class I or could bind *in vitro* with high affinity to the NK activating receptor, NKG2D. We found that infection with CPXVΔ012, CPXVΔ018, and CPXVΔ203, induced recruitment of NK cells to draining LNs in numbers equivalent to wild-type CPXV infection (Figure 38A, 38C, 38E). However, these NK cells still failed to produce

IFN-γ, indicating that these ORFs were not responsible for the inhibition of NK cells (Figure 38B, 38D, 38F).

Given the large number of CPXV specific ORFs identified in our screen, it seemed impractical to generate single mutant deletion viruses for all 36 ORFs and systematically examine them for an IFN-γ inhibition phenotype. Instead, we employed large deletion mutants generated by a collaborator to screen many ORFs at the same time. One of these mutants, A587 contains two deletions, one within each terminal region of the CPXV genome. ORFs 3-9 and 222-227 are missing from the A587 mutant and 7 of the CPXV unique ORFs fall within these deletions including ORF 3, 7, 8, 9, 222, 223, and 224. When the A587 mutant was used to infect mice, we found similar recruitment of NK cells to the draining LN (Figure 39A) but no IFN-γ producing NK cells (Figure 39B). Therefore the inhibition of NK production of IFN-γ was unchanged and we discounted those 7 predicted ORFs.

We next examined the A518 mutant, which has one large deletion of ORFs 11-36, including 7 unique to CPXV which were identified in our genomic screen: 12, 13, 17, 18 19, 20 and 31f. Again, recruitment of NK cells to the draining LN was comparable using the A518 mutant to recruitment following either CPXV or VV (Figure 40A). When we infected using this virus, we found a partial restoration of IFN-γ production (Figure 40B). The expression of CD69 was also observed at later time points after infection and appeared to correlate with the induction of IFN-γ expression (Figure 40C). In contrast, expression of CD25 did not appear to correlate with IFN-γ expression following CPXV and A518 mutant infection (Figure 40C). Given the partial restoration of IFN-γ and CD69 expression, we postulated that the inhibitory ORF lay within this deletion.

To determine whether a particular ORF was responsible for the lack of IFN-γ inhibition in the A518 mutant, we used two viruses with deletions within the A518 deleted region: one lacking ORFs 18-21 and another lacking ORFs 22-36. While both of these viruses recruited NK cells similarly to wild-type CPXV (Figure 41A), they also both recruited NK cells that produced intermediate IFN-γ levels similar to the A518 recruited NK cells (Figure 41B). These data suggest that CPXV inhibition of IFN-γ production by NK cells was the product of at least two ORFs in the 11-36 region, making inhibition multifactorial.

Discussion

Here we demonstrate that CPXV recruited NK cells were not fully mature, as demonstrated by decreased expression of surface maturation molecules and the inability to produce IFN-γ. CPXV recruited NK cells retain the ability to produce granzyme B and limit viral replication in the draining LN, and are therefore still functional despite incomplete maturation. Our data indicate that incomplete NK cell maturation is the product of active inhibition by CPXV. This inhibition is complex and multifactorial since it is partially abrogated during infection with CPXV mutants that contain large genomic deletions.

NK cells have both the capacity to directly lyse target cells and to induce cytokines which shape the adaptive immune response. Following CPXV infection, NK cells kill infected cells through direct lysis mediated through granzyme B, but are inhibited for IFN-γ production. One hypothesis which may explain this phenotype is that CPXV can inhibit only one of multiple activation signals that are required to stimulate different NK cell functions (151). Supporting this hypothesis, NK cells can express small

amounts of Klrg1 and normal granzyme B following CPXV infection. CD69 and IFN-γ are most highly expressed at early times after infection with VV, and both correspondingly decrease as the infection progresses. In either the A518 mutant or the co-infection model where a partial restoration of IFN-γ production was observed, a slight increase in CD69 is also observed. These data suggest that the same signal may be responsible for CD69 expression and IFN-γ induction while induction of granzyme B may occur following an alternate signal. Additionally, when examining expression of CD25, we observed that it does not appear to be linked to either IFN-γ or granzyme B expression, suggesting yet another signal might be important for NK cell survival. NK cells can respond to a variety of signals including type I IFNs, other pro-inflammatory cytokines and direct receptor ligation. Therefore it is possible that integration of multiple disparate signals result in different functionality of NK cells.

There are several alternate hypotheses that could explain this NK cell activation phenotype. It is also possible that NK cell stimulation following CPXV infection is interrupted and the phenotype results from partial activation by an immediate early or early CPXV ORF(s) before inhibition occurs. Additionally, NK cells can be directly infected by VV(152, 153), so it is possible they may also be infected by CPXV, limiting their activation. At this time, we have not examined CPXV tropism, but direct infection of NK cells by CPXV is an intriguing idea. Finally, incomplete activation of NK cells could result from a combination of any of these hypotheses.

When examining cytokine protein expression by multiplex analysis, we found a close correspondence between CPXV or VV infection and cytokine induction. Following VV infection, there was induction of both IL-6 and IFN-γ, both pro-inflammatory cytokines that may stimulate more rapid recruitment of inflammatory lymphocytes and

therefore early resolution of VV titers in the draining LN. In contrast, CPXV induced expression of these inflammatory molecules is delayed. Instead CPXV infection increased early expression of IL-10, which is known to be inhibitory towards maturation of DCs and macrophages and inhibit function of T and NK cells (150, 154). These cytokine expression profiles indicate a more inhibitory nature of CPXV infection in the draining LN.

Following CPXV infection IFN-γ protein expression was observed in the draining LN. Since we know that recruited NK cells are not responsible for production of this IFN-γ, another cell must be the source of this cytokine. The early expression of IFN-γ protein suggests that another innate lymphocyte may be responsible for its production. Several innate lymphocytes have been implicated in very early production of IFN-γ including NKT cells and an innate $CD8^+$ T cell population (131, 155). At this time, these populations have not been examined in the context of our CPXV footpad infection. IFN-γ production continues to increase in the draining LN following CPXV infection, peaking at 6 dpi, when adaptive $CD8^+$ T cells could be responsible for its production. While CPXV, like all orthopoxviruses, encodes an IFN-γ binding protein, this protein has been shown to be unable to bind murine IFN-γ (156). Thus it is likely that the induction of IFN-γ helps control CPXV infection in the draining LN.

The co-infection experiments indicate that CPXV produces an inhibitory molecule that dominates any potential VV derived activating molecule. Since co-infection of single cells is likely to be rare following injection with both CPXV and VV, we speculated that the inhibitory molecule was either a surface expressed molecule or secreted. If the inhibitory molecule was intracellular, then the cells infected with only VV during co-infection would be expected to stimulate IFN-γ production by recruited NK

cells and intermediate production of IFN-γ would be observed. However, the inhibition of IFN-γ was absolute at all time points observed following co-infection supporting our hypothesis that the inhibitory molecule is surface expressed or secreted.

In attempts to address this hypothesis of extracellular inhibition, we varied the ratio of CPXV and VV used during co-infection experiments. These experiments indicated that the amount of CPXV present was the limiting factor for inactivation of NK cells, again confirmed the dominance of the inhibitory molecule(s). Inhibitory molecules are often dominant to activating molecules, examples of which can be found within NK cell receptor signaling. NK cell inhibitory receptors that sense MHC class I on potential targets cells strongly inhibit activation of NK cells and viruses have evolved to exploit this interaction. They do so employing mechanisms including MHC class I mimicry and stabilization of Qa-I/HLA-E to signal inhibitory NKG2/CD94 receptors (157-160). Thus the strong inhibition of NK cell IFN-γ production by CPXV could be overpowering any potential ORF encoded by VV and future studies must be performed to determine if such an activating ORF exists.

Our attempt to identify the inhibitory ORF expressed by CPXV resulted in discovery of several mutants with intermediate IFN-γ production, including the the A518 mutant, CPXVΔ18-21 and CPXVΔ22-36. These findings lead to several potential hypotheses. First, it could be that there are multiple ORFs responsible for inhibition of IFN-γ production, located in this region that could be NK specific. Another possibility is that CPXV lacking the inhibitory ORF is not capable of inducing IFN-γ production to the levels that VV does. Experiments designed to test both of these hypotheses will be complicated by numerous non-NK specific inhibitory proteins encoded within the terminal regions of the CPXV genome, including multiple cytokine-binding proteins.

These data suggest that inhibition of IFN-γ is multifactorial and will be difficult to dissect using single deletion analysis.

Here we have examined the activation of NK cells following CPXV footpad infection. Surprisingly, given increased viral burdens in systemically NK cell depleted mice, NK cells recruited to the draining LN did not produce IFN-γ or up-regulate activation markers during CPXV infection. Control of viral replication may therefore involve granzyme B mediated target cell lysis, as expression of granzyme B remained unaffected following CPXV infection. Attempts to identify the CPXV ORFs responsible for NK cell inhibition have only underscored the complex, multifactorial nature of NK cell function, especially in the context of viral infection.

Figure 31: CPXV infection inhibited production of IFN-γ by NK cell recruited to the draining LN.
Age and sex matched C57BL/6 mice were infected with $1.5x10^6$ pfu/ms of CPXV or VV or $8.5x10^4$ pfu/ms MCMV and at indicated times, cells from the draining and non-draining LN were isolated and stained. Following extracellular staining, cells were fixed, permeablized and intracellularly stained for IFN-γ. Total IFN-γ producing NK cells ($NK1.1^+CD3^-CD19^-IFN\text{-}\gamma^+$) cells following (A) CPXV, VV or (B) MCMV infection are graphed. (A) The graph depict average of n=6 independent experiments (18 hpi), n=14 independent experiments (1 dpi), n=3 independent experiments (36hpi), n=8 independent experiments (2 & 3 dpi), and n=2 independent experiments (6 & 9 dpi).

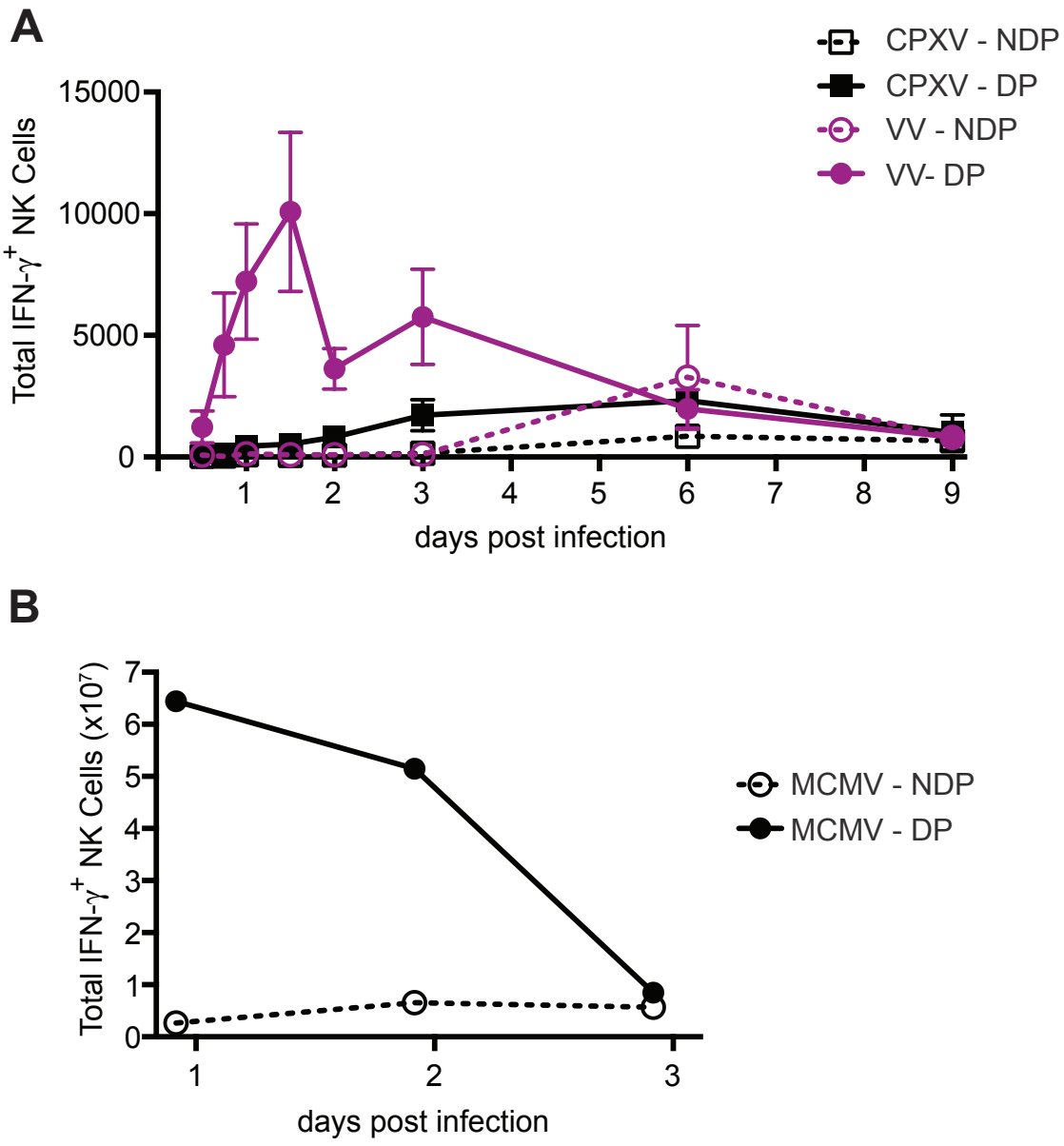
A
CPXV - NDP
CPXV - DP
VV - NDP
VV- DP
Total IFN-γ+ NK Cells
15000
10000
5000
0
1
2
3
4
5
6
7
8
9
days post infection
B
MCMV - NDP
MCMV - DP
Total IFN-γ+ NK Cells (x10⁷)
7
6
5
4
3
2
1
0
1
2
3
days post infection

Figure 32: VV infection but not CPXV infection stimulated NK production of IFN-γ in a dose dependent manner.
Age and sex matched C57BL/6 mice were infected with 3.75 x 10^3 pfu/mouse to 3.75 x 10^6 pfu/mouse of (A, C) CPXV or (B, D) VV. At indicated time points, cells from the draining and non-draining LN were isolated and stained. Following extracellular staining, cells were fixed, permeablized and intracellularly stained for IFN-γ. (A, B) Percent and (C, D) total IFN-γ producing NK Cells ($NK1.1^+CD3^-CD19^-IFN\text{-}\gamma^+$) cells following (A, C) CPXV and (B, D) VV infection are graphed.

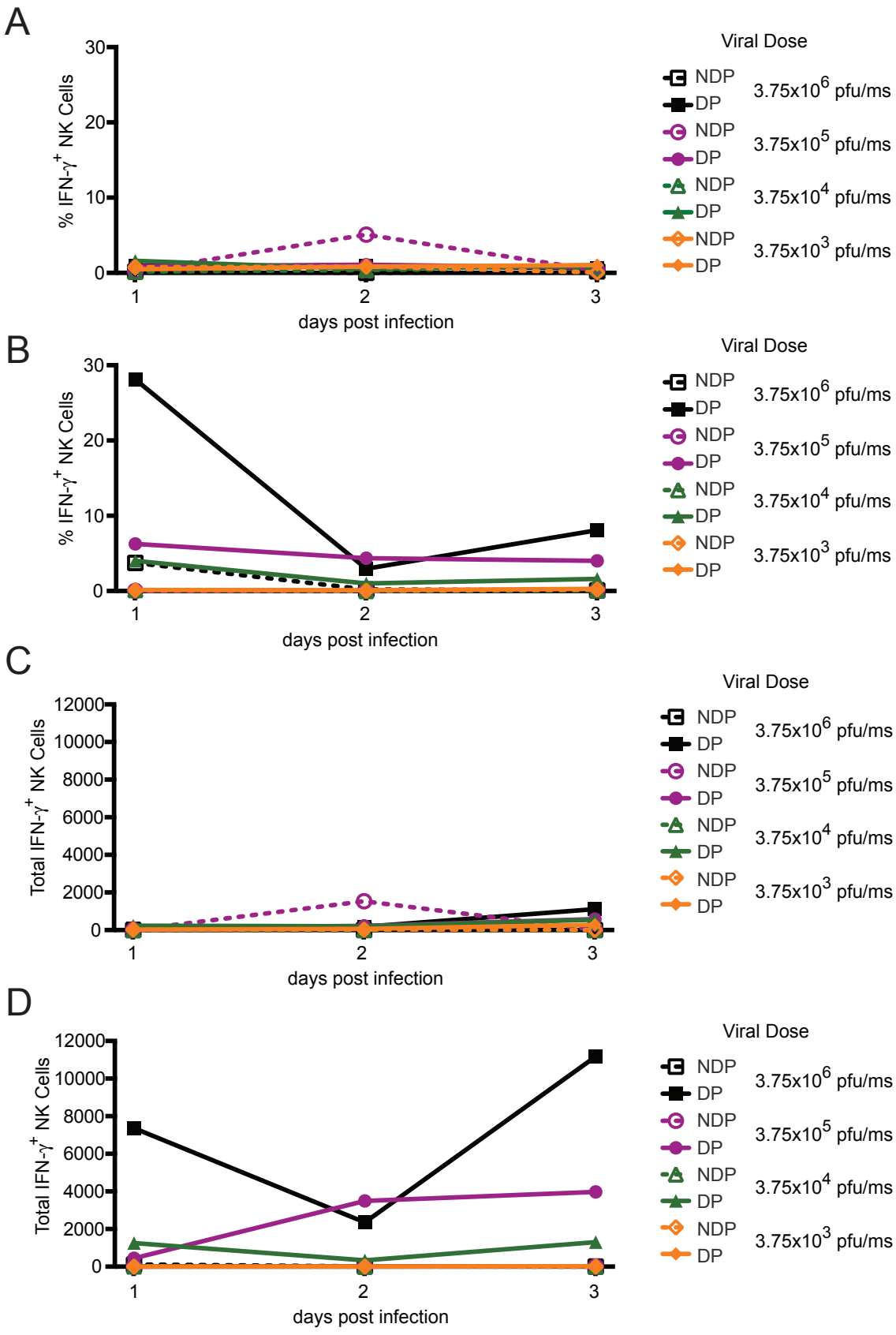
A
% IFN-γ+ NK Cells
30
20
10
0
1
2
3
days post infection
Viral Dose
NDP
DP
3.75x10^6 pfu/ms
NDP
DP
3.75x10^5 pfu/ms
NDP
DP
3.75x10^4 pfu/ms
NDP
DP
3.75x10^3 pfu/ms
B
% IFN-γ+ NK Cells
30
20
10
0
1
2
3
days post infection
Viral Dose
NDP
DP
3.75x10^6 pfu/ms
NDP
DP
3.75x10^5 pfu/ms
NDP
DP
3.75x10^4 pfu/ms
NDP
DP
3.75x10^3 pfu/ms
C
Total IFN-γ+ NK Cells
12000
10000
8000
6000
4000
2000
0
1
2
3
days post infection
Viral Dose
NDP
DP
3.75x10^6 pfu/ms
NDP
DP
3.75x10^5 pfu/ms
NDP
DP
3.75x10^4 pfu/ms
NDP
DP
3.75x10^3 pfu/ms
D
Total IFN-γ+ NK Cells
12000
10000
8000
6000
4000
2000
0
1
2
3
days post infection
Viral Dose
NDP
DP
3.75x10^6 pfu/ms
NDP
DP
3.75x10^5 pfu/ms
NDP
DP
3.75x10^4 pfu/ms
NDP
DP
3.75x10^3 pfu/ms

Figure 33: Kinetic analysis of cytokine expression in the draining LN following CPXV and VV infection.
Age and sex matched C57BL/6 mice were infected as before with CPXV or VV and at indicated times, LNs were isolated and homogenized by bead beating in RPMI. Cytokine production was measured using the mouse inflammation cytometric bead array. (A) IFN-γ, (B) IL-6, (C) IL-10 and (D) CCL2 (MCP-1) expression are graphed over time. The graph depicts the average of n=4 to 5 independently infected mice (1, 2, 3, 6, and 9 dpi) and n= 2 (CPXV) to 5 (VV) independently infected mice.

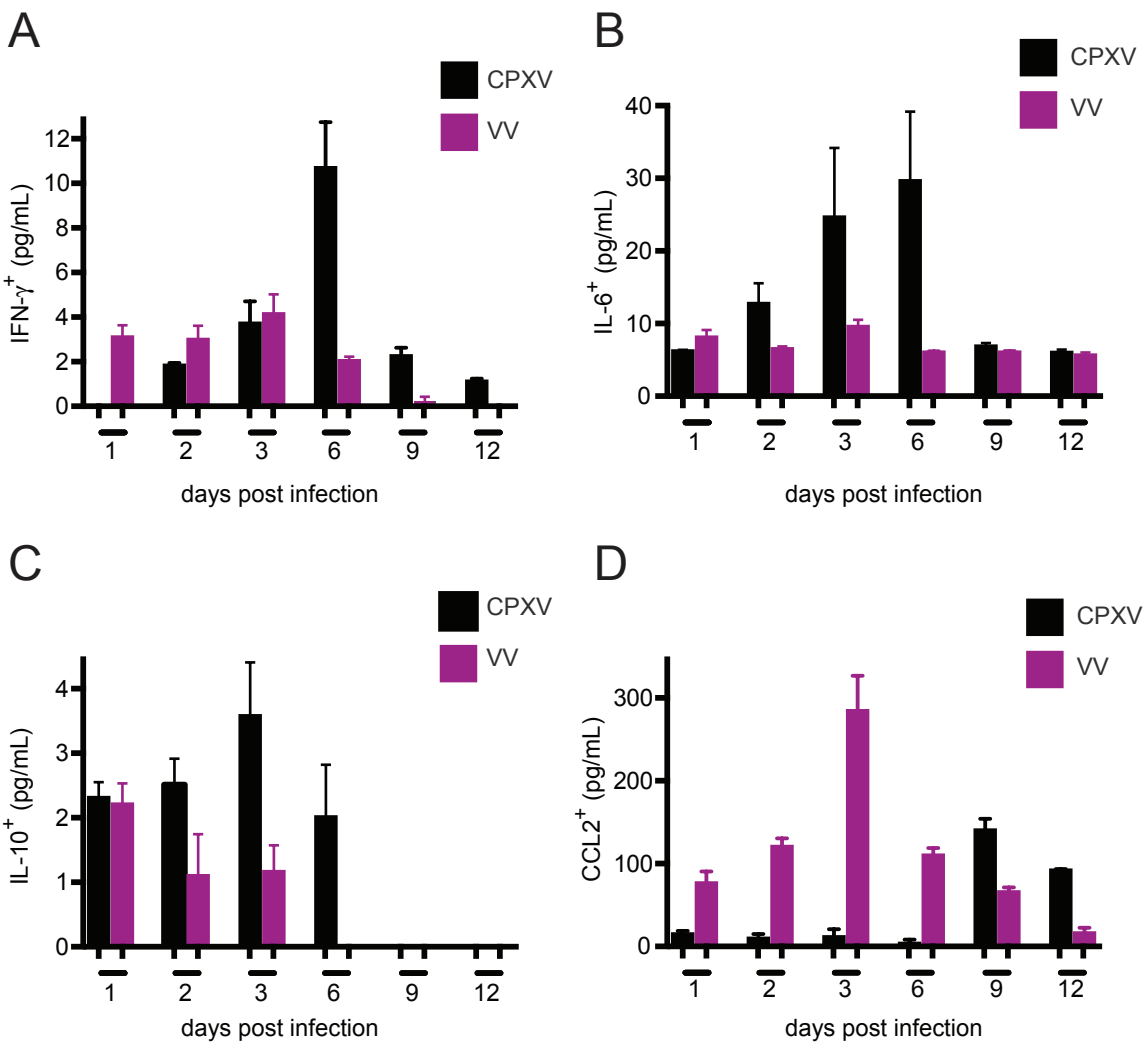
A
CPXV
VV
IFN-γ+ (pg/mL)
0
2
4
6
8
10
12
1
2
3
6
9
12
days post infection
B
CPXV
VV
IL-6+ (pg/mL)
0
10
20
30
40
1
2
3
6
9
12
days post infection
C
CPXV
VV
IL-10+ (pg/mL)
0
1
2
3
4
1
2
3
6
9
12
days post infection
D
CPXV
VV
CCL2+ (pg/mL)
0
100
200
300
1
2
3
6
9
12
days post infection

Figure 34: Kinetic analysis of NK cell expression of surface activation molecules following CPXV or VV infection.
Age and sex matched C57BL/6 mice were infected as before with CPXV or VV and at indicate times, lymphocytes from the draining and non-draining LN were isolated and stained. Following identification of NK cells ($NK1.1^{+}CD3^{-}CD19^{-}$), surface expression of CD69 and CD25 was determined. A representative result of 3 independent experiments is depicted.

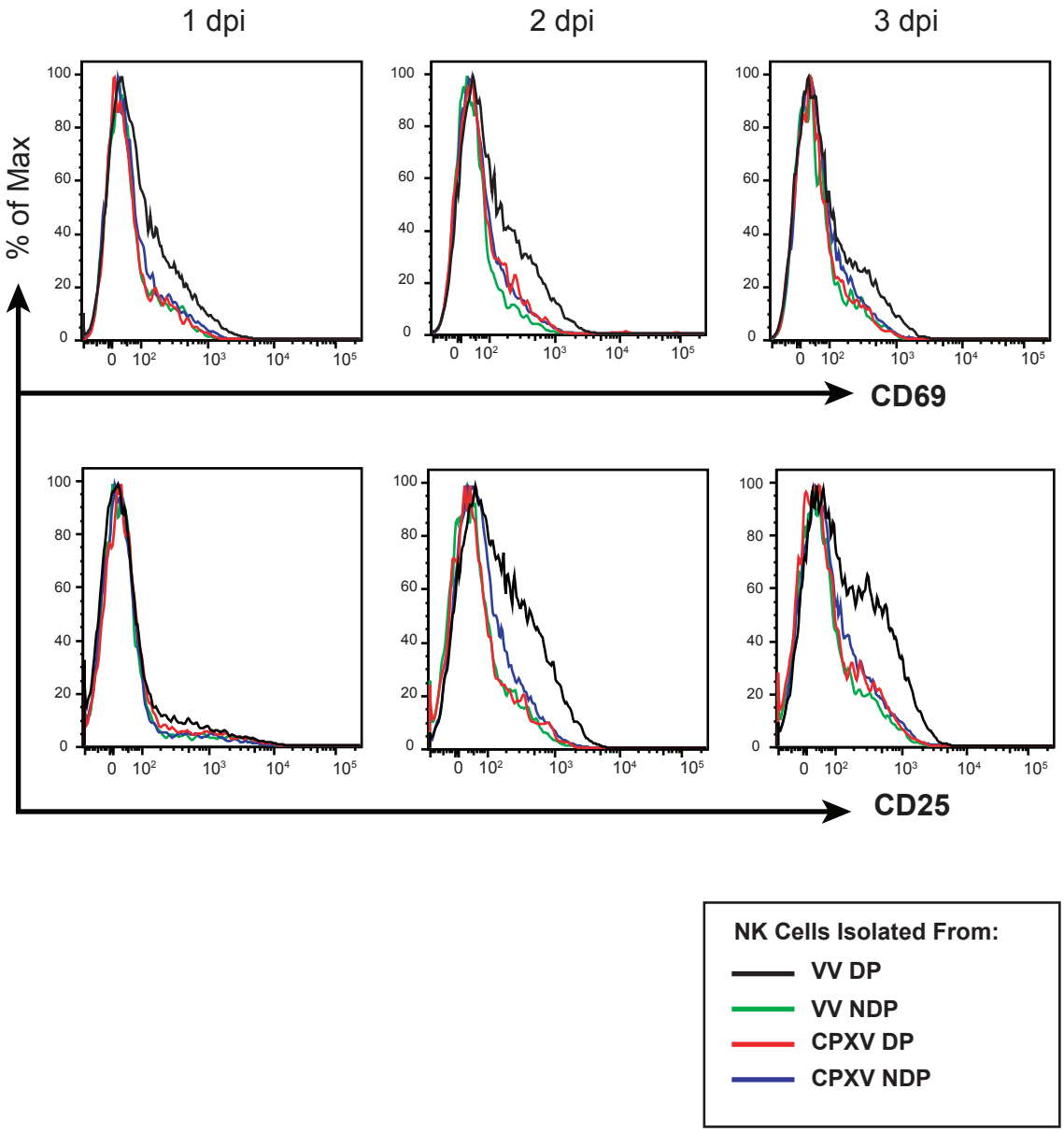
1 dpi
2 dpi
3 dpi
% of Max
CD69
CD25
NK Cells Isolated From:
VV DP
VV NDP
CPXV DP
CPXV NDP

Figure 35: NK cells produce granzyme B following CPXV and VV infection.
Age and sex matched C57BL/6 mice were infected as before and at indicated times, lymphocytes from the draining and non-draining LN were isolated and stained. Following extracellular staining, cells were fixed, permeablized and intracellularly stained for IFN-γ and granzyme B. Following identification of NK cells ($NK1.1^{+}CD3^{-}CD19^{-}$), IFN-γ and granzyme production was assessed. A representative dot plot from 10 independent experiments is shown.

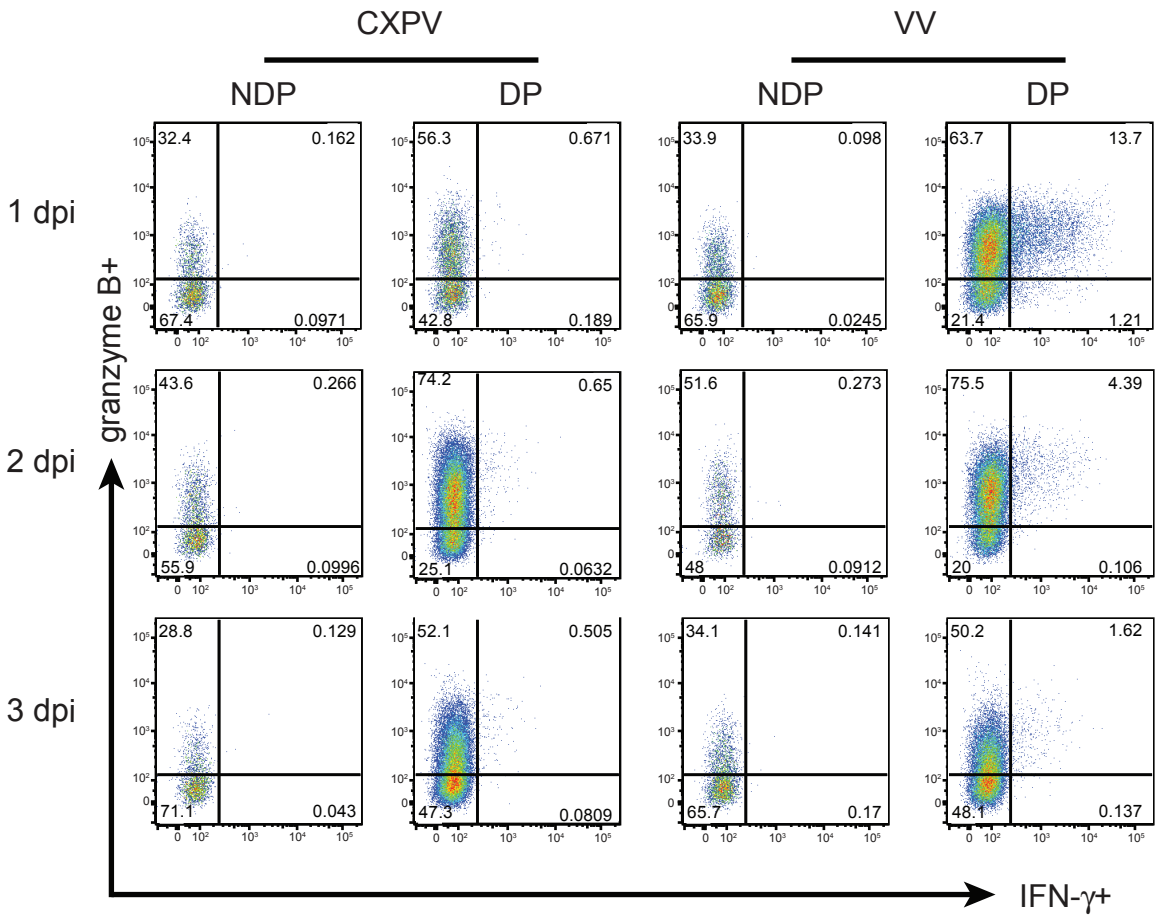
CXPV
VV
NDP
DP
NDP
DP
1 dpi
2 dpi
3 dpi
granzyme B+
IFN-γ+
32.4
0.162
67.4
0.0971
56.3
0.671
42.8
0.189
33.9
0.098
65.9
0.0245
63.7
13.7
21.4
1.21
43.6
0.266
55.9
0.0996
74.2
0.65
25.1
0.0632
51.6
0.273
48
0.0912
75.5
4.39
20
0.106
28.8
0.129
71.1
0.043
52.1
0.505
47.3
0.0809
34.1
0.141
65.7
0.17
50.2
1.62
48.1
0.137

Figure 36: NK cells do not produce IFN-γ following co-infection with CPXV and VV.

Age and sex matched C57BL/6 mice were infected with $1.5x10^6$ pfu/ms CPXV, VV or a 1:1 mixture of CPXV and VV. At indicated times, lymphocytes from the draining and non-draining LN were isolated and stained. Following extracellular staining, cells were fixed, permeablized and intracellularly stained for IFN-γ. (A) Percent and (B) total IFN-γ producing NK cells ($NK1.1^+CD3^-CD19^-IFN\text{-}\gamma^+$) for 4 independent experiments are depicted. (C) C57BL/6 mice were injected with $1.5x10^6$ pfu/ms CPXVΔ203-GFP, VV or a 1:1 mixture of CPXVΔ203-GFP and draining LNs were titered on CV-1 monolayers. GFP-expressing plaques were counted prior to crystal violet staining. Data represent the average of 1 mouse from 2 independent experiments.

A

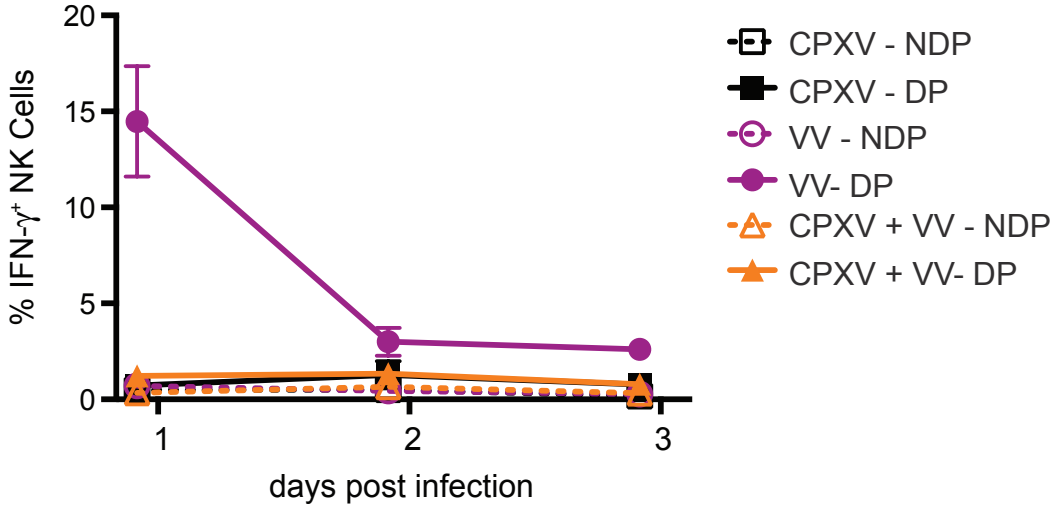
20
15
10
5
0
% IFN-γ+ NK Cells
1
2
3
days post infection
CPXV - NDP
CPXV - DP
VV - NDP
VV- DP
CPXV + VV - NDP
CPXV + VV- DP

B

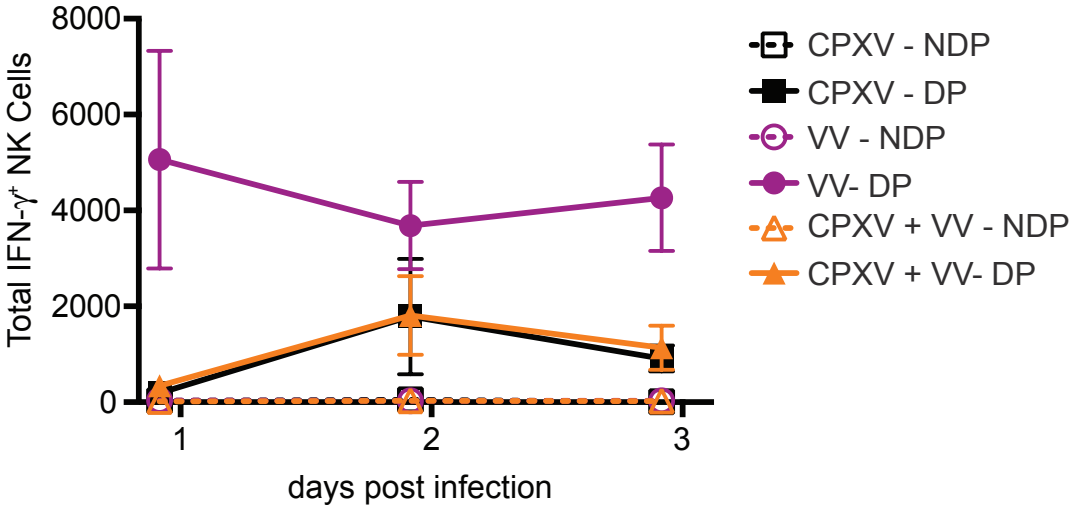
8000
6000
4000
2000
0
Total IFN-γ+ NK Cells
1
2
3
days post infection
CPXV - NDP
CPXV - DP
VV - NDP
VV- DP
CPXV + VV - NDP
CPXV + VV- DP

C

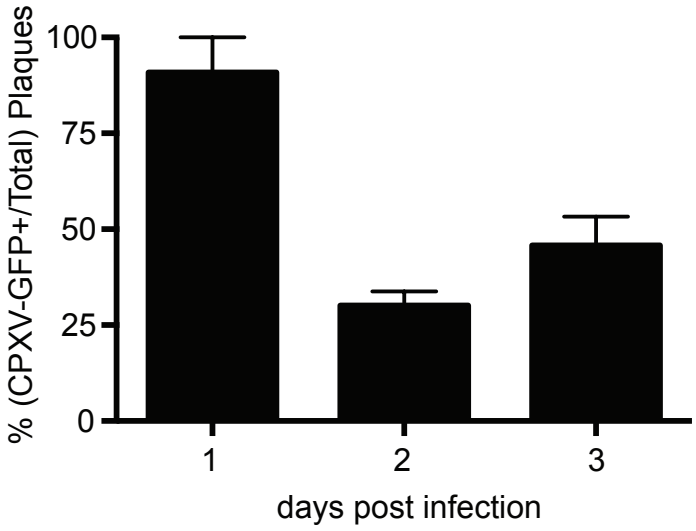
100
75
50
25
0
% (CPXV-GFP+/Total) Plaques
1
2
3
days post infection

Figure 37: Inhibition of NK cell IFN-γ production can be overcome.
Age and sex matched C57BL/6 mice were infected with CPXV, VV or with 0.1:1, 1:1 or 1:10 mixtures of CPXV and VV. Lymphocytes from the draining and non-draining LN were isolated and stained 1 dpi. Following extracellular staining, cells were fixed, permeablized and intracellularly stained for IFN-γ. (A) Percent and (B) total IFN-γ producing NK cells ($NK1.1^{+}CD3^{-}CD19^{-}IFN\text{-}\gamma^{+}$) are graphed. The graph depicts the average of data from 2 to 4 independent experiments. (C) C57BL/6 mice were infected with CPXV and lymphocytes were isolated at 1, 2 or 3 dpi and stimulated with PMA/ionomycin for 8 hours. Following identification of NK cells ($NK1.1^{+}CD3^{-}CD19^{-}$), IFN-γ expression was assessed. A representative result of 4 independent experiments is depicted.

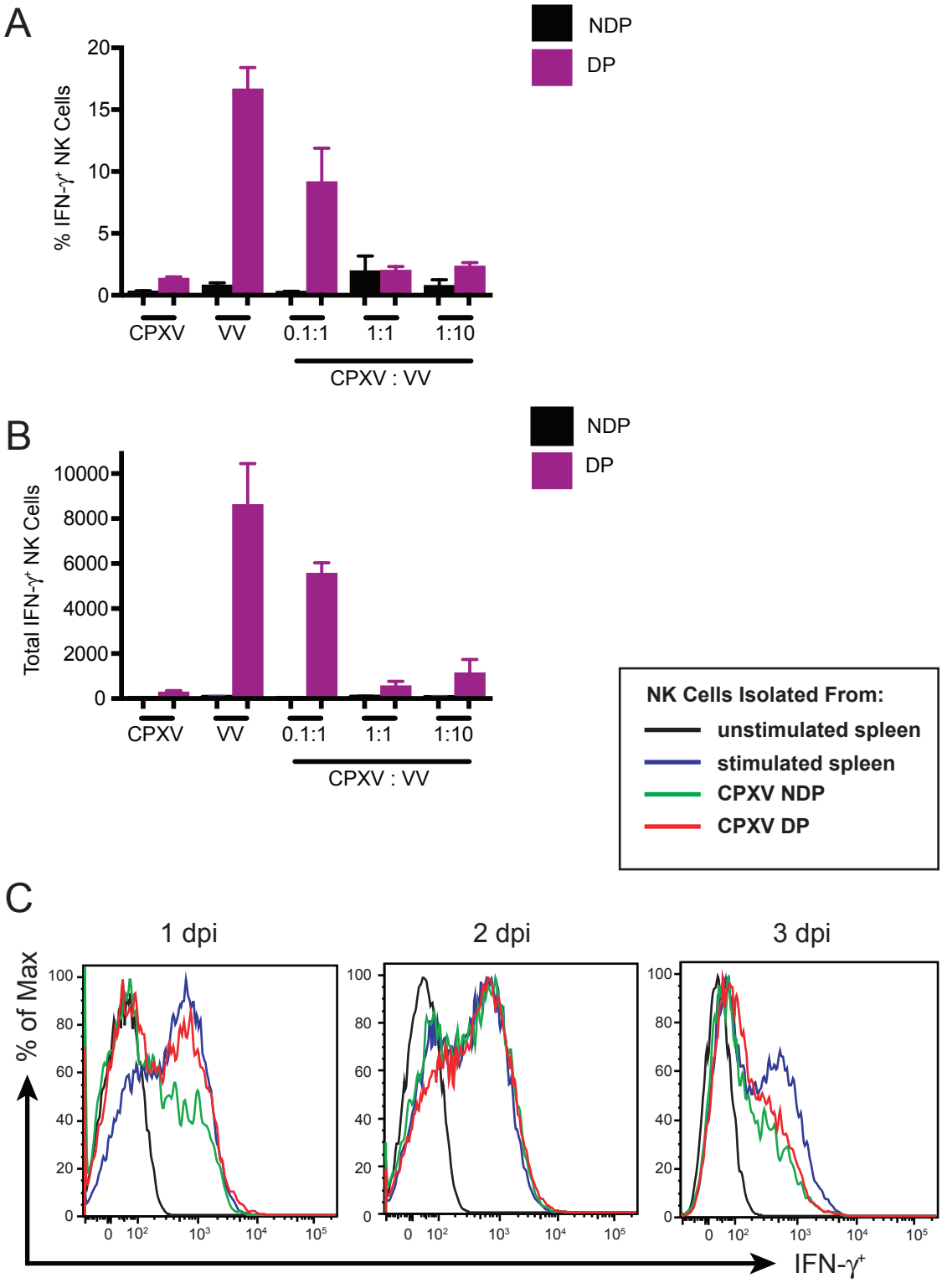
A
NDP
DP
% IFN-γ+ NK Cells
20
15
10
5
0
CPXV
VV
0.1:1
1:1
1:10
CPXV : VV
B
NDP
DP
Total IFN-γ+ NK Cells
10000
8000
6000
4000
2000
0
CPXV
VV
0.1:1
1:1
1:10
CPXV : VV
NK Cells Isolated From:
unstimulated spleen
stimulated spleen
CPXV NDP
CPXV DP
C
1 dpi
2 dpi
3 dpi
% of Max
100
80
60
40
20
0
0
10²
10³
10⁴
10⁵
IFN-γ+

Table 2: ORFs found in CPXV but not ECTV or VV.
This table lists ORFs determined by comparing the genomes of CPXV-Brighton Red, VV-Western Reserve, and ECTV-moscow strains using 80% identity threshold. The screen identified 36 ORFs that were unique to CPXV-Brighton Red.

Predicted Protein Information	**CPXV ORF**
1 or 2 predicted membrane spanning sequences	1, 3, 7, 47, 58, 63, 119a, 130, 160, 170, 192, 214, 224, 229
Ankryin domain	8, 17, 19, 220, 223
Secretory signal peptide	18, 170
Homologous to CMPX TLR inhibitor	9, 222
MHC I downregulation	12, 203
Galactose oxidase / transcriptional repression	13
Viral sensitivity to α-amanitin	10
no information	2, 31f, 51a, 78a, 96, 116, 152a, 216, 228

Figure 38: The inhibition of IFN-γ production by NK cells is unaffected in the absence of CPXV012, CPXV018 and CPXV203.
Age and sex matched C57BL/6 mice were infected with $1.5x10^6$ pfu/ms wild-type CPXV, VV or (A) CPXVΔ012, (B) CPXVΔ018 or (C) CPXVΔ203. Lymphocytes from the draining and non-draining LN were isolated and stained 1 dpi. Following extracellular staining, cells were fixed, permeablized and intracellularly stained for IFN-γ. NK cells ($NK1.1^+CD3^-CD19^-$) were identified and IFN-γ expression was assessed. Both percent and total IFN-γ producing cells are depicted.

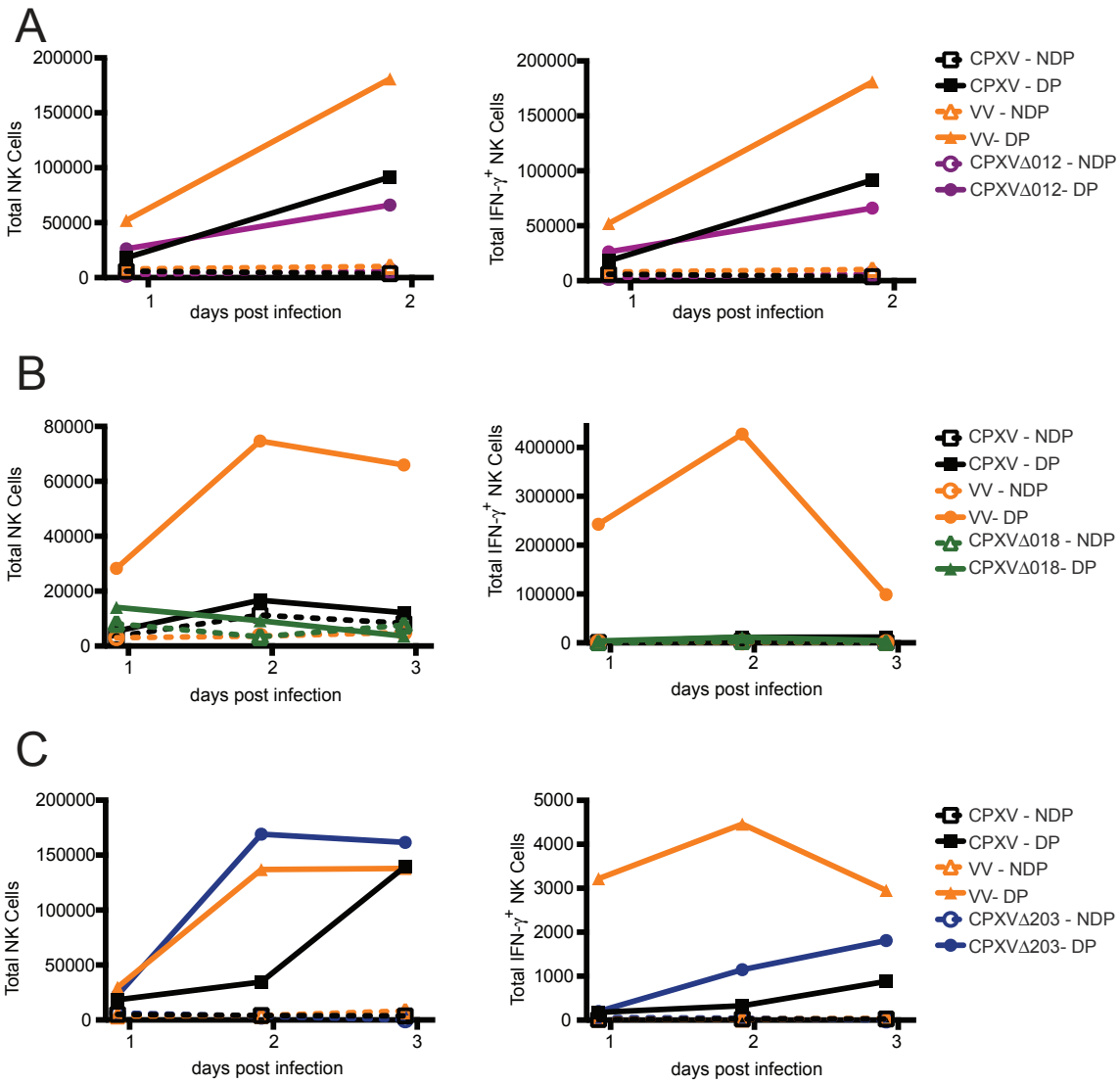
A
Total NK Cells
200000
150000
100000
50000
0
1
2
days post infection
Total IFN-γ+ NK Cells
200000
150000
100000
50000
0
1
2
days post infection
CPXV - NDP
CPXV - DP
VV - NDP
VV- DP
CPXVΔ012 - NDP
CPXVΔ012- DP
B
Total NK Cells
80000
60000
40000
20000
0
1
2
3
days post infection
Total IFN-γ+ NK Cells
400000
300000
200000
100000
0
1
2
3
days post infection
CPXV - NDP
CPXV - DP
VV - NDP
VV- DP
CPXVΔ018 - NDP
CPXVΔ018- DP
C
Total NK Cells
200000
150000
100000
50000
0
1
2
3
days post infection
Total IFN-γ+ NK Cells
5000
4000
3000
2000
1000
0
1
2
3
days post infection
CPXV - NDP
CPXV - DP
VV - NDP
VV- DP
CPXVΔ203 - NDP
CPXVΔ203- DP

Figure 39: The A587 mutant inhibits NK cell IFN-γ production.
Age and sex matched C57BL/6 mice were infected with $1.5x10^6$ pfu/ms wild-type CPXV, VV or A587. Lymphocytes from the draining and non-draining LN were isolated and stained 1 dpi. Following extracellular staining, cells were fixed, permeablized and intracellularly stained for IFN-γ. NK cells ($NK1.1^+CD3^-CD19^-$) were identified and IFN-γ expression was assessed. (A) Percent and (B) total IFN-γ producing NK cells ($NK1.1^+CD3^-CD19^-IFN\text{-}\gamma^+$) are graphed.

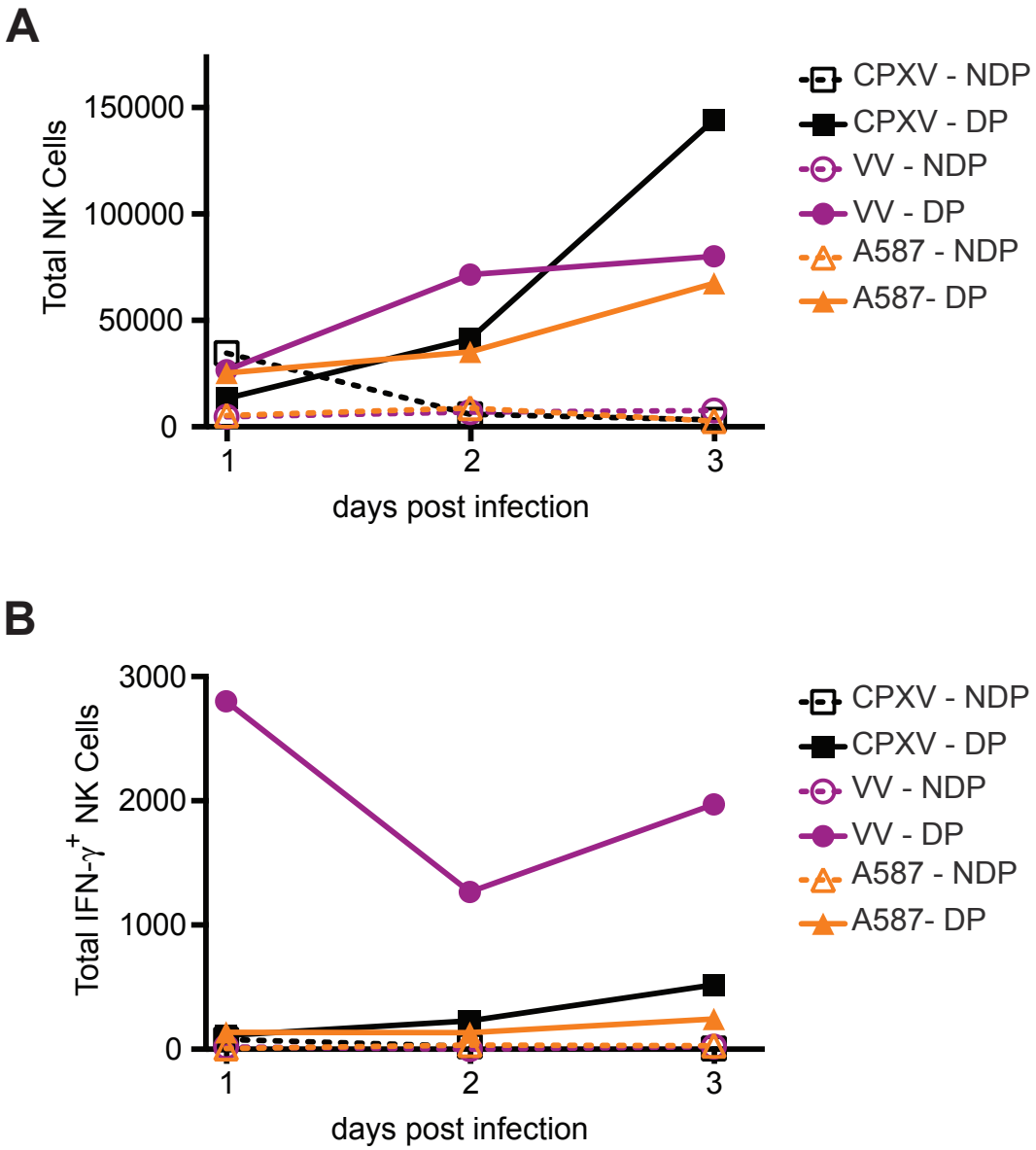
A
Total NK Cells
150000
100000
50000
0
1
2
3
days post infection
CPXV - NDP
CPXV - DP
VV - NDP
VV - DP
A587 - NDP
A587- DP
B
Total IFN-γ+ NK Cells
3000
2000
1000
0
1
2
3
days post infection
CPXV - NDP
CPXV - DP
VV - NDP
VV - DP
A587 - NDP
A587- DP

Figure 40: NK cells activation is partially restored following infection with the A518 mutant.
Age and sex matched C57BL/6 mice were infected with $1.5x10^6$ pfu/ms wild-type CPXV, VV or A518. Lymphocytes from the draining and non-draining LN were isolated and stained 1 dpi. Following extracellular staining, cells were fixed, permeablized and intracellularly stained for IFN-γ. (A) Percent and (B) total IFN-γ producing NK cells ($NK1.1^+CD3^-CD19^-IFN\text{-}\gamma^+$) are graphed. Data from 5 independent experiments are depicted. (C) Following identification of NK cells ($NK1.1^+CD3^-CD19^-$), CD69 and CD25 surface expression was assessed. A representative result of 2 independent experiments is depicted.

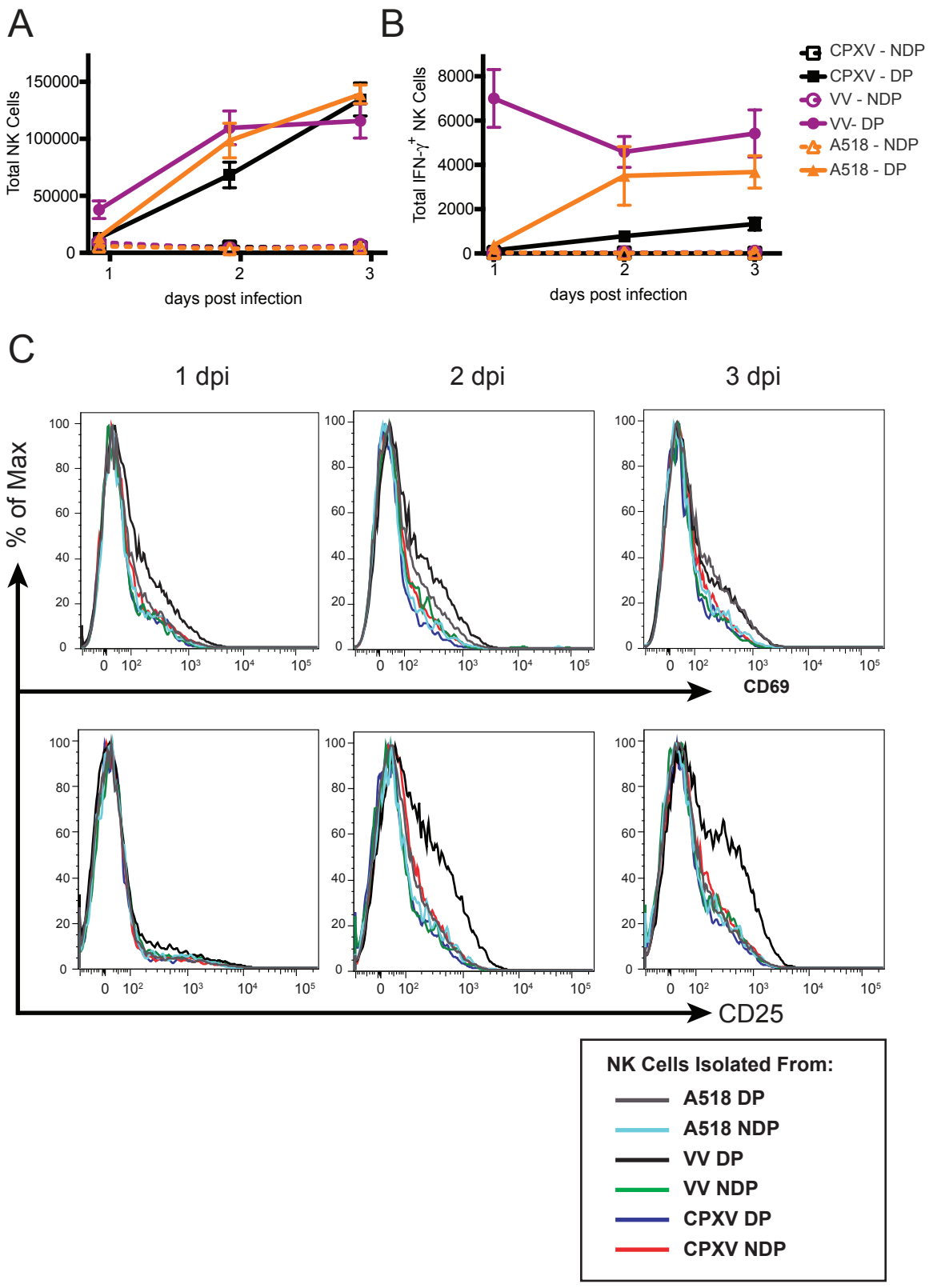
A
Total NK Cells
150000
100000
50000
0
1
2
3
days post infection
B
Total IFN-γ+ NK Cells
8000
6000
4000
2000
0
1
2
3
days post infection
CPXV - NDP
CPXV - DP
VV - NDP
VV- DP
A518 - NDP
A518 - DP
C
1 dpi
2 dpi
3 dpi
% of Max
CD69
CD25
NK Cells Isolated From:
A518 DP
A518 NDP
VV DP
VV NDP
CPXV DP
CPXV NDP

Figure 41: CPXV inhibition of NK cell IFN-γ production is control by multiple ORFs.
Age and sex matched C57BL/6 mice were infected with $1.5x10^6$ pfu/ms wild-type CPXV, VV, A518, CPXVΔ018-021, or CPXVΔ022-036. Lymphocytes from the draining and non-draining LN were isolated and stained 1 dpi. Following extracellular staining, cells were fixed, permeablized and intracellularly stained for IFN-γ. (A) Percent and (B) total IFN-γ producing NK cells ($NK1.1^+CD3^-CD19^-IFN\text{-}\gamma^+$) are graphed. The graphs depict the average of data from 3 to 5 independent experiments.

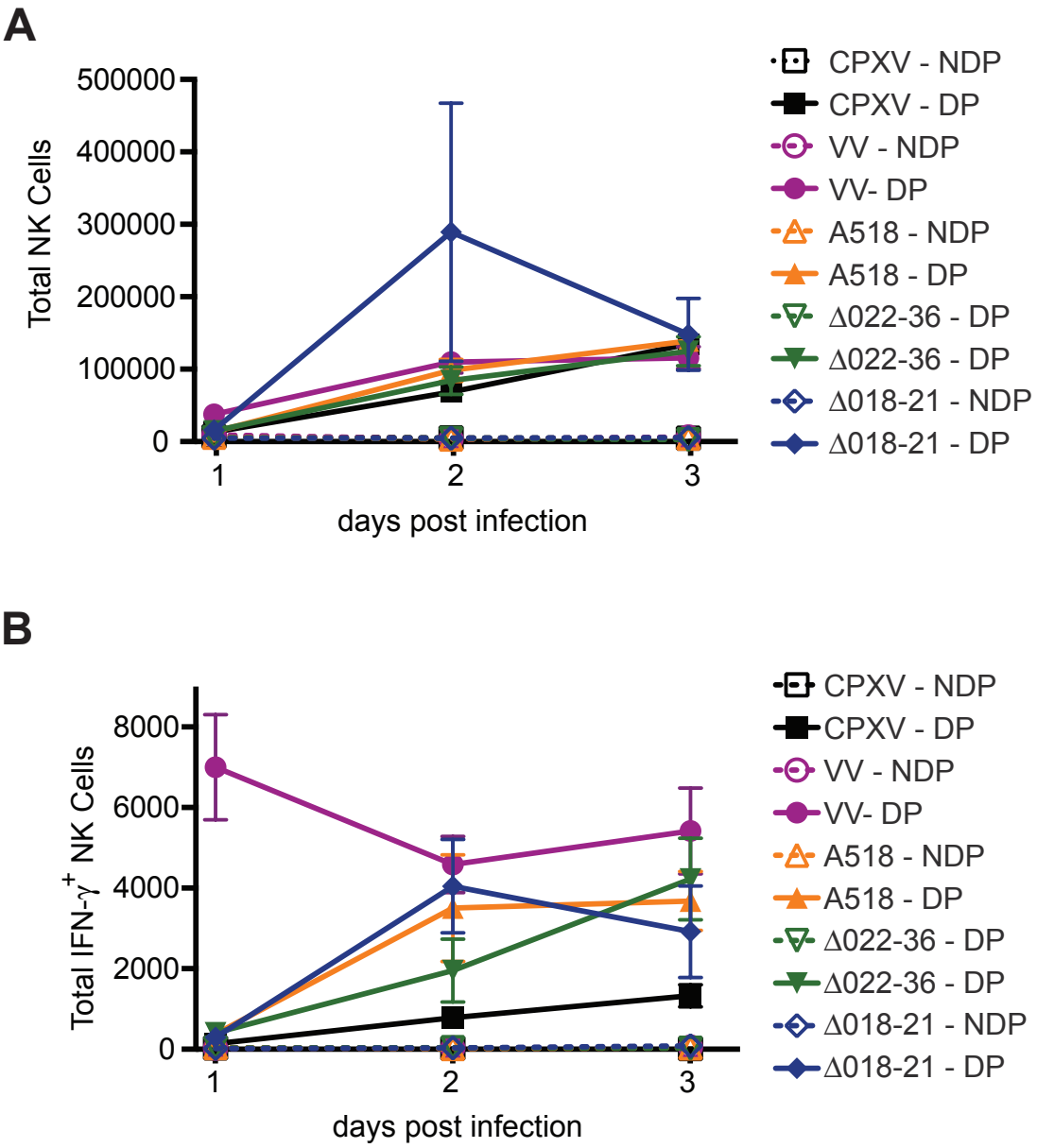
A
500000
400000
300000
200000
100000
0
Total NK Cells
1
2
3
days post infection
CPXV - NDP
CPXV - DP
VV - NDP
VV- DP
A518 - NDP
A518 - DP
Δ022-36 - DP
Δ022-36 - DP
Δ018-21 - NDP
Δ018-21 - DP
B
8000
6000
4000
2000
0
Total IFN-γ+ NK Cells
1
2
3
days post infection
CPXV - NDP
CPXV - DP
VV - NDP
VV- DP
A518 - NDP
A518 - DP
Δ022-36 - DP
Δ022-36 - DP
Δ018-21 - NDP
Δ018-21 - DP

CHAPTER 8:

Conclusions and Future Directions

Cowpox Footpad Infection Provides a Relevant Model for Zoonotic Infection

Orthopoxviruses cause zoonotic infection and several have been well characterized in existing laboratory models. Most investigation of orthopoxvirus pathogenesis employ intravenous or intranasal infection (30, 39, 90). Intravenous infection simulates systemic infection while intranasal infection simulates aerosolized infection and models inoculation following natural smallpox infection or predicted dissemination during a bioterrorist event. However the literature demonstrate that most CPXV infections occur through contact-mediated spread within the host reservoir and to zoonotic hosts (6, 8, 91). Previous investigations of CPXV infection in a footpad mouse model have been limited in scope and did not examine the host response (90, 93). We have developed a footpad model of CPXV infection in mice and have demonstrated establishment of infection at the site of inoculation and in the draining LN, from where secondary dissemination originates at later times. This footpad model more closely parallels infection with orthopoxviruses such as zoonotic CPXV infection of humans, where viral replication has been observed only at the site of infection (9). In zoonotic CPXV infections, lymphadenopathy results from recruitment of lymphocytes to draining LNs. In mice, CPXV footpad inoculation stimulated recruitment of many lymphocytes to the draining LN, including NK cells, which highlights the relevance of our footpad model for the study of *in vivo* CPXV infection. We have shown that our model can provide a unique opportunity to study immune responses following inoculation with CPXV via its natural route of infection.

NK Cells are Required for Resistance to but Not Survival of CPXV Footpad Infection

Immediately following infection, innate lymphocytes are recruited to the site of infection and the draining LN. Here they stimulate an inflammatory response and directly control infection while an adaptive immune response is primed. One innate lymphocyte that is important at early times following infection is the NK cell, which produces cytokines and lyses infected cells. Under homeostatic conditions, murine NK cells are a rare LN population (74), so observation of rapid and robust expansion of NK cell numbers in the draining LN following CPXV infection suggested that they were important for resistance to this pathogen.

Since CPXV encodes many unique inhibitory proteins, we hypothesized that NK cell function might be inhibited following CPXV infection. However, following systemic NK cell depletion, CPXV replication in the draining LN was significantly increased, indicating NK cells were functional following CPXV infection. It has been demonstrated that splenic titers of ECTV are increased following footpad inoculation in the absence of NK cells (81). Following inoculation with CPXV in the footpad, we observed early spread to the lungs and the spleen in the absence of NK cells. These data demonstrate that NK cells are important for limiting viral replication and spread following both ECTV and CPXV infection. Therefore, we concluded that the unique inhibitory proteins of CPXV do not completely neutralize NK cell control of replication and dissemination.

We examined the importance of NK cell control of viral replication and spread by observing survival following CPXV infection in the NK cell depleted mice. In contrast to previous studies using ECTV and VV which demonstrate a requirement of NK cells for survival (80-82), depletion of NK cells prior to CPXV infection did not lead to increased mortality. These novel findings indicate that there are differential requirements for NK cells following orthopoxviral infections. Another possibility is that since intravenous

inoculation was used to examine the requirement of NK cells for survival following VV infection, it is possible that following footpad inoculation in the absence of NK cells, lethality may not occur. It is also possible that we did not observe CPXV lethality because the infectious dose of CPXV was too low. Dose-response experiments could be performed examining the NK cell requirement for survival following larger infectious doses of CPXV in the footpad model. However, high-dose inoculation following contact-mediated spread within the host reservoir or to zoonotic hosts seems unlikely. We have concluded that NK cells are important for limiting viral replication and dissemination following CPXV infection but are not essential for survival at the dose examined.

Mechanisms of NK Cell Recruitment

Expansion of the NK cell population in the draining LN following CPXV infection resulted from chemokine-mediated recruitment rather than *in situ* proliferation of relatively rare resident cells. The role of chemokine receptor-mediated trafficking of murine NK cells to the site of infection has been studied in the context of several pathogens, but no commonly required chemokine receptor has been identified (64, 75, 76, 108, 140). NK cells are recruited to sites of inflammation despite expression of a variety of inflammatory chemokines in the context of different pathogens. Therefore NK cells must express an array of inflammatory chemokine receptors to mediate this response (65). Additionally, expression of multiple chemokine receptors adds a protective level of redundancy for host resistance to infection.

Previous studies have not identified specific chemokine receptors that mediate NK cell recruitment following orthopoxvirus infection. Here we demonstrated an intrinsic requirement for CXCR3 expression on the NK cell which mediates recruitment

to the draining LN following CPXV infection. Meanwhile, CCR2 and CCR5, which have been shown to be required following infection with MCMV, HSV-2, *Aspergillus fumigatus and Toxoplasma gondi* (64, 75, 76, 108), were not found to be individually necessary to mediate NK cell recruitment. While this work was in progress, it was demonstrated that MVA, a highly attenuated orthopoxvirus, stimulates recruitment of NK cells to draining LNs in a CXCR3-dependent and CCR5-independent manner (140), confirming our results. Additionally, CXCR3 has been demonstrated to be responsible for NK cell recruitment several inflammatory but non-infectious responses and for re-localization of NK cells from the red pulp to the T cell zone in the spleen following MCMV infection (105-107, 109). CXCR3 receptor-mediated NK cell recruitment is perhaps unsurprising, since inflammation often results in the production of IFN-γ and expression of the chemokine ligands for CXCR3 is induced by this cytokine (104). Since a role for CXCR3 has not been examined in response to other pathogens, it may indeed be a commonly required chemokine receptor for NK cell trafficking. Expression of CXCR3 has been suggested as a marker of mature, cytotoxic NK cells (161), supporting the hypothesis that CXCR3 is ubiquitously expressed on many NK cells. Therefore, CXCR3 may be a commonly important receptor for recruitment of NK cells to sites of inflammation and infection.

We also determined that there was a requirement for IFN-γ following CPXV infection. As discussed above, IFN-γ is important for induction of inflammatory chemokines including CXCR3. However, in the absence of CXCR3, NK cell recruitment was decreased but not abolished. This indicated that IFN-γ was also inducing other inflammatory mediators, possibly other inflammatory chemokines. Since IFN-γ is upstream of multiple processes, only one of which is recruitment of NK cells, its role in

mediating CXCR3-independent NK cell recruitment following CPXV infection is likely to be complex and difficult to dissect.

A Role for DC-Mediated NK Cell Recruitment is Difficult to Ascertain

It has previously been demonstrated that footpad injection of LPS-matured DCs results in the trafficking of DCs from the periphery to the draining LN, where they stimulate recruitment of NK cells that produce IFN-γ to prime a T_H1 response (107). This interaction, in combination with many documented interplays between NK cells and DCs (44, 45, 53, 117), raises the possibility that DCs mediate recruitment of NK cells in response to CPXV infection. The migration of DCs from the periphery to the draining LN is dependent on the up-regulation of CCR7 and does not occur in mice deficient for CCR7 (162). We did not observe NK cell recruitment to the draining LN in CCR7-deficient mice, supporting the hypothesis that DCs recruit NK cells to draining LNs. However, the LN architecture is disorganized in CCR7-deficient mice which likely leads to defective trafficking of many lymphocytes, complicating interpretation of this experiment (99). To further investigate the hypothesis that DCs recruit NK cells, we examined the recruitment of migratory DCs from the periphery to the draining LN following CPXV infection. Surprisingly, given the commonly accepted paradigm of pathogen recognition stimulating migration of DCs from the periphery to the draining LN, we observed comparable populations of migratory DCs in non-draining and draining LNs. These data suggested that following CPXV footpad inoculation, DCs were not migrating from the periphery at a greater rate or in greater numbers than under homeostatic conditions. Additionally, while CD11c-DTR diphtheria toxin-depleted mice showed major defects in NK cell recruitment, macrophages and other cells ectopically

express CD11c and are depleted, confounding interpretation of these results (133, 138). Attempts to restore DC populations in deficient systems did not result in increased NK cell trafficking following CPXV infection. While data from several different experiments suggest that DCs may play a role in recruitment of NK cells to the draining LN following CPXV infection, we have been unable to establish a system that can conclusively identify a role in NK cell recruitment. These data raise the possibility that DCs may be important, but not sufficient for NK cell recruitment in this system.

A Novel Macrophage and NK Cell Interaction

SCS macrophages can phagocytose and detect free viral particles arriving from the periphery through the lymphatic system (94, 129, 130). Following diphtheria toxin-mediated depletion of CD11c-DTR transgenic mice, SCS macrophages were depleted, raising the possibility that they may be required for NK cell recruitment to the draining LN following CPXV infection (133). To test this hypothesis, we infected macrophage-depleted mice with CPXV and examined NK cell recruitment to the draining LN. Mice that lacked macrophages in the draining LN exhibited no NK cell recruitment indicating a novel interaction between macrophages and NK cells. During our subsequent studies, several reports were published that also observed NK cell interactions with $CD169^+$ SCS macrophages and a requirement of macrophages for NK cell recruitment (131, 139, 140). Our findings, in combination with these recently reported results, indicate a novel interaction between macrophages and NK cells.

Macrophages can detect infection and induce inflammation, including through production of IFN-γ-induced CXCL9 and CXCL10 (134, 135). We therefore hypothesized that macrophages mediated NK cell recruitment to the draining LN

following CPXV infection in a CXCR3-dependent manner. However, depletion of macrophages and subsequent CPXV infection induced comparable levels of *Cxcl9* and *Cxcl10* expression as in non-depleted mice. These data indicate that macrophages recruit NK cells in a CXCR3-independent manner. However, the mechanism of macrophage-mediated NK cell recruitment is currently unknown. One possibility to explain macrophage-mediated recruitment is that SCS macrophages are the preferentially infected cell in the draining LN following CPXV infection, and removal of macrophages results in diminished host recognition and therefore decreased inflammation and lymphocyte recruitment. Another possibility is that while *Cxcl9* and *Cxcl10* expression was unaffected, many viruses stimulate type I IFN production, which can lead to expression of different chemokines such as CCL3 (77). We observed increased expression of *Ccl3* transcripts following both CPXV and VV infection, so it is possible that macrophages induce type I IFN and mediate recruitment of NK cells through alternate inflammatory chemokines. These data indicate that there are two, non-overlapping pathways to recruit NK cells to the draining LN following infection, emphasizing the importance of the expansion of the NK cell population in the draining LN in response to viral infection.

Inappropriate Association of NK Cell Resistance and NK Cell Recruitment

NK cell-mediated resistance to ECTV infection has been inferred by the expansion of IFN-γ and granzyme B producing NK cells in the draining LN (80, 81). However, control of ECTV in the draining LN in the presence or absence of NK cells has not been described in the literature. Here we have demonstrated that recruitment of NK cells was unnecessary for control of viral replication in the draining LN or spread to the

spleen and lungs. While NK cells were essential for control of viral burden in these organs, their specific recruitment was not necessary and rare NK cells present in the draining LN controlled viral replication in the absence of NK cell recruitment. While this could be a function of CPXV infection in comparison to ECTV infection, it does not appear that expansion of the population and control of infection can be linked.

Incomplete NK Cell Maturation Despite Cytotoxic Function

When examining the maturation phenotype of NK cells isolated from the draining LN following CPXV infection, we observed that NK cells did not produce IFN-γ or up-regulate some surface activation markers. This inhibition was CPXV specific and could be overcome *ex vivo* by stimulating with PMA and ionomycin or *in vivo* by limiting the infectious dose of CPXV during a co-infection with VV. Although CPXV inhibited NK cell production of IFN-γ, systemic depletion of NK cells resulted in increased local and systemic viral burden. These data suggest that NK cells are partially activated following infection and their function is likely due to production of granzyme B. Since it has been demonstrated that stimulation of NK cells by cytokines and through activating receptors results in different NK cell functions, CPXV may block one but not all activation signals, resulting in this partially activated phenotype. Most infections lead to both NK cell cytotoxicity and cytokine production, but it has been reported that following Lymphocytic Choriomeningitis (LCMV) infection, NK cells have cytotoxic function but do not produce IFN-γ due to the lack of IL-12 induction (163). To our knowledge, no IL-12 binding protein has been identified in CPXV, but it is likely that CPXV has other mechanisms to subvert IL-12 production. It is then possible that a lack of IL-12 production may be a shared mechanism of NK cell inhibition following CPXV and

LCMV infection. It is also possible that these systems may share additional stimulatory and/or inhibitory signals. Thus determining shared activation and inhibition signals during viral infection may help further understanding of differential NK cell activation signals.

CPXV-mediated inhibition of IFN-γ was multifactorial, suggesting the involvement of both NK cell specific and non-NK cell specific virally encoded inhibitory proteins. Partial restoration of IFN-γ production by recruited NK cells was observed following infection with the A518 mutant, CPXVΔ018-021 and CPXVΔ022-36. CPXV018 inhibits NKG2D activation *in vitro* (85), but CPXVΔ018 did not recruit IFN-γ producing NK cells to the draining LN, suggesting an additional mechanism of IFN-γ inhibition. Induction of IFN-γ production in NK cells can be stimulated by IL12, IL-15 and IL-18 and inhibited by IL-10 in the absence of IL-12 (54, 154, 164-166). CPXV encodes an IL-18 binding protein and induces sustained high levels of IL-10 which may non-specifically contribute to NK cell inhibition (34, 39). VV hemagglutinin expression is recognized by NKp30 and NKp46 in HeLa cells, resulting in NK cell inhibition (167-169). The ability of CPXV hemagglutinin to bind these natural cytotoxicity receptors has not been examined, but it is possible that CPXV also mediates NK cell inhibition through this mechanism. The numerous CPXV inhibitory proteins and their individual and synergistic effects on the host response clearly confer a strong advantage to CPXV during infection of the host, but will also complicate any attempt to discern individual contributions of each inhibitory protein to CPXV immune evasion.

Although NK cells did not produce IFN-γ following CPXV infection, increased viral burden following systemic NK cell depletion indicated that NK cells were an important component of the host response. Additionally, given the number of viral

inhibitory proteins that directly or indirectly impact NK cell activation, it must be advantageous for CPXV to even partially inhibit NK cell function. It is interesting to speculate about the ability of CPXV to infect and disseminate within the host in the context of uninhibited NK cell activation. Several experiments could be designed to overcome the *in vivo* inhibition of NK cells. The importance of IL-12 and IL-18 for NK cell activation has been demonstrated following ECTV and VV suggesting they might also be important following CPXV infection (41, 42). Since inhibition may occur through or be modulated by virally encoded cytokine binding proteins, treatment with IL-12 and/or IL-18 or infection with CPXV which recombinantly expresses either cytokine could result in saturation of virally encoded cytokine binding proteins, allowing NK cell activation. Another way to restore NK cell functionality might be examine NK cell activation following infection with the CPXVΔ018 mutant. Although our studies have demonstrated that lack of CPXV018 does not restore IFN-γ production, it is possible that CPXV018 may also inhibit cytotoxic NK cell function. Inhibition of NK cell function may be essential for establishment CPXV infection and dissemination within the host. These proposed experiments may help dissect the reason CPXV encodes many inhibitory proteins against NK cell function.

Aside from cytotoxicity and stimulation of inflammation, NK cell production of IFN-γ also shapes the T_H1 response (107). It is possible that priming of the adaptive immune response is delayed following CPXV infection in comparison to VV or ECTV infection in the absence of NK cell produced IFN-γ. The scope of these studies did not include an examination of this process, but systemic depletion of NK cells did result in delayed viral clearance in the draining LN and the foot, suggesting a delay in the adaptive immune response. Therefore, CPXV inhibition of IFN-γ may be beneficial for both

suppressing NK lysis of CPXV infected cells and delaying the priming of a T_H1 response, resulting in prolonged CPXV infection.

Clinical Relevance

Many studies use members of the orthopoxvirus genus to model smallpox virus infection, but symptoms, viral spread and disease course vary greatly between these orthopoxviruses. Despite the lack of lethality following CPXV infection in the mouse model, footpad infection of mice closely mimics zoonotic infection making it a relevant model to study vacciniation and zoonotic infection following a range of non-lethal orthopoxvirus infections. Vaccination of patients that are immunocompromised or have atopic dermatitis is not advised, but with increasing numbers of emerging and zoonotic poxvirus infections, safer vaccine development is crucial. Many strategies have been employed to generate new vaccines, including directed deletion of inhibitory proteins. Since NK cells are important for limiting early viral replication, inducing inflammation and priming the adaptive immune response, removal of virally encoded NK cell specific and non-NK cell specific inhibitors from novel candidate vaccine strains is important. Conversely, in inflammatory diseases where NK cells are inappropriately activated, identification of virally encoded NK cell specific inhibitors may be a useful therapeutic treatment.

Concluding Remarks

Studies examining the host response to viral infection and viral immune evasion provide insight into the complexity of host-pathogen interaction. In these studies, we have demonstrated the relevance of studying CPXV in a footpad model of infection to

further characterize and understand zoonotic orthopoxvirus infections. We have highlighted the importance of NK cells following CPXV infection, studied the mechanism of NK cell recruitment in the context of natural infection and the complicated and multifactorial nature of viral inhibition of NK cell function. Further investigation will help illuminate and dissect these intricate host-pathogen interactions.

REFERENCES

1. Fenner F (1988) *Smallpox and its eradication* (The World Health Organization).
2. Riedel S (2005) Edward Jenner and the history of smallpox and vaccination. *Proceedings (Baylor University Medical Center)* 18:21.
3. Parker S, Nuara A, Buller RML, Schultz DA (2007) Human monkeypox: an emerging zoonotic disease. *Future Microbiol* 2:17–34.
4. Ligon BL (2004) Monkeypox: a review of the history and emergence in the Western hemisphere. *Semin Pediatr Infect Dis* 15:280–287.
5. Jezek Z et al. (1986) Four generations of probable person-to-person transmission of human monkeypox. *Am J Epidemiol* 123:1004–1012.
6. Campe H et al. (2009) Cowpox virus transmission from pet rats to humans, Germany. *Emerging Infect Dis* 15:777–780.
7. Wollenberg A et al. (2012) The Munich Outbreak of Cutaneous Cowpox Infection: Transmission by Infected Pet Rats. *Acta Derm Venerol* 92:126–131.
8. Ninove L et al. (2009) Cowpox virus transmission from pet rats to humans, France. *Emerging Infect Dis* 15:781–784.
9. Vorou RM, Papavassiliou VG, Pierroutsakos IN (2008) Cowpox virus infection: an emerging health threat. *Curr Opin Infect Dis* 21:153–156.
10. Chantrey J et al. (1999) Cowpox: reservoir hosts and geographic range. *Epidemiology and Infection* 122:455.
11. Pelkonen PM et al. (2003) Cowpox with Severe Generalized Eruption, Finland. *Emerging Infect Dis* 9:1458.
12. Mack TM (1972) Smallpox in Europe, 1950-1971. *J Infect Dis* 125:161–169.
13. Kim S-H, Oh M-D (2007) Persistence of cell-mediated immunity to vaccinia virus. *J Infect Dis* 196:805–806.
14. Amanna IJ, Slifka MK, Crotty S (2006) Immunity and immunological memory following smallpox vaccination. *Immunol Rev* 211:320–337.
15. Baxby D (1977) The origins of vaccinia virus. *J Infect Dis* 136:453–455.
16. R HI, Bowie AG (2005) Evasion of innate immunity by vaccinia virus. *Parasitology* 130:S11.
17. Moss B (2011) Smallpox vaccines: targets of protective immunity. *Immunol Rev* 239:8–26.
18. Verardi PH, Titong A, Hagen CJ (2012) A vaccinia virus renaissance: New vaccine and immunotherapeutic uses after smallpox eradication. *Hum Vaccin Immunother* 8:961–970.
19. Gomes JAS et al. (2012) Immune Modulation in Primary Vaccinia virus Zoonotic Human Infections. *Clinical and Developmental Immunology* 2012:1–11.
20. Carroll DS et al. (2011) Chasing Jenner's Vaccine: Revisiting Cowpox Virus Classification. *PLoS One* 6:e23086.
21. Bennett M et al. (1997) Cowpox in British voles and mice. *J Comp Pathol* 116:35–44.
22. Upton C, Slack S, Hunter AL, Ehlers A, Roper RL (2003) Poxvirus Orthologous Clusters: toward Defining the Minimum Essential Poxvirus Genome. *J Virol* 77:7590–7600.
23. Seet BT et al. (2003) Poxviruses and immune evasion. *Annu Rev Immunol* 21:377–423.

24. Alzhanova D, Früh K (2010) Modulation of the host immune response by cowpox virus. *Microbes Infect* 12:900–909.
25. Delaloye J et al. (2009) Innate Immune Sensing of Modified Vaccinia Virus Ankara (MVA) Is Mediated by TLR2-TLR6, MDA-5 and the NALP3 Inflammasome. *PLoS Pathog* 5:e1000480.
26. Samuelsson C et al. (2008) Survival of lethal poxvirus infection in mice depends on TLR9, and therapeutic vaccination provides protection. *The Journal of Clinical Investigation* 118:1776.
27. Zhu J, Martinez J, Huang X, Yang Y (2007) Innate immunity against vaccinia virus is mediated by TLR2 and requires TLR-independent production of IFN. *The Journal of Clinical Investigation* 109:619–625.
28. González JM, Esteban M (2010) A poxvirus Bcl-2-like gene family involved in regulation of host immune response: sequence similarity and evolutionary history. *Virol J* 7:59.
29. Byun M, Wang X, Pak M, Hansen TH, Yokoyama WM (2007) Cowpox virus exploits the endoplasmic reticulum retention pathway to inhibit MHC class I transport to the cell surface. *Cell Host Microbe* 2:306–315.
30. Byun M et al. (2009) Two mechanistically distinct immune evasion proteins of cowpox virus combine to avoid antiviral CD8 T cells. *Cell Host Microbe* 6:422–432.
31. Dasgupta A, Hammarlund E, Slifka MK, Früh K (2007) Cowpox virus evades CTL recognition and inhibits the intracellular transport of MHC class I molecules. *J Immunol* 178:1654–1661.
32. Alzhanova D et al. (2009) Cowpox virus inhibits the transporter associated with antigen processing to evade T cell recognition. *Cell Host Microbe* 6:433–445.
33. Katze MG, He Y, Gale M (2002) Viruses and interferon: A fight for supremacy. *Nat Rev Immunol* 2:675–687.
34. Reading P, Smith G (2003) Vaccinia virus interleukin-18-binding protein promotes virulence by reducing gamma interferon production and natural killer and T-cell activity. *J Virol* 77:9960–9968.
35. Perdiguero B, Esteban M (2009) The Interferon System and Vaccinia Virus Evasion Mechanisms. *Journal of Interferon & Cytokine Research* 29:581–598.
36. Mahalingam S, Karupiah G (2000) Modulation of chemokines by poxvirus infections. *Current Opinion in Immunology* 12:409–412.
37. Vaheri A, Nepomnyashchikh TS, Shchelkunov SN (2010) SECRET domain of variola virus CrmB protein can be a member of poxviral type II chemokine-binding proteins family. *BMC Research Notes* 3:271.
38. Alcami A, Lira SA (2010) Modulation of chemokine activity by viruses. *Curr Opin Immunol* 22:482–487.
39. Spesock AH et al. (2011) Cowpox virus induces interleukin-10 both in vitro and in vivo. *Virology* 417:87–97.
40. Kennedy RB, Ovsyannikova IG, Jacobson RM, Poland GA (2009) The immunology of smallpox vaccines. *Current Opinion in Immunology* 21:314–320.
41. Wang Y, Chaudhri G, Jackson R, Karupiah G (2009) IL-12p40 and IL-18 play pivotal roles in orchestrating the cell-mediated immune response to a poxvirus infection. *J Immunol* 183:3324–3331.
42. Gherardi MM (2003) IL-12 and IL-18 act in synergy to clear vaccinia virus infection: involvement of innate and adaptive components of the immune system.

Journal of General Virology 84:1961–1972.
43. Perera LP, Goldman CK, Waldmann TA (2001) Comparative assessment of virulence of recombinant vaccinia viruses expressing IL-2 and IL-15 in immunodeficient mice. *Proc Natl Acad Sci USA* 98:5146–5151.
44. Moretta L et al. (2006) Effector and regulatory events during natural killer-dendritic cell interactions. *Immunol Rev* 214:219–228.
45. Cooper MA, Fehniger TA, Fuchs A, Colonna M, Caligiuri MA (2004) NK cell and DC interactions. *Trends Immunol* 25:47–52.
46. Yammani RD et al. (2008) Regulation of maturation and activating potential in CD8+ versus CD8− dendritic cells following in vivo infection with vaccinia virus. *Cell* 378:142–150.
47. Hansen SJ et al. (2011) Cowpox virus inhibits human dendritic cell immune function by nonlethal, nonproductive infection. *Cell* 412:411–425.
48. Engelmayer J et al. (1999) Vaccinia virus inhibits the maturation of human dendritic cells: a novel mechanism of immune evasion. *J Immunol* 163:6762–6768.
49. Rivera R et al. (2007) Murine alveolar macrophages limit replication of vaccinia virus. *Virology* 363:48–58.
50. Humlová Z, Vokurka M, Esteban M, Mělková Z (2002) Vaccinia virus induces apoptosis of infected macrophages. *J Gen Virol* 83:2821–2832.
51. Jonsson AH, Yokoyama WM (2009) Natural killer cell tolerance licensing and other mechanisms. *Adv Immunol* 101:27–79.
52. Yokoyama WM, Plougastel BFM (2003) Immune functions encoded by the natural killer gene complex. *Nat Rev Immunol* 3:304–316.
53. Andrews DM, Scalzo AA, Yokoyama WM, Smyth MJ, Degli-Esposti MA (2003) Functional interactions between dendritic cells and NK cells during viral infection. *Nat Immunol* 4:175–181.
54. Christine A Biron, Khuong B Nguyen, Gary C Pien, Leslie P Cousens, Salazar-Mather TP (1999) Natural Killer Cells in Antiviral Defense: Function and Regulation by Innate Cytokines. *Annu Rev Immunol* 17:189–220.
55. Kärre K, Ljunggren HG, Piontek G, Kiessling R (1986) Selective rejection of H-2-deficient lymphoma variants suggests alternative immune defence strategy. *Nature* 319:675–678.
56. Gasser S, Raulet DH (2006) Activation and self-tolerance of natural killer cells. *Immunol Rev* 214:130–142.
57. Scalzo AA, Yokoyama WM (2008) Cmv1 and natural killer cell responses to murine cytomegalovirus infection. *Curr Top Microbiol Immunol* 321:101–122.
58. Loh J, Chu DT, O'Guin AK, Yokoyama WM, Virgin HW (2004) Natural Killer Cells Utilize both Perforin and Gamma Interferon To Regulate Murine Cytomegalovirus Infection in the Spleen and Liver. *J Virol* 79:661–667.
59. Fehniger TA et al. (2007) Acquisition of murine NK cell cytotoxicity requires the translation of a pre-existing pool of granzyme B and perforin mRNAs. *Immunity* 26:798–811.
60. Kim S, Yokoyama WM (1998) NK Cell Granule Exocytosis and Cytokine Production Inhibited by Ly-49A Engagement. *Cellular Immunology* 183:106–112.
61. Yokoyama WM, Kim S, French AR (2004) The dynamic life of natural killer cells. *Annu Rev Immunol* 22:405–429.

62. Arase H, Arase N, Saito T (1996) Interferon gamma production by natural killer (NK) cells and NK1.1+ T cells upon NKR-P1 cross-linking. *The Journal of Experimental Medicine* 183:2391.
63. Dorner BG et al. (2004) Coordinate expression of cytokines and chemokines by NK cells during murine cytomegalovirus infection. *J Immunol* 172:3119–3131.
64. Salazar-Mather TP, Orange JS, Biron CA (1998) Early murine cytomegalovirus (MCMV) infection induces liver natural killer (NK) cell inflammation and protection through macrophage inflammatory protein 1alpha (MIP-1alpha)-dependent pathways. *J Exp Med* 187:1–14.
65. Moser B, Willimann K (2004) Chemokines: role in inflammation and immune surveillance. *Ann Rheum Dis* 63 Suppl 2:ii84–ii89.
66. Cyster JG (1999) Chemokines and cell migration in secondary lymphoid organs. *Science* 286:2098–2102.
67. Müller M, Carter S, Hofer MJ, Campbell IL (2010) Review: The chemokine receptor CXCR3 and its ligands CXCL9, CXCL10 and CXCL11 in neuroimmunity - a tale of conflict and conundrum. *Neuropathology and Applied Neurobiology* 36:368–387.
68. Hokeness KL, Kuziel WA, Biron CA, Salazar-Mather TP (2005) Monocyte chemoattractant protein-1 and CCR2 interactions are required for IFN-alpha/beta-induced inflammatory responses and antiviral defense in liver. *J Immunol* 174:1549–1556.
69. Sunny C Yung PMM (2012) Antimicrobial Chemokines. *Frontiers in Immunology* 3.
70. Allen SJ, Crown SE, Handel TM (2007) Chemokine: receptor structure, interactions, and antagonism. *Annu Rev Immunol* 25:787–820.
71. Deng Q, Barbieri JT (2008) Molecular mechanisms of the cytotoxicity of ADP-ribosylating toxins. *Annu Rev Microbiol* 62:271–288.
72. Robertson MJ (2002) Role of chemokines in the biology of natural killer cells. 71:173–183.
73. Maghazachi AA (2003) G protein-coupled receptors in natural killer cells. *J Leukoc Biol* 74:16–24.
74. Grégoire C et al. (2007) The trafficking of natural killer cells. *Immunol Rev* 220:169–182.
75. Morrison BE, Park SJ, Mooney JM, Mehrad B (2003) Chemokine-mediated recruitment of NK cells is a critical host defense mechanism in invasive aspergillosis. *J Clin Invest* 112:1862–1870.
76. Khan IA et al. (2006) CCR5 Is Essential for NK Cell Trafficking and Host Survival following Toxoplasma gondii Infection. *PLoS Pathog* 2:e49.
77. Salazar-Mather TP, Lewis CA, Biron CA (2002) Type I interferons regulate inflammatory cell trafficking and macrophage inflammatory protein 1α delivery to the liver. *Journal of Clinical Investigation* 110:321.
78. Hsu KM, Pratt JR, Akers WJ, Achilefu SI, Yokoyama WM (2009) Murine cytomegalovirus displays selective infection of cells within hours after systemic administration. *J Gen Virol* 90:33–43.
79. Paust S et al. (2010) Critical role for the chemokine receptor CXCR6 in NK cell–mediated antigen-specific memory of haptens and viruses. *Nat Immunol* 11:1127–1135.
80. Parker AK, Parker S, Yokoyama WM, Corbett JA, Buller M (2007) Induction of

Natural Killer Cell Responses by Ectromelia Virus Controls Infection. *Journal of Virology* 81:4070–4079.
81. Fang M, Lanier LL, Sigal LJ (2008) A Role for NKG2D in NK Cell–Mediated Resistance to Poxvirus Disease. *PLoS Pathogens* 4:e30.
82. Kennedy M et al. (2000) Reversible defects in natural killer and memory CD8 T cell lineages in interleukin 15-deficient mice. *J Exp Med* 191:771–780.
83. Fang M et al. (2011) CD94 Is Essential for NK Cell-Mediated Resistance to a Lethal Viral Disease. *Immunity* 34:579–589.
84. Gillard GO et al. (2011) Thy1+ Nk Cells from Vaccinia Virus-Primed Mice Confer Protection against Vaccinia Virus Challenge in the Absence of Adaptive Lymphocytes. *PLoS Pathog* 7:e1002141.
85. Campbell JA, Trossman DS, Yokoyama WM, Carayannopoulos LN (2007) Zoonotic orthopoxviruses encode a high-affinity antagonist of NKG2D. *J Exp Med* 204:1311–1317.
86. Xue X et al. (2011) Structural Basis of Chemokine Sequestration by CrmD, a Poxvirus-Encoded Tumor Necrosis Factor Receptor. *PLoS Pathog* 7:e1002162.
87. Epperson ML, Lee CA, Fremont DH (2012) Subversion of cytokine networks by virally encoded decoy receptors. *Immunol Rev* 250:199–215.
88. Hildner K et al. (2008) Batf3 Deficiency Reveals a Critical Role for CD8 + Dendritic Cells in Cytotoxic T Cell Immunity. *Science* 322:1097–1100.
89. Joachimiak MP, Weisman JL, May BC (2006) JColorGrid: software for the visualization of biological measurements. *BMC Bioinformatics* 7:225.
90. Knorr CW, Allen SD, Torres AR, Smee DF (2006) Effects of cidofovir treatment on cytokine induction in murine models of cowpox and vaccinia virus infection. *Antiviral Res* 72:125–133.
91. Begon M et al. (1999) Transmission dynamics of a zoonotic pathogen within and between wildlife host species. *Proc Biol Sci* 266:1939–1945.
92. Subrahmanyan TP (1968) A study of the possible basis of age-dependent resistance of mice to poxvirus diseases. *Aust J Exp Biol Med Sci* 46:251–265.
93. Mims CA (1968) The response of mice to the intravenous injection of cowpox virus. *Br J Exp Pathol* 49:24–32.
94. Andrian Von UH, Mempel TR (2003) Homing and cellular traffic in lymph nodes. *Nat Rev Immunol* 3:867–878.
95. Murray PJ, Wynn TA (2011) Protective and pathogenic functions of macrophage subsets. *Nat Rev Immunol* 11:723–737.
96. Beauvillain C et al. (2011) CCR7 is involved in the migration of neutrophils to lymph nodes. *The Journal of Clinical Investigation* 117:1196–1204.
97. Naik SH (2008) Demystifying the development of dendritic cell subtypes, a little. *Immunol Cell Biol* 86:439–452.
98. Heath W, Carbone F (2009) Dendritic cell subsets in primary and secondary T cell responses at body surfaces. *Nat Immunol* 10:1237–1244.
99. Forster R et al. (1999) CCR7 coordinates the primary immune response by establishing functional microenvironments in secondary lymphoid organs. *Cell* 99:23–33.
100. Seaman WE, Sleisenger M, Eriksson E, Koo GC (1987) Depletion of natural killer cells in mice by monoclonal antibody to NK-1.1. Reduction in host defense against malignancy without loss of cellular or humoral immunity. *J Immunol* 138:4539–4544.

101. Vosshenrich CAJ et al. (2006) A thymic pathway of mouse natural killer cell development characterized by expression of GATA-3 and CD127. *Nat Immunol* 7:1217–1224.
102. Vargas CL, Poursine-Laurent J, Yang L, Yokoyama WM (2011) Development of thymic NK cells from double negative 1 thymocyte precursors. *Blood* 118:3570–3578.
103. Cella M et al. (2009) A human natural killer cell subset provides an innate source of IL-22 for mucosal immunity. *Nature* 457:722–725.
104. Groom JR, Luster AD (2011) CXCR3 ligands: redundant, collaborative and antagonistic functions. *Immunol Cell Biol* 89:207–215.
105. Liu Q, Smith CW, Zhang W, Burns AR, Li Z (2012) NK Cells Modulate the Inflammatory Response to Corneal Epithelial Abrasion and Thereby Support Wound Healing. *Am J Pathol* 181:452–462.
106. Wendel M, Galani IE, Suri-Payer E, Cerwenka A (2008) Natural Killer Cell Accumulation in Tumors Is Dependent on IFN- and CXCR3 Ligands. *Cancer Research* 68:8437–8445.
107. Martín-Fontecha A et al. (2004) Induced recruitment of NK cells to lymph nodes provides IFN-γ for TH1 priming. *Nat Immunol* 5:1260–1265.
108. Thapa M, Kuziel WA, Carr DJJ (2007) Susceptibility of CCR5-Deficient Mice to Genital Herpes Simplex Virus Type 2 Is Linked to NK Cell Mobilization. *J Virol* 81:3704–3713.
109. Gregoire C et al. (2008) Intrasplenic trafficking of natural killer cells is redirected by chemokines upon inflammation. *Eur J Immunol* 38:2076–2084.
110. Mills GB, Moolenaar WH (2003) The emerging role of lysophosphatidic acid in cancer. *Nat Rev Immunol* 3:582–591.
111. Moulton EA, Bertram P, Chen N, Buller RML, Atkinson JP (2010) Ectromelia Virus Inhibitor of Complement Enzymes Protects Intracellular Mature Virus and Infected Cells from Mouse Complement. *J Virol* 84:9128–9139.
112. Palumbo GJ, Pickup DJ, Fredrickson TN, McIntyre LJ, Buller RM (1989) Inhibition of an inflammatory response is mediated by a 38-kDa protein of cowpox virus. *Virology* 172:262–273.
113. Palumbo GJ, Glasgow WC, Buller RM (1993) Poxvirus-induced alteration of arachidonate metabolism. *Proc Natl Acad Sci USA* 90:2020–2024.
114. Walzer T et al. (2007) Natural killer cell trafficking in vivo requires a dedicated sphingosine 1-phosphate receptor. *Nat Immunol* 8:1337–1344.
115. Randolph GJ, Ochando J, Partida-Sánchez S (2008) Migration of dendritic cell subsets and their precursors. *Annu Rev Immunol* 26:293–316.
116. Martin-Fontecha A et al. (2003) Regulation of dendritic cell migration to the draining lymph node: impact on T lymphocyte traffic and priming. *J Exp Med* 198:615–621.
117. Gerosa F et al. (2002) Reciprocal activating interaction between natural killer cells and dendritic cells. *J Exp Med* 195:327–333.
118. Bar-On L, Jung S (2010) Defining in vivo dendritic cell functions using CD11c-DTR transgenic mice. *Methods Mol Biol* 595:429–442.
119. Jung S et al. (2002) In vivo depletion of CD11c+ dendritic cells abrogates priming of CD8+ T cells by exogenous cell-associated antigens. *Immunity* 17:211–220.
120. Naik SH et al. (2005) Cutting edge: generation of splenic CD8+ and CD8-

dendritic cell equivalents in Fms-like tyrosine kinase 3 ligand bone marrow cultures. *J Immunol* 174:6592–6597.
121. Jenne L, Hauser C, Arrighi JF, Saurat JH, Hügin AW (2000) Poxvirus as a vector to transduce human dendritic cells for immunotherapy: abortive infection but reduced APC function. *Gene Ther* 7:1575–1583.
122. Winter S et al. (2011) Manifestation of spontaneous and early autoimmune gastritis in CCR7-deficient mice. *Am J Pathol* 179:754–765.
123. Davalos-Misslitz ACM et al. (2007) Generalized multi-organ autoimmunity in CCR7-deficient mice. *Eur J Immunol* 37:613–622.
124. Shortman K, Heath WR (2010) The CD8+ dendritic cell subset. *Immunol Rev* 234:18–31.
125. Bedoui S et al. (2009) Cross-presentation of viral and self antigens by skin-derived CD103+ dendritic cells. *Nat Immunol* 10:488–495.
126. Liard C et al. (2012) Intradermal immunization triggers epidermal Langerhans cell mobilization required for CD8 T-cell immune responses. *J Invest Dermatol* 132:615–625.
127. Allan RS et al. (2003) Epidermal viral immunity induced by CD8alpha+ dendritic cells but not by Langerhans cells. *Science* 301:1925–1928.
128. Martin-Fontecha A, Lanzavecchia A, Sallusto F (2009) Dendritic cell migration to peripheral lymph nodes. *Handb Exp Pharmacol*:31–49.
129. Oussoren C, Storm G (1999) Role of macrophages in the localisation of liposomes in lymph nodes after subcutaneous administration. *Int J Pharm* 183:37–41.
130. Junt T et al. (2007) Subcapsular sinus macrophages in lymph nodes clear lymph-borne viruses and present them to antiviral B cells. *Nature* 450:110–114.
131. Kastenmüller W, Torabi-Parizi P, Subramanian N, Lämmermann T, Germain RN (2012) A Spatially-Organized Multicellular Innate Immune Response in Lymph Nodes Limits Systemic Pathogen Spread. *Cell* 150:1235–1248.
132. Norbury CC, Malide D, Gibbs JS, Bennink JR, Yewdell JW (2002) Visualizing priming of virus-specific CD8+ T cells by infected dendritic cells in vivo. *Nat Immunol* 3:265–271.
133. Probst H et al. (2005) Histological analysis of CD11c-DTR/GFP mice after in vivo depletion of dendritic cells. *Clin Exp Immunol* 141:398–404.
134. Melchjorsen J (2006) Induction of cytokine expression by herpes simplex virus in human monocyte-derived macrophages and dendritic cells is dependent on virus replication and is counteracted by ICP27 targeting NF- B and IRF-3. *Journal of General Virology* 87:1099–1108.
135. Hardison JL, Wrightsman RA, Carpenter PM, Lane TE, Manning JE (2006) The Chemokines CXCL9 and CXCL10 Promote a Protective Immune Response but Do Not Contribute to Cardiac Inflammation following Infection with Trypanosoma cruzi. *Infect Immun* 74:125.
136. Zitvogel L (2002) Dendritic and natural killer cells cooperate in the control/switch of innate immunity. *J Exp Med* 195:F9–14.
137. Orange JS, Biron CA (1996) Characterization of early IL-12, IFN-alphabeta, and TNF effects on antiviral state and NK cell responses during murine cytomegalovirus infection. *J Immunol* 156:4746–4756.
138. Bennett CL, Clausen BE (2007) DC ablation in mice: promises, pitfalls, and challenges. *Trends Immunol* 28:525–531.

139. Coombes JL, Han S-J, van Rooijen N, Raulet DH, Robey EA (2012) Infection-induced regulation of natural killer cells by macrophages and collagen at the lymph node subcapsular sinus. *Cell Rep* 2:124–135.
140. Garcia Z et al. (2012) Subcapsular sinus macrophages promote NK cell accumulation and activation in response to lymph borne viral particles. *The Journal of Clinical Investigation*.
141. Tsai WC et al. (2000) CXC chemokine receptor CXCR2 is essential for protective innate host response in murine Pseudomonas aeruginosa pneumonia. *Infect Immun* 68:4289–4296.
142. Eisele NA, Lee-Lewis H, Besch-Williford C, Brown CR, Anderson DM (2011) Chemokine Receptor CXCR2 Mediates Bacterial Clearance Rather Than Neutrophil Recruitment in a Murine Model of Pneumonic Plague. *Am J Pathol* 178:1190–1200.
143. Herbold W et al. (2010) Importance of CXC Chemokine Receptor 2 in Alveolar Neutrophil and Exudate Macrophage Recruitment in Response to Pneumococcal Lung Infection. *Infect Immun* 78:2620–2630.
144. Rothenberg ME, Hogan SP (2006) The Eosinophil. *Annu Rev Immunol* 24:147–174.
145. Essbauer S, Pfeffer M, Meyer H (2010) Zoonotic poxviruses. *Vet Microbiol* 140:229–236.
146. Dixon H et al. (2006) The role of Th2 cytokines, chemokines and parasite products in eosinophil recruitment to the gastrointestinal mucosa during helminth infection. *Eur J Immunol* 36:1753–1763.
147. Ancuta P et al. (2006) CD16+ monocyte-derived macrophages activate resting T cells for HIV infection by producing CCR3 and CCR4 ligands. *J Immunol* 176:5760–5771.
148. Strowig T, Brilot F, Münz C (2008) Noncytotoxic functions of NK cells: direct pathogen restriction and assistance to adaptive immunity. *J Immunol* 180:7785–7791.
149. Kishimoto T (2010) IL-6: from its discovery to clinical applications. *Int Immunol* 22:347–352.
150. Couper KN, Blount DG, Riley EM (2008) IL-10: the master regulator of immunity to infection. *J Immunol* 180:5771–5777.
151. Sun JC, Lanier LL (2011) NK cell development, homeostasis and function: parallels with CD8+ T cells. *Nat Rev Immunol* 11:645–657.
152. Kirwan S, Merriam D, Barsby N, McKinnon A, Burshtyn DN (2006) Vaccinia virus modulation of natural killer cell function by direct infection. *Virology* 347:75–87.
153. Parker AK, Yokoyama WM, Corbett JA, Chen N, Buller RML (2008) Primary naive and interleukin-2-activated natural killer cells do not support efficient ectromelia virus replication. *Journal of General Virology* 89:751–759.
154. Grütz G (2005) New insights into the molecular mechanism of interleukin-10-mediated immunosuppression. *J Leukoc Biol* 77:3–15.
155. Berg RE, Forman J (2006) The role of CD8 T cells in innate immunity and in antigen non-specific protection. *Curr Opin Immunol* 18:338–343.
156. A Alcamí GLS (1995) Vaccinia, cowpox, and camelpox viruses encode soluble gamma interferon receptors with novel broad species specificity. *Journal of Virology* 69:4633–4639.

157. Lisnić VJ, Krmpotić A, Jonjić S (2010) Modulation of natural killer cell activity by viruses. *Current Opinion in Microbiology* 13:530–539.
158. Yang Z, Bjorkman PJ (2008) Structure of UL18, a peptide-binding viral MHC mimic, bound to a host inhibitory receptor. *Proc Natl Acad Sci U S A* 105:10095–10100.
159. Braud VM et al. (1998) HLA-E binds to natural killer cell receptors CD94/NKG2A, B and C. *Nature* 391:795–799.
160. Vance RE, Kraft JR, Altman JD, Jensen PE, Raulet DH (1998) Mouse CD94/NKG2A Is a Natural Killer Cell Receptor for the Nonclassical Major Histocompatibility Complex (MHC) Class I Molecule Qa-1b. *The Journal of Experimental Medicine* 188:1841.
161. Marquardt N, Wilk E, Pokoyski C, Schmidt RE, Jacobs R (2010) Murine CXCR3+CD27bright NK cells resemble the human CD56bright NK-cell population. *Eur J Immunol* 40:1428–1439.
162. Braun A et al. (2011) Afferent lymph–derived T cells and DCs use different chemokine receptor CCR7–dependent routes for entry into the lymph node and intranodal migration. *Nat Immunol* 12:879–887.
163. Orange JS, Biron CA (1996) An absolute and restricted requirement for IL-12 in natural killer cell IFN-gamma production and antiviral defense. Studies of natural killer and T cell responses in contrasting viral infections. *J Immunol* 156:1138–1142.
164. Akira S (2000) The role of IL-18 in innate immunity. *Curr Opin Immunol* 12:59–63.
165. Brandstadter JD, Yang Y (2011) Natural killer cell responses to viral infection. *J Innate Immun* 3:274–279.
166. Fehniger TA et al. (1999) Differential cytokine and chemokine gene expression by human NK cells following activation with IL-18 or IL-15 in combination with IL-12: implications for the innate immune response. *J Immunol* 162:4511–4520.
167. Seidel E, Glasner A, Mandelboim O (2012) Virus-mediated inhibition of natural cytotoxicity receptor recognition. *Cell Mol Life Sci*.
168. Chisholm SE, Reyburn HT (2006) Recognition of vaccinia virus-infected cells by human natural killer cells depends on natural cytotoxicity receptors. *J Virol* 80:2225–2233.
169. Jarahian M et al. (2011) Modulation of NKp30- and NKp46-Mediated Natural Killer Cell Responses by Poxviral Hemagglutinin. *PLoS Pathog* 7:e1002195.